

Meanders and the Temperley-Lieb algebra

P. Di Francesco,

O. Golinelli

and

E. Guitter*,

*Service de Physique Théorique,
C.E.A. Saclay,
F-91191 Gif sur Yvette Cedex, France*

The statistics of meanders is studied in connection with the Temperley-Lieb algebra. Each (multi-component) meander corresponds to a pair of reduced elements of the algebra. The assignment of a weight q per connected component of meander translates into a bilinear form on the algebra, with a Gram matrix encoding the fine structure of meander numbers. Here, we calculate the associated Gram determinant as a function of q , and make use of the orthogonalization process to derive alternative expressions for meander numbers as sums over correlated random walks.

* e-mails: philippe,golinelli,gutter@amoco.saclay.cea.fr

1. Introduction

The meander problem is one of these fundamental combinatorial problems with a simple formulation, which resist the repeated attempts to solve them. The problem is to count the number M_n of meanders of order n , i.e. of inequivalent configurations of a closed non-self-intersecting loop crossing an infinite line through $2n$ points. The infinite line may be viewed as a river flowing from east to west, and the loop as a closed circuit crossing this river through $2n$ bridges. Two configurations are considered as equivalent if they are smooth deformations of one another.

Apparently, the meander problem dates back the work of Poincaré about differential geometry. Since then, it arose in various domains such as mathematics, physics, computer science [1] and fine arts [2]. In the late 80's, Arnold reactualized this problem in relation with Hilbert's 16th problem, concerning the enumeration of ovals of planar algebraic curves [3]. Meanders also emerged in the classification of 3-manifolds [4]. More recently, random matrix model techniques, borrowed from quantum field theory, were applied to this problem [5] [6]. As such, the meander problem seems to belong to the same class as large N QCD [7].

In a previous paper [6], we made our first incursion into the meander problem, in trying to solve the *compact folding* problem of a polymer chain. Considering indeed a long closed polymer chain of say $2n$ identical monomers, we ask the question of counting the inequivalent ways of folding the whole chain onto itself, forbidding interpenetration of monomers. By compact folding, we mean that all the monomers are packed on top of each other. Accordingly, folding is a simple realization of objects with self-avoiding constraints. The reader may bear in mind the simple image of the folding of a closed strip of $2n$ stamps, with all stamps piled up on top of each other [8] [9].

The equivalence between this folding problem and the meander problem may be seen as follows. As illustrated in Fig.1, drawing a line (river) across the $2n$ constituents (bridges) of the folded polymer, and pulling them apart, produces a meander of order n . The folding of a *closed* polymer chain and the meander problem are therefore completely identical. By analogy, we were led to define the meander counterpart of the folding problem of an *open* polymer chain: the semi-meanders. The latter are defined in the same way as meanders, except that the river is now semi-infinite, i.e. it has a source, around which the semi-meander is allowed to wind freely. We denote by \bar{M}_n the number of semi-meanders of order n , namely with n bridges.

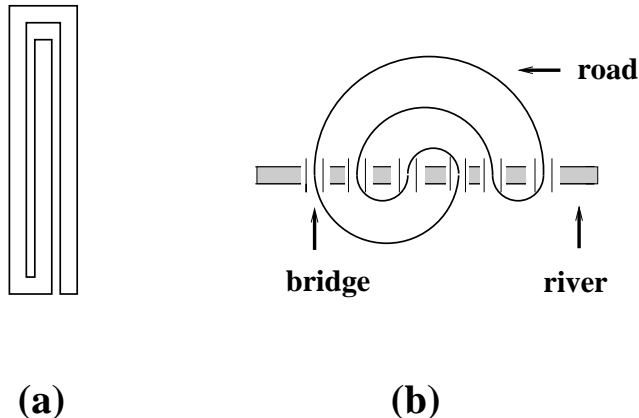


Fig. 1: A compactly folded polymer (a) with $2n = 6$ monomers, and the associated meander (b), obtained by drawing a line (river) horizontally through the monomers. Each monomer becomes a bridge, and each hinge a segment of road between two bridges.

In this paper, we reconsider the meander and semi-meander problems in the framework of the Temperley-Lieb algebra [10]. This is based on a one-to-one correspondence between (multicomponent) semi-meanders and reduced elements of the Temperley-Lieb algebra. Similarly, (multicomponent) meanders are associated to *pairs* of such elements. More precisely, the Temperley-Lieb algebra is endowed with a bilinear structure out of which a Gram matrix can be constructed. In our language, the bilinear form associates to each pair of elements of the algebra a weight q^c , where c denotes the number of connected components of the associated meander. In particular, the Gram matrix, as a polynomial of q , encodes all the relevant information about meander and semi-meander numbers.

Here we obtain as a main result an exact compact expression for the determinant of the Gram matrix, referred to as the *meander determinant*. Far from solving the question of enumerating meanders, this gives however some partial information on the problem, and produces an exact solution to a meander-flavored issue. This result is summarized in Eq.(5.6), and proved by explicit orthogonalization of the Gram matrix. In a second step, we make use of the precise form of the change of basis in the orthogonalization process to derive various expressions for the semi-meander (Eq.(6.62)) and meander (Eq.(6.63)) numbers as statistical sums over paths, with an interpretation as Solid On Solid (SOS) model partition functions.

The paper is organized as follows. We start in Sect.2 by giving basic definitions of (multi-component) meander (Eq.(2.1)) and semi-meander (Eq.(2.3)) numbers and associated polynomials in which a weight q is assigned to each connected component. The

relation between (semi-)meanders and both arch configurations and walk diagrams is then discussed, and known results for $q = \pm 1$ are reviewed (Eqs.(2.6)-(2.8)). Various conjectured and/or numerical asymptotic behaviors for large n are given (Eqs.(2.11)-(2.18)). In Sect.3, we introduce the Temperley-Lieb algebra $TL_n(q)$, and discuss its relation with walk diagrams and arch configurations, in one-to-one correspondence with reduced elements of the algebra. These reduced elements form a natural basis (basis 1) of $TL_n(q)$. The contact with meanders is made through the introduction of a trace and a bilinear form on $TL_n(q)$ (Eqs.(3.11) and (3.14)). When evaluated on pairs of reduced elements (of the basis 1), this form generates the Gram matrix (Eq.(3.15)), which encodes the fine structure of meander numbers. In Sect.4, we make a change from basis 1 to a new basis 2, in which the Gram matrix is diagonal. This allows for the calculation of the Gram determinant as a function of q (Eq.(5.6)), and the identification of its zeros (Eq.(5.10)) and their multiplicities (Eq.(5.23)). These results, together with a complete combinatorial proof are detailed in Sect.5. The matrix for the change of basis $1 \rightarrow 2$ is studied in great detail in Sect.6, where it is shown to obey a simple recursion relation (Eq.(6.29)). This equation is explicitly solved, in the form of matrix elements between two walk diagrams, factorized into a selection rule (with value 0 or 1, see Eq.(6.38)) multiplied by some weight, with a local dependence on the heights of the walk diagrams (Eq.(6.43)). This leads to expressions for the meander and semi-meander polynomials as sums over selected walk diagrams (Eqs.(6.62) and (6.63)). Analogous formulas are derived within the framework of SOS models (Eq.(6.90)), leading to various conjectures as to the asymptotic form of the meander and semi-meander polynomials for $q \geq 2$. Sect.7 is devoted to a refinement of the meander determinant for semi-meanders with fixed number of windings around the source of the river (Eq.(7.5)). A few concluding remarks are gathered in Sect.8. Some technical ingredients are detailed in Appendices A,B and C.

2. Definitions

2.1. Meanders

A *meander* of order n is a planar configuration of a closed non-self-intersecting loop (road) crossing an infinite oriented line (river flowing from east to west) through $2n$ points (bridges). We denote by M_n the number of topologically inequivalent meanders of order n . We extend the definition to a set of k roads (i.e., a meander with k possibly interlocking connected components). The number of meanders with k connected components is denoted



Fig. 2: The four meanders of order $n = 2$, i.e. with $2n = 4$ bridges. The two first ones have $k = 1$ connected component, the two other have $k = 2$ connected components.

by $M_n^{(k)}$. Note that necessarily $1 \leq k \leq n$. These numbers are summarized in the meander polynomial

$$m_n(q) = \sum_{k=1}^n M_n^{(k)} q^k \quad (2.1)$$

The various meanders corresponding to $n = 2$ are depicted in Fig.2. They correspond to the polynomial

$$m_2(q) = 2q + 2q^2 \quad (2.2)$$

The numbers $M_n^{(k)}$ are listed in [6] for $1 \leq k \leq n \leq 12$.

2.2. Semi-meanders

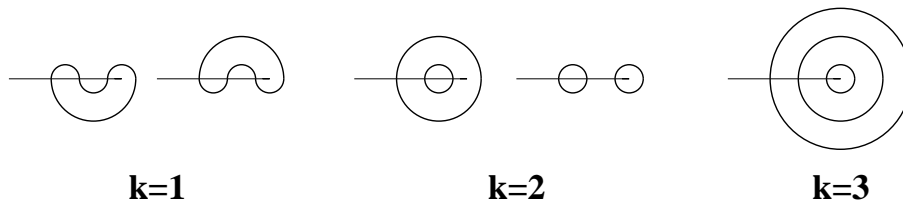


Fig. 3: The five semi-meanders of order $n = 3$, arranged according to their numbers $k = 1, 2, 3$ of connected components.

A *semi-meander* of order n is a planar configuration of a closed non-self-intersecting loop (road) crossing a semi-infinite line (river with a source) through n points (bridges). Note that, in a semi-meander, the road may wind around the source of the river. We denote by \bar{M}_n the number of topologically inequivalent semi-meanders of order n , and by $\bar{M}_n^{(k)}$ the number of semi-meanders with k connected components, $1 \leq k \leq n$. We also

have the semi-meander polynomial

$$\bar{m}_n(q) = \sum_{k=1}^n \bar{M}_n^{(k)} q^k \quad (2.3)$$

The various semi-meanders corresponding to $n = 3$ are depicted in Fig.3. They correspond to the polynomial

$$\bar{m}_3(q) = 2q + 2q^2 + q^3 \quad (2.4)$$

The numbers $\bar{M}_n^{(k)}$ are listed in [6] for $1 \leq k \leq n \leq 14$.

2.3. Arch configurations and (semi) meanders

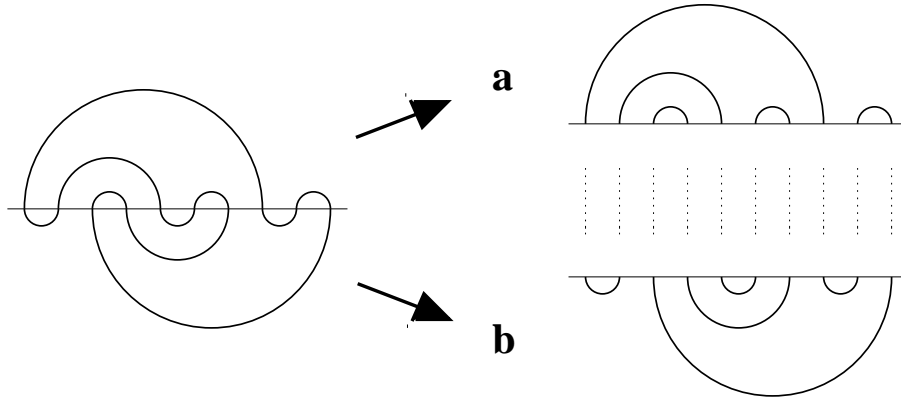


Fig. 4: Any meander is obtained as the superimposition of a top (*a*) and bottom (*b*) arch configurations of same order ($n = 5$ here). An arch configuration is a planar pairing of the $(2n)$ bridges through n non-intersecting arches lying above the river (by convention, we represent the lower configuration *b* reflected with respect to the river).

A multicomponent meander may be viewed as the superimposition of two (top and bottom) *arch configurations* of order n , corresponding respectively to the configurations of the road on both sides of the river, as shown in Fig.4. An arch configuration is simply a configuration of n planar non-intersecting arches (lying, say, above the river) linking the $2n$ bridges by pairs. The number of arch configurations of order n is given by the Catalan number

$$c_n = \frac{(2n)!}{(n+1)!n!} \quad (2.5)$$

The set of arch configurations of order n is denoted by A_n .

As an immediate consequence, as arbitrary multicomponent meanders are obtained by superimpositions of arbitrary top and bottom arch configurations, we have

$$m_n(1) = (c_n)^2 \tag{2.6}$$

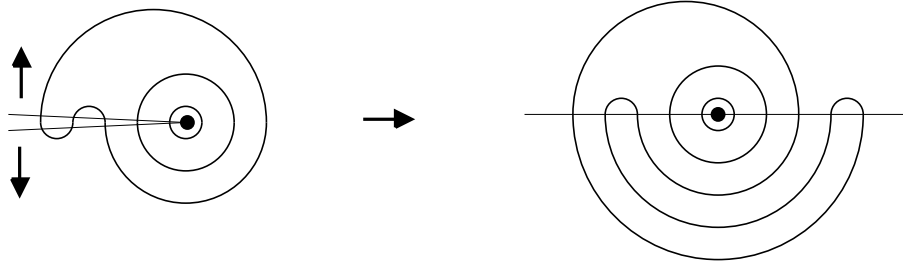


Fig. 5: Any semi-meander may be viewed as a particular meander by opening the semi-infinite river as indicated by the arrows. This doubles the number of bridges in the resulting meander, hence the order is conserved ($n = 5$ here). By construction, the lower arch configuration of the meander is always a rainbow arch configuration of same order. The number of connected components ($k = 3$ here) is conserved in the transformation.

As for semi-meanders, upon opening the semi-infinite river and dedoubling the bridges (cf. Fig.5), they can also be viewed as the superimposition of a top arch configuration of order n , and of a particular bottom “rainbow” arch configuration (namely that linking the i -th bridge to the $(2n + 1 - i)$ -th one, $i = 1, 2, \dots, n$). Therefore arbitrary multicomponent semi-meanders may be obtained by superimposing an arbitrary arch configuration with a rainbow of order n , leading to

$$\bar{m}_n(1) = c_n \tag{2.7}$$

In ref.[6], we have also proved the following results

$$\begin{aligned} m_n(-1) &= \begin{cases} 0 & \text{if } n = 2p \\ -(c_p)^2 & \text{if } n = 2p + 1 \end{cases} \\ \bar{m}_n(-1) &= \begin{cases} 0 & \text{if } n = 2p \\ -(c_p) & \text{if } n = 2p + 1 \end{cases} \end{aligned} \tag{2.8}$$

Note that the one-component meander and semi-meander numbers are recovered in the $q \rightarrow 0$ limit of respectively $m_n(q)/q$ and $\bar{m}_n(q)/q$.

2.4. Walk diagrams

An arch configuration of order n may be viewed as a closed random walk of $2n$ steps on a semi-infinite line, or equivalently its two-dimensional extent, which we call a *walk diagram*, defined as follows. Let us first label the segments of river between consecutive bridges, namely the segment i lies between the i -th and the $(i + 1)$ -th bridge, for $i = 1, 2, \dots, 2n - 1$. Let us also label by 0 and $2n$, the semi-infinite portions of river respectively to the left of the first bridge and to the right of the last one. To each portion of river i , we attach a height ℓ_i equal to the number of arches passing at the vertical of i . The nonnegative integers ℓ_i satisfy the following conditions

$$\begin{aligned} \ell_0 &= \ell_{2n} = 0 \\ \ell_{i+1} - \ell_i &\in \{\pm 1\} \quad i = 0, 1, \dots, 2n - 1 \end{aligned} \tag{2.9}$$

The diagram formed by the broken line joining the successive points (i, ℓ_i) , $i = 0, 1, \dots, 2n$, is the walk diagram corresponding to the initial arch configuration. This diagram represents the two-dimensional extent of a walk of $2n$ steps on the semi-infinite line $\ell \geq 0$ starting and ending at its origin.

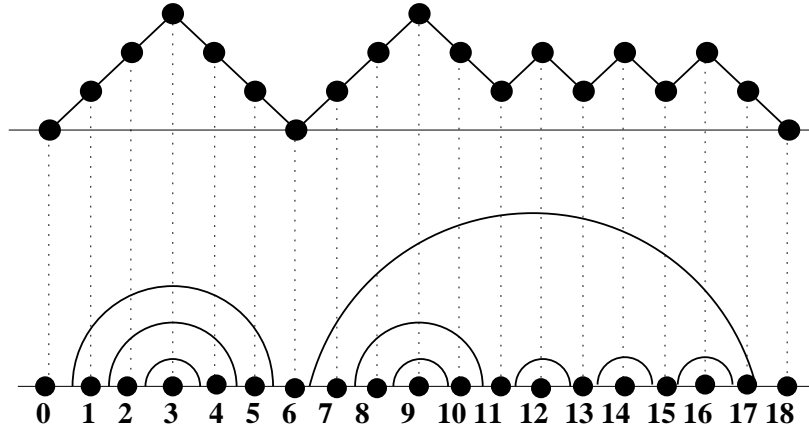


Fig. 6: A walk diagram of 18 steps, and the corresponding arch configuration. Each dot corresponds to a segment of river. The height on the walk diagram is given by the number of arches intersected by the vertical dotted line.

Conversely, any walk diagram of $2n$ steps, characterized by integer heights $\ell_i \geq 0$, $i = 0, \dots, 2n$, satisfying (2.9), corresponds to a unique arch configuration of order n . To construct the arch configuration corresponding to a walk diagram, notice that, going from left to right along the river, whenever $\ell_i - \ell_{i-1} = 1$, a new arch originates from the bridge

i , whereas when $\ell_i - \ell_{i-1} = -1$, an arch terminates at the bridge i . We denote by W_n the set of walk diagrams of $2n$ steps. We have the identification

$$W_n \equiv A_n \tag{2.10}$$

In this paper, we will alternatively use the arch configuration and walk diagram pictures.

2.5. Asymptotics

Earlier numerical work [9] [5] [6] suggests that the (one-component) meander and semi-meander numbers behave in the large n limit as respectively

$$\begin{aligned} M_n &\sim \frac{R^n}{n^\alpha} \\ \bar{M}_n &\sim \frac{\bar{R}^n}{n^\gamma} \end{aligned} \tag{2.11}$$

with

$$\begin{aligned} \bar{R} &\simeq 3.5\dots & R &= \bar{R}^2 \\ \alpha &= 7/2 & \gamma &= 2 \end{aligned} \tag{2.12}$$

The values of the exponents α and γ are conjectured to be exact. The relation $R = \bar{R}^2$ is a consequence of the polymer folding interpretation [6]: the entropy per monomer is the same for the open and closed polymer folding problems. Note however that the configuration exponents α and γ depend on the boundary conditions (open or closed). A natural quantity of interest for the study of semi-meanders is the *winding*, namely the number of times the road winds around the source of the river in the river/road picture of the semi-meander. In the arch configuration picture, the winding of a semi-meander is the number of arches of the upper configuration passing at the vertical of the middle point; representing the upper arch configuration as a walk diagram a , the winding of the semi-meander is simply ℓ_n^a . Denoting by $c(a)$ the number of connected components of the superimposition of the arch configuration a and of a rainbow configuration of order n , the average winding in semi-meanders of order n reads

$$w_n(q) = \frac{\sum_{a \in W_n} \ell_n^a q^{c(a)}}{\sum_{a \in W_n} q^{c(a)}} \underset{n \rightarrow \infty}{\sim} n^{\nu(q)} \tag{2.13}$$

where we have identified a winding exponent $\nu(q) \in [0, 1]$. In this paper, we give strong analytical evidence that $\nu(q) = 1$ for all $q \geq 2$. For $0 < q < 2$, numerical work seems to indicate that $1/2 \leq \nu(q) < 1$.

More generally, we expect the meander and semi-meander polynomials to behave for large n as

$$\begin{aligned} m_n(q) &\sim \frac{R(q)^n}{n^{\alpha(q)}} \\ \bar{m}_n(q) &\sim \frac{\bar{R}(q)^n}{n^{\gamma(q)}} \end{aligned} \tag{2.14}$$

where $R(q) = \bar{R}(q)^2$ like in the $q = 0$ case, but only for $q < 2^1$

As an element of comparison, by using Stirling's formula for factorials, we have

$$\begin{aligned} \bar{m}_n(1) &= c_n \sim \frac{4^n}{n^{3/2}} \\ m_n(1) &= (c_n)^2 \sim \frac{4^{2n}}{n^3} \end{aligned} \tag{2.15}$$

hence $\bar{R}(1) = 4$ and

$$\alpha(1) = 3 \quad \gamma(1) = 3/2 \tag{2.16}$$

We also have the obvious large q asymptotics

$$\begin{aligned} \bar{m}_n(q) &\sim q^n \\ m_n(q) &\sim c_n q^n \sim \frac{(4q)^n}{n^{3/2}} \end{aligned} \tag{2.17}$$

hence $R(q) \sim 4q$ and $\bar{R}(q) \sim q$, whereas

$$\alpha(\infty) = \frac{3}{2} \quad \gamma(\infty) = 0 \tag{2.18}$$

¹ This relation is only expected insofar as $\nu(q) < 1$. Indeed, in this case, comparing the numbers $m_n(q)$ and $\bar{m}_{2n}(q)$ of respectively meanders and semi-meanders with $(2n)$ bridges, we see that the semi-meanders with significant winding (i.e., $w_n \sim n$) are negligible, hence we expect the two numbers to be of the same order, namely

$$m_n(q) \sim R(q)^n \sim \bar{m}_{2n}(q) \sim \bar{R}(q)^{2n}$$

hence $R(q) = \bar{R}(q)^2$. According to the previous discussion, this fails for $q \geq 2$, where $\nu(q) = 1$. Indeed, it is easy to see that, for large q , $R(q)/\bar{R}(q)^2 \sim 4/q \rightarrow 0$, as $m_n(q) \sim c_n q^n \sim (4q)^n$ and $\bar{m}_{2n}(q) \sim q^{2n}$.

3. Temperley-Lieb algebra and meanders

3.1. The Temperley-Lieb algebra and arch configurations

The Temperley-Lieb algebra of order n and parameter q , denoted by $TL_n(q)$, is defined through its n generators $1, e_1, e_2, \dots, e_{n-1}$ subject to the relations

$$\begin{aligned}
 (i) \quad e_i^2 &= q e_i \quad i = 1, 2, \dots, n-1 \\
 (ii) \quad [e_i, e_j] &= 0 \quad \text{if } |i-j| > 1 \\
 (iii) \quad e_i e_{i\pm 1} e_i &= e_i \quad i = 1, 2, \dots, n-1
 \end{aligned}
 \tag{3.1}$$

This definition becomes clear in the ‘‘braid’’ pictorial representation, where the generators act on n parallel strings as follows:

$$1 = \begin{array}{|c|} \hline \hline \hline \hline \hline \hline \\ \hline \end{array} \begin{array}{c} 1 \\ \vdots \\ i \\ i+1 \\ \vdots \\ n \end{array} \quad e_i = \begin{array}{|c|} \hline \hline \hline \hline \hline \hline \\ \hline \end{array} \begin{array}{c} \vdots \\ \vdots \\ \vdots \\ \vdots \\ \vdots \end{array} \begin{array}{c} i \\ i+1 \end{array} \tag{3.2}$$

and a product of elements is represented by the juxtaposition of the corresponding braid diagrams. The relation (ii) expresses the locality of the e ’s, namely that the e ’s commute whenever they involve distant strings. The relations (i) and (iii) read respectively

$$\begin{aligned}
 (i) \quad e_i^2 &= \begin{array}{|c|} \hline \hline \hline \hline \hline \hline \\ \hline \end{array} \begin{array}{c} \vdots \\ \vdots \\ \vdots \\ \vdots \\ \vdots \end{array} \begin{array}{c} i \\ i+1 \end{array} = q \begin{array}{|c|} \hline \hline \hline \hline \hline \hline \\ \hline \end{array} \begin{array}{c} \vdots \\ \vdots \\ \vdots \\ \vdots \\ \vdots \end{array} \begin{array}{c} i \\ i+1 \end{array} = q e_i \\
 (iii) \quad e_i e_{i+1} e_i &= \begin{array}{|c|} \hline \hline \hline \hline \hline \hline \\ \hline \end{array} \begin{array}{c} \vdots \\ \vdots \\ \vdots \\ \vdots \\ \vdots \end{array} \begin{array}{c} i \\ i+1 \end{array} = \begin{array}{|c|} \hline \hline \hline \hline \hline \hline \\ \hline \end{array} \begin{array}{c} \vdots \\ \vdots \\ \vdots \\ \vdots \\ \vdots \end{array} \begin{array}{c} i \\ i+1 \end{array} = e_i
 \end{aligned}
 \tag{3.3}$$

In the relation (i), the loop has been erased, but affected the weight q . The relation (iii) is simply obtained by stretching the $(i+2)$ -th string.

3.2. The basis 1

The algebra $TL_n(q)$ is built out of arbitrary products of generators e_i . Up to numerical factors depending on q , any such product can be reduced by using the relations (i)-(iii). The algebra $TL_n(q)$, as a real vector space, is therefore naturally endowed with the basis

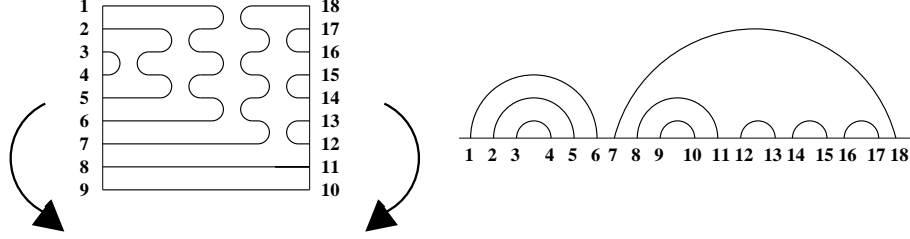


Fig. 7: The transformation of a reduced element of $TL_9(q)$ into an arch configuration of order 9. The reduced element reads $e_3e_4e_2e_5e_3e_1e_6e_4e_2$.

formed by all the distinct reduced elements of the algebra. This basis will be referred to as *basis 1* in the following. For illustration, the reduced elements of $TL_3(q)$ read

$$\begin{aligned}
 1 &= \text{[Diagram: 3 horizontal strands]} & e_1 &= \text{[Diagram: 3 strands, first two cross]} & e_2 &= \text{[Diagram: 3 strands, last two cross]} \\
 e_1e_2 &= \text{[Diagram: 3 strands, first two cross then last two cross]} & e_2e_1 &= \text{[Diagram: 3 strands, last two cross then first two cross]}
 \end{aligned} \tag{3.4}$$

Let us now show that the reduced elements of $TL_n(q)$ are in one to one correspondence with arch configurations of order n . This is most clearly seen by considering the braid pictorial representation of a reduced element. Such a diagram has no internal loop (by virtue of (i)), and all its strings are stretched (using (iii)). As shown in Fig.7, one can construct a unique arch configuration of order n by deforming the diagram so as to bring the $(2n)$ ends of the strings on a line. This deformation is invertible, and we conclude that, as a vector space, $TL_n(q)$ has dimension

$$\dim(TL_n(q)) = c_n \tag{3.5}$$

The basis 1 is best expressed in the language of walk diagrams. The walk diagrams of $2n$ steps are arranged according to their middle height $\ell_n = h$, where $h = n - 2p$, $0 \leq p \leq n/2$. For each value of h , the basic reduced element

$$f_h^{(n)} = e_1e_3e_5\dots e_{2p-1} \quad f_n^{(n)} = 1 \tag{3.6}$$

corresponds to the lowest walk diagram $\mathcal{W}_h^{(n)}$ with middle height h , namely

$$\mathcal{W}_h^{(n)} = \text{[Diagram: A walk diagram with 2n steps, starting at 0, ending at 2n, with a peak at n. The x-axis is labeled 0, 2, 4, ..., 2p, ..., n, ..., 2(n-p), ..., 2n. The y-axis represents height.] } \tag{3.7}$$

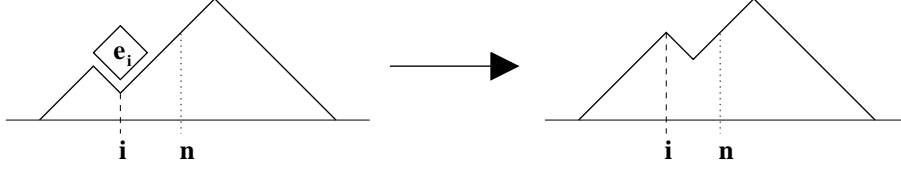


Fig. 8: An example of allowed left multiplication by e_i . The initial walk diagram must have a minimum at the vertical of the point i . This operation adds a box to the walk diagram at the vertical of the point $i < n$.

with

$$\begin{aligned}
 \ell_0 &= \ell_2 = \dots = \ell_{2p} = 0 \\
 \ell_1 &= \ell_3 = \dots = \ell_{2p-1} = 1 \\
 \ell_{2p+j} &= j \quad j = 1, 2, \dots, h \\
 \ell_{2n-j} &= \ell_j \quad j = 0, 1, 2, \dots, n
 \end{aligned} \tag{3.8}$$

It is then easy to see that any reduced element corresponding to a walk diagram with middle height $\ell_n = h$ is obtained by repeated appropriate multiplications to the left or to the right of $f_h^{(n)}$ with e 's. The walk diagrams of middle height h are constructed univocally by adding “boxes” to the diagram $\mathcal{W}_h^{(n)}$. As illustrated on Fig.8, adding a box to a diagram \mathcal{W} at the vertical of the point i is allowed only if i is a minimum of \mathcal{W} , namely $\ell_{i+1} = \ell_{i-1} = \ell_i + 1$, in which case the new diagram, with the box added, has $\ell_i \rightarrow \ell_i + 2$. For the associated basis 1 elements, this addition of a box corresponds to the left (resp. right) multiplication by e_i (resp. e_{2n-i}) when $i < n$ (resp. $i > n$). This does not affect the middle height $\ell_n = h$. For illustration, we list the elements of the basis 1 for $TL_3(q)$ together with the corresponding walk diagram (the middle height ℓ_3 takes only the values 1 (in 4 diagrams) and 3 (in 1 diagram))

$$\begin{aligned}
 e_1 &= f_1^{(3)} = \text{walk diagram 1} \\
 e_2 e_1 &= e_2 f_1^{(3)} = \text{walk diagram 2} \\
 e_1 e_2 &= f_1^{(3)} e_2 = \text{walk diagram 3} \\
 e_2 &= e_2 f_1^{(3)} e_2 = \text{walk diagram 4} \\
 1 &= f_3^{(3)} = \text{walk diagram 5}
 \end{aligned} \tag{3.9}$$

To avoid confusion, we will denote by $(a)_1$ the basis 1 element corresponding to the walk diagram (or arch configuration) $a \in W_n (\equiv A_n)$.

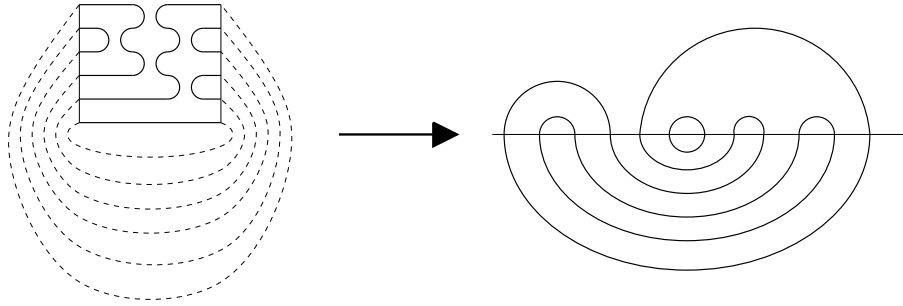


Fig. 9: The trace of an element $e \in TL_6(q)$ is obtained by identifying the left and right ends of its strings (dashed lines). In the arch configuration picture, this amounts to closing the upper configuration by a rainbow of order 6. The corresponding semi-meander has 3 connected components, hence $\text{Tr}(e) = q^3$.

3.3. Scalar product and meanders

The standard scalar product on $TL_n(q)$ is defined as follows. First one introduces a trace over $TL_n(q)$. From the relation (i) of (3.1), we see that in any element e of $TL_n(q)$ each closed loop may be erased and replaced by a prefactor q . Taking the trace of a basis 1 element e corresponds to identifying the left and right ends of each string as in Fig.9, and assigning an analogous factor to each closed loop, which results in a factor

$$\text{Tr}(e) = q^{c(e)} \quad (3.10)$$

where $c(e)$ is the number of connected components of the closure of e . The definition of the trace is extended to any linear combination of basis elements by linearity. Note that, with this definition, the trace is cyclic, namely $\text{Tr}(ef) = \text{Tr}(fe)$. In the arch configuration picture, $c(e)$ is easily identified as the number of connected components of the semi-meander obtained by superimposing the arch configuration a corresponding to e and the rainbow of order n : indeed, the rainbow connects the i -th bridge to the $(2n + 1 - i)$ -th, which exactly corresponds to the above identification of string ends. In particular, this permits to identify the semi-meander polynomial (2.3) as

$$\boxed{\bar{m}_n(q) = \sum_{e \in \text{basis } 1} q^{c(e)} = \sum_{a \in W_n} \text{Tr}((a)_1)} \quad (3.11)$$

We also define the transposition on $TL_n(q)$, by its action on the generators $e_i^t = e_i$, and the relation $(ef)^t = f^t e^t$ for any $e, f \in TL_n(q)$. The definition extends to real linear

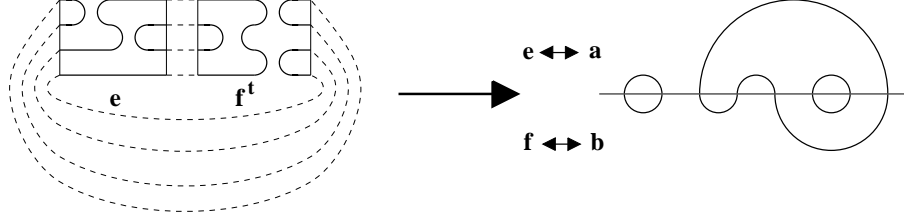


Fig. 10: The scalar product (e, f) is obtained by first multiplying e with f^t , and then identifying the left and right ends of the strings (by the dashed lines). Here we have $(e, f) = q^3$. The corresponding meander is obtained by superimposition of the upper arch configuration a corresponding to e and lower arch configuration b corresponding to f (the transposition of f is crucial to recover b as lower arch configuration). Here the meander has $c(a, b) = c(e, f) = 3$ connected components.

combinations by $(\lambda e + \mu f)^t = \lambda e^t + \mu f^t$. In the arch configuration picture, this corresponds to the reflection $i \rightarrow (2n + 1 - i)$ of the bridges. In the walk diagram picture, this is the reflection $i \rightarrow (2n - i)$.

For any two elements e and $f \in TL_n(q)$, the scalar product is defined as

$$(e, f) = \text{Tr}(e f^t) \quad (3.12)$$

This has a simple interpretation in terms of meanders. We have indeed

$$(e, f) = q^{c(e, f)} = q^{c(a, b)} \quad (3.13)$$

where $c(e, f) = c(a, b)$ is the number of connected components of the meander obtained by superimposing the a and b arch configurations corresponding respectively to e and f (see Fig.10 for an example). This permits to identify the meander polynomial as

$$m_n(q) = \sum_{a, b \in A_n} q^{c(a, b)} = \sum_{a, b \in W_n} ((a)_1, (b)_1) \quad (3.14)$$

Note that $(e, 1) = \text{Tr}(e)$, hence the semi-meander expression (3.11) corresponds to taking $(b)_1 = 1$ in the above and summing over $a \in W_n$ only. This agrees with the abovementioned fact that the semi-meanders are particular meanders, namely with lower arch configuration fixed to be a rainbow. Indeed, the unit $1 \in TL_n(q)$ corresponds in the arch configuration picture to the rainbow of order n , $(r_n)_1 = 1$.

3.4. Gram matrix

The Gram matrix $\mathcal{G}_n(q)$ of the basis 1 of $TL_n(q)$ is the $c_n \times c_n$ symmetric matrix with entries equal to the scalar products of the basis elements, namely

$$\boxed{[\mathcal{G}_n(q)]_{a,b} = ((a)_1, (b)_1) = q^{c(a,b)} \quad \forall a, b \in A_n \equiv W_n} \quad (3.15)$$

For instance, $\mathcal{G}_3(q)$ reads, in the basis 1 (3.9):

$$\mathcal{G}_3(q) = \begin{pmatrix} q^3 & q^2 & q^2 & q & q^2 \\ q^2 & q^3 & q & q^2 & q \\ q^2 & q & q^3 & q^2 & q \\ q & q^2 & q^2 & q^3 & q^2 \\ q^2 & q & q & q^2 & q^3 \end{pmatrix} \quad (3.16)$$

The meander and semi-meander polynomials are easily expressed in terms of the Gram matrix. Arranging the elements of basis 1 by growing middle height of the walk diagrams (in particular, the unit 1 is the last element), and defining the c_n -dimensional vectors

$$\vec{u} = (1, 1, 1, \dots, 1) \quad \vec{v} = (0, 0, \dots, 0, 1) \quad (3.17)$$

we have

$$\begin{aligned} m_n(q) &= \vec{u} \cdot \mathcal{G}_n(q) \vec{u} \\ \bar{m}_n(q) &= \vec{v} \cdot \mathcal{G}_n(q) \vec{u} \end{aligned} \quad (3.18)$$

where $\vec{x} \cdot \vec{y}$ denotes the ordinary Euclidian scalar product of \mathbb{R}^{c_n} . Moreover, we also have

$$m_n(q^2) = \text{tr}(\mathcal{G}_n(q)^2) \quad (3.19)$$

The Gram matrix $\mathcal{G}_n(q)$ contains therefore all the information we need about meanders. The remainder of the paper is devoted to a thorough study of this matrix and of the consequences on meanders.

4. The basis 2

The multiplication of elements of the basis 1 involves many reductions, and therefore is quite complicated. In this section, we describe another basis for $TL_n(q)$, which we refer to as *basis 2*, in which the products of basis elements are trivialized, namely the product of any two basis 2 elements is either 0 or equal to another basis element. This second basis, described in detail in [11], will be instrumental in writing alternative expressions of the meander and semi-meander polynomials.

4.1. Definition of the basis 2

We need a few preliminary definitions. The Chebishev polynomials of the second kind are defined by the initial data $U_0(x) = 1$ and $U_1(x) = x$ and the recursion relation

$$U_{n+1}(x) = xU_n(x) - U_{n-1}(x) \quad (4.1)$$

or equivalently by

$$U_n\left(z + \frac{1}{z}\right) = \frac{z^{n+1} - z^{-n-1}}{z - z^{-1}} \quad (4.2)$$

We also introduce the fractions

$$\mu_n = \frac{U_{n-1}(q)}{U_n(q)} \quad (4.3)$$

subject to the recursion relation

$$\frac{1}{\mu_{n+1}} = \frac{1}{\mu_1} - \mu_n \quad (4.4)$$

To describe the basis 2, we use a walk diagram picture analogous to that for basis 1. Each basis element will be attached to a walk diagram of $2n$ steps. As in the case of basis 1, we start from the definition of the fundamental element $\varphi_h^{(n)}$, corresponding to $\mathcal{W}_h^{(n)}$, the lowest walk diagram with middle height $\ell_n = h = n - 2p$ (3.7), namely

$$\varphi_h^{(n)} = (\mu_1)^p e_1 e_3 \cdots e_{2p-1} E_h(e_{2p+1}, e_{2p+2}, \dots, e_{n-1}) \quad (4.5)$$

where the elements E_h are defined recursively by

$$\begin{aligned} E_0 &= E_1 = 1 \\ E_{h+1}(e_i, e_{i+1}, \dots, e_{i+h-1}) & \\ &= E_h(e_i, e_{i+1}, \dots, e_{i+h-2})(1 - \mu_h e_{i+h-1}) E_h(e_i, e_{i+1}, \dots, e_{i+h-2}) \end{aligned} \quad (4.6)$$

For instance, we have

$$\begin{aligned} E_2(e_i) &= 1 - \mu_1 e_i \\ E_3(e_i, e_{i+1}) &= (1 - \mu_1 e_i)(1 - \mu_2 e_{i+1})(1 - \mu_1 e_i) \\ &= 1 - \mu_2(e_i + e_{i+1}) + \mu_1 \mu_2(e_i e_{i+1} + e_{i+1} e_i) \end{aligned} \quad (4.7)$$

Note that E_h is a projector² ($E_h^2 = E_h$), and that the normalization factor in (4.5) ensures that $\varphi_h^{(n)}$ is a projector too.

² This is easily proved by recursion on h , by simultaneously proving that $E_h^2 = E_h$ and $(E_h(e_i, \dots, e_{i+h-2})e_{i+h-1})^2 = \mu_h^{-1} E_h(e_i, \dots, e_{i+h-2})e_{i+h-1}$.

In a second step, we construct the other basis elements corresponding to walk diagrams with middle height h . The latter are obtained by repeated left and right additions of boxes on the basic diagram $\mathcal{W}_h^{(n)}$. To define the corresponding basis 2 elements, it is sufficient to give the multiplication rule corresponding to a box addition (see Fig.8). The rule reads as follows. If a box is added on a minimum ($\ell_{i+1} = \ell_{i-1} = \ell_i + 1$) of the walk diagram at the vertical of the point $i < n$ (resp. $2n - i > n$), the corresponding basis element is multiplied to the left (resp. right) by the quantity

$$\sqrt{\frac{\mu_{\ell_i+2}}{\mu_{\ell_i+1}}}(e_i - \mu_{\ell_i+1}) \quad (4.8)$$

Applying these rules in the case of $TL_3(q)$, we find the following basis 2 elements

$$\begin{aligned}
\begin{array}{c} \bullet \\ \diagup \quad \diagdown \\ \bullet \quad \bullet \\ \diagup \quad \diagdown \\ \bullet \quad \bullet \quad \bullet \\ \diagup \quad \diagdown \\ \bullet \quad \bullet \quad \bullet \quad \bullet \end{array} &= \varphi_1^{(3)} = \mu_1 e_1 \\
\begin{array}{c} \bullet \\ \diagup \quad \diagdown \\ \bullet \quad \bullet \\ \diagup \quad \diagdown \\ \bullet \quad \bullet \quad \bullet \\ \diagup \quad \diagdown \\ \bullet \quad \bullet \quad \bullet \quad \bullet \end{array} &= \sqrt{\frac{\mu_2}{\mu_1}}(e_2 - \mu_1)\mu_1 e_1 \\
&= \sqrt{\mu_1 \mu_2}(e_2 e_1 - \mu_1 e_1) \\
\begin{array}{c} \bullet \\ \diagup \quad \diagdown \\ \bullet \quad \bullet \\ \diagup \quad \diagdown \\ \bullet \quad \bullet \quad \bullet \\ \diagup \quad \diagdown \\ \bullet \quad \bullet \quad \bullet \quad \bullet \end{array} &= \mu_1 e_1 \sqrt{\frac{\mu_2}{\mu_1}}(e_2 - \mu_1) \\
&= \sqrt{\mu_1 \mu_2}(e_1 e_2 - \mu_1 e_1) \\
\begin{array}{c} \bullet \\ \diagup \quad \diagdown \\ \bullet \quad \bullet \\ \diagup \quad \diagdown \\ \bullet \quad \bullet \quad \bullet \\ \diagup \quad \diagdown \\ \bullet \quad \bullet \quad \bullet \quad \bullet \end{array} &= \sqrt{\frac{\mu_2}{\mu_1}}(e_2 - \mu_1)\mu_1 e_1 \sqrt{\frac{\mu_2}{\mu_1}}(e_2 - \mu_1) \\
&= \mu_2(e_2 - \mu_1)(e_1 e_2 + e_2 e_1) + \mu_1^2 e_1 \\
\begin{array}{c} \bullet \\ \diagup \quad \diagdown \\ \bullet \quad \bullet \\ \diagup \quad \diagdown \\ \bullet \quad \bullet \quad \bullet \\ \diagup \quad \diagdown \\ \bullet \quad \bullet \quad \bullet \quad \bullet \end{array} &= \varphi_3^{(3)} = E_3(e_1, e_2) \\
&= 1 - \mu_2(e_1 + e_2) + \mu_1 \mu_2(e_1 e_2 + e_2 e_1)
\end{aligned} \quad (4.9)$$

4.2. Properties of the basis 2

The construction of the basis 2 basic elements $\varphi_h^{(n)}$ is entirely dictated by the requirement that

$$e_j E_h(e_i, e_{i+1}, \dots, e_{i+h-1}) = 0 \quad \text{for } j = i, i+1, \dots, i+h-1 \quad (4.10)$$

These relations were indeed used in [11] as a defining property for the E_h 's.

The multiplication rule (4.8) ensures that whenever the multiplication by e_i acts on a slope of the corresponding walk diagram (i.e., when $\ell_{i+1} + \ell_{i-1} - 2\ell_i = 0$), the result vanishes. In other words,

$$e_i (a)_2 = 0 \quad \text{whenever } \ell_{i+1}^a + \ell_{i-1}^a - 2\ell_i^a = 0 \quad (4.11)$$

These rules are also responsible for the following main property of the basis 2 elements. To write it explicitly, we need a more detailed notation for the walk diagrams of middle height $\ell_n = h$, and the associated basis 2 elements. Such a diagram will be denoted $a = lr$, where l (resp. r) denotes the left (resp. right) half of the walk diagram, with $i = 0, 1, \dots, n$ (resp. $i = 2n, 2n - 1, \dots, n$), namely

$$l = \{(i, \ell_i)\} \quad r = \{(i, \ell_{2n-i})\} \quad (4.12)$$

for $i = 0, 1, 2, \dots, n$. Note that l is read from left to right on a and that r is read from right to left. Moreover,

$$(lr)^t = (rl) \quad (4.13)$$

Both half-walks start at height $\ell_0 = \ell_{2n} = 0$ and end at height $\ell_n = h$. To avoid confusion, we will denote the corresponding basis 1,2 elements by $(lr)_1, (lr)_2$ respectively.

The main property satisfied by the basis 2 elements reads, for any elements $(a)_2, (a')_2$ of the basis 2, $a = lr$ and $a' = l'r'$:

$$(lr)_2 (l'r')_2 = \delta_{r,l'} (lr')_2 \quad (4.14)$$

On this relation, we learn that all the self-transposed elements (i.e., with $(a)_2 = (a)_2^t$), namely those attached to symmetric walk diagrams (i.e., with $l = r$), are projectors. In particular, we recover the fact that $\varphi_h^{(n)} = (\mathcal{W}_h^{(n)})_2$ is a projector. As we shall see in the next section, the relation (4.14) implies also that the basis 2 is orthogonal with respect to the scalar product (3.12).

5. The meander determinant

5.1. The Gram matrix for basis 2

Thanks to the main property (4.14), the Gram matrix $\Gamma_n(q)$ of the basis 2 elements takes a particularly simple diagonal form. Its $c_n \times c_n$ entries read

$$[\Gamma_n(q)]_{a,a'} = ((a)_2, (a')_2) \quad (5.1)$$

Let us compute the scalar product

$$\begin{aligned} ((a)_2, (a')_2) &= \text{Tr}((lr)_2 (l'r')_2^t) = \text{Tr}((lr)_2 (r'l')_2) = \delta_{r,l'} \text{Tr}((ll')_2) \\ &= \text{Tr}((l'r')_2^t (lr)_2) = \text{Tr}((r'l')_2 (lr)_2) = \delta_{l,l'} \text{Tr}((rr')_2) \\ &= \delta_{a,a'} \text{Tr}((a)_2 (a)_2^t) \end{aligned} \quad (5.2)$$

by direct application of (4.14) and use of the cyclicity of the trace and of (4.13). Hence the matrix $\Gamma_n(q)$ is diagonal. Moreover

$$\mathrm{Tr}((a)_2(a)_2^t) = \mathrm{Tr}((rr)_2) = \mathrm{Tr}((ll)_2) \quad (5.3)$$

for any r, l , does not depend on the half-path r of final height $\ell_n = h$. It may be evaluated on the left half-path ρ_h corresponding to the walk diagram $\mathcal{W}_h^{(n)}$ of (3.7). A simple calculation shows that

$$\mathrm{Tr}((\rho_h \rho_h)_2) = \mathrm{Tr}(\varphi_h^{(n)}) = U_h(q) \quad (5.4)$$

where U denotes the Chebishev polynomial (4.1). Hence $\Gamma_n(q)$ is simply the diagonal matrix with the c_n entries

$$[\Gamma_n(q)]_{a,a} = U_{\ell_n^a}(q) \quad (5.5)$$

where ℓ_n^a denotes the middle height of the walk diagram a .

We conclude that the basis 2 is orthogonal with respect to the scalar product $(,)$.

5.2. Main result

This remarkable property of the basis 2 will enable us to compute the determinant $D_n(q)$ of the Gram matrix $\mathcal{G}_n(q)$ for the basis 1, also referred to as *meander determinant*. The result reads³

$$\boxed{\begin{aligned} D_n(q) &= \det(\mathcal{G}_n(q)) = \prod_{i=1}^n U_i(q)^{a_{n,i}} \\ a_{n,i} &= \binom{2n}{n-i} - 2\binom{2n}{n-i-1} + \binom{2n}{n-i-2} \end{aligned}} \quad (5.6)$$

where $U_i(q)$ are the Chebishev polynomials (4.1), and we use the convention that $\binom{j}{k} = 0$ if $j < 0$. For instance, the determinant of the matrix $\mathcal{G}_3(q)$ (3.16) reads

$$D_3(q) = U_1(q)^4 U_2(q)^4 U_3(q) = q^5 (q^2 - 1)^4 (q^2 - 2) \quad (5.7)$$

³ Ref. [4] presents a recursive algorithm for computing this determinant, which relies on direct manipulations of lines and columns of \mathcal{G}_n . The main result of [4] is the identification of the zeros of $D_n(q)$. Here we also give their multiplicities.

As a nontrivial check, let us first compute the degree of $D_n(q)$ as a polynomial in q

$$\deg(D_n(q)) = \sum_{i=1}^n i a_{n,i} = \binom{2n}{n-1} = n c_n \quad (5.8)$$

which is in agreement with the definition of the Gram matrix \mathcal{G}_n : the term with highest degree in the expansion of the determinant comes from the product of the diagonal elements of \mathcal{G}_n , namely

$$\prod_{a \in W_n} q^{c(a,a)} = \prod_{a \in W_n} q^n = q^{n c_n} \quad (5.9)$$

as all the meanders with identical top and bottom arch configurations have the maximal number n of connected components.

5.3. The zeros of the meander determinant and their multiplicities

Before going into the proof of the formula (5.6), let us describe a few consequences of this result. The zeros $z_{k,l}$ of the polynomial $D_n(q)$ are those of the $U_k(q)$, for $k = 1, \dots, n$, namely, using (4.2)

$$z_{k,l} = 2 \cos \pi \frac{l}{k+1} \quad 1 \leq l \leq k \leq n$$

(5.10)

hence we may rewrite

$$D_n(q) = \prod_{1 \leq l \leq k \leq n} \left(q - 2 \cos \pi \frac{l}{k+1} \right)^{a_{n,k}} \quad (5.11)$$

This yields the multiplicity $d_n(z_{k,l})$ of each zero $z_{k,l}$, when $(k+1)$ and l are coprime integers, and $l \leq (k+1)/2$ ($z_{k,k+1-l} = -z_{k,l}$ has the same multiplicity as $z_{k,l}$)

$$d_n(z_{k,l}) = \sum_{m=1}^{[(n+1)/(k+1)]} a_{n,m(k+1)-1} \quad (5.12)$$

For $k = 1, l = 1$ this yields the multiplicity of the zero $q = 0$

$$d_n(0) = \sum_{m=1}^{[(n+1)/2]} a_{n,2m-1} = \binom{2n}{n} - \binom{2n}{n-1} = c_n \quad (5.13)$$

The fact that the zero $q = 0$ of $d_n(q)$ has multiplicity c_n enables us to write, in the limit $q \rightarrow 0$

$$D_n(q) \sim q^{c_n} D'_n(0) \quad (5.14)$$

where $D'_n(0) \neq 0$ is the determinant of the matrix $\mathcal{G}'_n(0)$ with entries

$$[\mathcal{G}'_n(0)]_{a,b} = \begin{cases} 1 & \text{if } c(a,b) = 1 \\ 0 & \text{otherwise} \end{cases} \quad (5.15)$$

hence $\mathcal{G}'_n(0)$ is the one-connected component piece of the Gram matrix $\mathcal{G}_n(q)$. For instance,

$$\mathcal{G}'_3(0) = \begin{pmatrix} 0 & 0 & 0 & 1 & 0 \\ 0 & 0 & 1 & 0 & 1 \\ 0 & 1 & 0 & 0 & 1 \\ 1 & 0 & 0 & 0 & 0 \\ 0 & 1 & 1 & 0 & 0 \end{pmatrix} \quad D'_3(0) = -2 \quad (5.16)$$

Noting that in the limit $q \rightarrow 0$

$$U_{2i}(q) \rightarrow (-1)^i \quad U_{2i-1}(q)/q \rightarrow i(-1)^{i-1} \quad (5.17)$$

the limit $q \rightarrow 0$ of (5.6) yields

$$\begin{aligned} D'_n(0) &= \prod_{i=1}^{[n/2]} (-1)^{ia_{n,2i}} \prod_{i=1}^{[(n+1)/2]} [i(-1)^{i-1}]^{a_{n,2i-1}} \\ &= (-1)^{(n-1)c_n/2} \prod_{i=1}^{[(n+1)/2]} i^{a_{n,2i-1}} \end{aligned} \quad (5.18)$$

Therefore

$$\begin{aligned} \log |D'_n(0)| &= \sum_{i=1}^{[(n+1)/2]} \left[\binom{2n}{n-2i} - 2 \binom{2n}{n-2i-1} + \binom{2n}{n-2i-2} \right] \log i \\ &\sim \frac{4^n}{2n} \sim \frac{\sqrt{\pi n}}{2} c_n \end{aligned} \quad (5.19)$$

where the asymptotic estimate results from a saddle-point approximation to the sum. If most of the eigenvalues λ of the matrix $\mathcal{G}'_n(0)$ were of the same order

$$\lambda \sim (D'_n(0))^{1/c_n} \sim e^{\sqrt{\pi n}/2} \quad (5.20)$$

we would have a meander polynomial, expressed through (3.19), of the order

$$m_n(q^2) \sim q^2 \sum_{\lambda} (\lambda)^2 \sim q^2 e^{\sqrt{\pi n}} c_n \quad (5.21)$$

which clearly is incompatible with the numerical estimate

$$m_n(q^2)/q^2 \underset{q \rightarrow 0}{\sim} M_n \sim \frac{\bar{R}^{2n}}{n^{7/2}} \quad (5.22)$$

We conclude that the eigenvalues λ of $\mathcal{G}'_n(0)$ do not have a localized distribution when n becomes large. This is also the case when $q = 1$. Indeed, the matrix $\mathcal{G}_n(q = 1)$ is simply the $c_n \times c_n$ matrix with all entries equal to 1. It has the eigenvalue 0, with degeneracy $(c_n - 1)$, and the nondegenerate eigenvalue c_n . This permits to recover the sum rules (2.6)-(2.7) easily. In this case, the distribution of eigenvalues of the Gram matrix is certainly not localized when $n \rightarrow \infty$, as the only eigenvalue which matters diverges while all the other eigenvalues remain 0.

More generally, the expression (5.12) can be resummed to yield

$$\boxed{c_n - d_n(z_{k,l}) = \frac{1}{2(k+1)} \sum_{m=1}^k \left(2 \sin \frac{\pi m}{k+1}\right)^2 \left(2 \cos \frac{\pi m}{k+1}\right)^{2n}} \quad (5.23)$$

(see Appendix A for a detailed proof). The result is independent of l , under the requirement that l and k be coprime. For instance, for $k = 2, 3, 4, 5$ and n , we find

$$\begin{aligned} d_n(\pm 1) &= c_n - 1 \\ d_n(\pm \sqrt{2}) &= c_n - 2^{n-1} \\ d_n\left(\pm \frac{\sqrt{5} \pm 1}{2}\right) &= c_n - \frac{1}{\sqrt{5}} \left[\left(\frac{\sqrt{5} + 1}{2}\right)^{2n-1} + \left(\frac{\sqrt{5} - 1}{2}\right)^{2n-1} \right] \\ d_n(\pm \sqrt{3}) &= c_n - \frac{3^{n-1} + 1}{2} \\ d_n\left(2 \cos \frac{\pi l}{n+1}\right) &= 1 \quad \text{for } l \text{ and } (n+1) \text{ coprime} \end{aligned} \quad (5.24)$$

The r.h.s. of (5.23) appears to be an integer in the following interpretation. Let \mathcal{A}_k be the $k \times k$ symmetric matrix, with entries

$$[\mathcal{A}_k]_{r,s} = \delta_{s,r+1} + \delta_{s,r-1} \quad (5.25)$$

for $r, s = 1, 2, \dots, k$. This matrix diagonalizes in the orthonormal basis $\{\mathbf{v}_r, r = 1, 2, \dots, k\}$, where

$$[\mathbf{v}_r]_s = \sqrt{\frac{2}{k+1}} \sin \frac{\pi r s}{k+1} \quad (5.26)$$

are the entries of the eigenvector \mathbf{v}_r of \mathcal{A}_k , for the eigenvalue $\beta_r^k = 2 \cos \pi r / (k + 1)$. Hence, the r.h.s. of (5.23) is nothing but

$$c_n - d_n(z_{k,l}) = \sum_{m=1}^k [\mathbf{v}_m]_1 (\beta_m^k)^{2n} [\mathbf{v}_m]_1 = [(\mathcal{A}_k)^{2n}]_{1,1} \quad (5.27)$$

This expression is clearly an integer, as a matrix element of the $(2n)$ -th power of an integral matrix. Moreover, this permits to interpret the number $c_n - d_n(z_{k,l})$ as counting the number of distinct closed walks of $(2n)$ steps on a *segment* of size k , which start and end up at a fixed end of the segment. Indeed, \mathcal{A}_k is the adjacency matrix of a chain of k vertices, labeled $1, 2, \dots, k$. The quantity $[(\mathcal{A}_k)^{2n}]_{1,1}$ counts the number of distinct paths of length $(2n)$ on the chain which start and end up at the vertex 1. In the language of walk diagrams, this is the number of walk diagrams $w \in W_n$ whose heights do not exceed $(k - 1)$. Denoting by

$$W_{n,j} = \{a \in W_n \mid \ell_i^a \leq j \text{ for } i = 0, 1, \dots, 2n\} \quad (5.28)$$

eq.(5.27) may be rephrased into

$$c_n - d_n(z_{k,l}) = \text{card}(W_{n,k-1}) \quad (5.29)$$

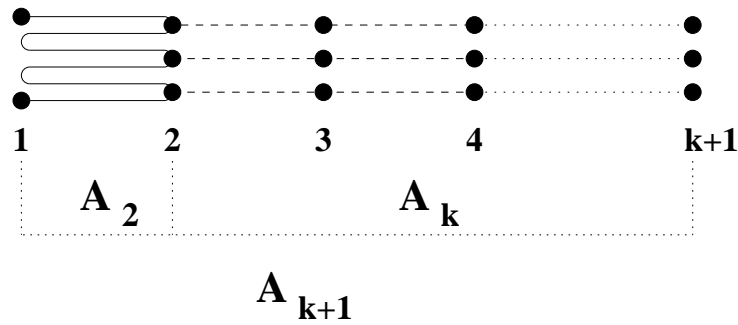


Fig. 11: Any walk on \mathcal{A}_{k+1} may be viewed as the prolongation of a walk on \mathcal{A}_2 , by one or several walks on \mathcal{A}_k , at each visit of the vertex 2. Here we have represented a walk on \mathcal{A}_2 , of length 6, corresponding to the term x^3 in $G_2(x)$. Each of its three visits of the vertex 2 may be arbitrarily prolonged by walks on \mathcal{A}_k (vertices 2, 3, ..., $k + 1$ on the figure), to generate all the walks on \mathcal{A}_{k+1} , resulting in the substitution $x^3 \rightarrow (xG_k(x))^3$ in the corresponding generating function.

This interpretation permits to write a very simple generating function for the multiplicities $d_n(z_{k,l})$. Indeed, for $k \geq 1$, let

$$G_k(x) = \sum_{n=0}^{\infty} x^n (c_n - d_n(z_{k,l})) \quad (5.30)$$

When $k = 1$, we set $G_1(x) = 1$, deciding by convention that $d_0(0) = 0$, whereas $c_0 = 1$. When $k = 2$, we are simply counting the only path of length $2n$, going back and forth between the origin and the other vertex of the chain. Each such come and go picks a factor of x , resulting in the generating function

$$G_2(x) = 1 + x + x^2 + \dots = \frac{1}{1-x} \quad (5.31)$$

in agreement with the first line of (5.24). To compute $G_{k+1}(x)$, knowing $G_k(x)$, we may view all the walks on \mathcal{A}_{k+1} , as an arbitrary insertion of walks on \mathcal{A}_k at each visit of the vertex 2 by arbitrary walks on \mathcal{A}_2 , as indicated in Fig.11. This leads to the following composition of generating functions

$$G_{k+1}(x) = G_2(xG_k(x)) = \frac{1}{1-xG_k(x)} = \frac{1}{1-\frac{x}{1-\frac{x}{\ddots_{1-x}}}} \quad (5.32)$$

where the fraction is iterated k times. Together with the initial condition $G_1(x) = 1$, eq.(5.32) completely determines $G_k(x)$ for all k . In fact, we find the following simple expression in terms of the Chebishev polynomials (4.2) and the function $\mu_k(q)$ (4.3)

$$\boxed{G_k(x) = \frac{U_1(1/\sqrt{x})U_{k-1}(1/\sqrt{x})}{U_k(1/\sqrt{x})} = \frac{1}{\sqrt{x}} \mu_k\left(\frac{1}{\sqrt{x}}\right)} \quad (5.33)$$

where we have identified the recursion relation (5.32) with (4.4) upon a mutliplicative redefinition of μ (which also gives $G_1(x) = 1$) and the change of variable $q = 1/\sqrt{x}$. Note that the expression (5.33) is valid as a series expansion in powers of x for small enough x . This in turn translates into the following expression for the generating function for the multiplicities $d_n(z_{k,l})$

$$\boxed{F_k(x) = \sum_{n=0}^{\infty} x^n d_n(z_{k,l}) = C(x) - \frac{1}{\sqrt{x}} \mu_k\left(\frac{1}{\sqrt{x}}\right)} \quad (5.34)$$

where

$$C(x) = \sum_{n=0}^{\infty} x^n c_n = \frac{1 - \sqrt{1 - 4x}}{2x} \quad (5.35)$$

denotes the generating function of the Catalan numbers (2.5). The results (5.24) may be easily recovered from the expression (5.34), for $k = 2, 3, 4, 5$. Note that the series $F_k(x)$ has the valuation k , namely $F_k(x) \sim x^k$ when $x \rightarrow 0$, as $d_n(z_{k,l}) = 0$, for $n \leq k - 1$, and $d_k(z_{k,l}) = 1$ for $n = k$. Hence $\lim_{k \rightarrow \infty} F_k(x) = 0$ uniformly for small enough x , which means that $G_k(x)$ converges to $C(x)$ uniformly when $k \rightarrow \infty$: this establishes a link between the Chebishev polynomials and the Catalan numbers.

Remarkably, the formula (5.23), together with the above interpretation (5.27), suggest a relation between the multiplicities $d_n(z_{k,l})$ of the zeros of $D_n(q)$ and the rank $r_n(z_{k,l}) = \dim \text{Im } \mathcal{G}_n(z_{k,l})$ of the matrix $\mathcal{G}_n(q = z_{k,l})$, namely that

$$d_n(z_{k,l}) + r_n(z_{k,l}) = c_n = \dim(TL_n(q)) \quad (5.36)$$

or in other words that

$$\dim \text{Ker } \mathcal{G}_n(z_{k,l}) = d_n(z_{k,l}) \quad (5.37)$$

Indeed, the matrix $\mathcal{G}_n(0) = 0$ has rank 0, whereas $\mathcal{G}_n(1)$ has rank 1 as all its lines are identical and non-vanishing. We also checked that $\mathcal{G}_n(\sqrt{2})$ has rank 2^{n-1} for $n = 1, 2, 3, 4, 5$. Eqs. (5.27) and (5.36) would imply in general that the rank of the matrix $\mathcal{G}_n(z_{k,l})$ (for l and $(k + 1)$ coprime) is equal to the number of walk diagrams $w \in W_n$, whose heights are *less or equal to* $(k - 1)$, i.e., $\text{card}(W_{n,k-1})$. Assuming that (5.36) is true, it is tempting to conjecture that the lines of $\mathcal{G}_n(z_{k,l})$ corresponding to the diagrams $a \in W_{n,k-1}$ form a collection of $r_n(z_{k,l})$ independent vectors, of which any other line of $\mathcal{G}_n(z_{k,l})$ is a linear combination. In particular, the last line of $\mathcal{G}_n(z_{k,l})$, corresponding to the diagram $\mathcal{W}_n^{(n)}$, should be a linear combination (with coefficients λ_a^n) of the lines of $\mathcal{G}_n(z_{k,l})$ pertaining to the diagrams $a \in W_{n,k-1}$. This would result in a relation

$$(z_{k,l})^{c(\mathcal{W}_n^{(n)}, b)} = \sum_{a \in W_{n,k-1}} \lambda_a^n (z_{k,l})^{c(a,b)} \quad (5.38)$$

Summing this over $b \in W_n$ would give a new expression for the semi-meander polynomial at $q = z_{k,l}$, as a linear combination of the polynomials corresponding to the diagrams $a \in W_{n,k-1}$, namely

$$\bar{m}_n(z_{k,l}) = \sum_{a \in W_{n,k-1}} \lambda_a^n \bar{m}(a, z_{k,l}) \quad (5.39)$$

where

$$\bar{m}(a, q) = \sum_{b \in W_n} q^{c(a,b)} \quad (5.40)$$

This conjecture is illustrated in appendix B, for $q = \sqrt{2}$ ($k = 3, l = 1$).

5.4. Proof of the main result

We now turn to the proof of the formula (5.6) expressing the meander determinant. Since the Gram matrix (5.5) is trivial in basis 2, we simply have to compute the determinant of the matrix of the change of basis 1 to 2. This is done by first showing that this matrix can be put in an upper triangular form and computing the product of its diagonal entries. The result, combined with (5.5), is identified with the desired expression (5.6) through a subtle mapping of walk diagrams.

Preliminaries. Let $\mathcal{P}_n(q)$ denote the matrix of the change of basis 1 to 2, made of the column vectors of the basis 2 expressed in the basis 1. It satisfies

$$(b)_2 = \sum_{a \in W_n} [\mathcal{P}_n(q)]_{a,b} (a)_1 \quad (5.41)$$

Let us show that the walk diagrams indexing the vectors of both bases can be ordered in such a way that the matrix $\mathcal{P}_n(q)$ is upper triangular.

The basic element $\varphi_h^{(h)}$ is, according to (4.5)(4.6), a linear combination of the basis 1 elements of $TL_h(q)$ of the form

$$\varphi_h^{(h)} = \sum_{a \in W_h} \lambda_a (a)_1(e_1, \dots, e_{h-1}) \quad (5.42)$$

where the sum extends over all the diagrams of $2h$ steps, which are all *included* in the walk $\mathcal{W}_h^{(h)}$. By inclusion of diagrams $a, b \in W_n$, we mean

$$a \subset b \quad \text{iff} \quad l_i^a \leq l_i^b \quad \forall i = 0, 1, \dots, 2n \quad (5.43)$$

Similarly, the basic element $\varphi_h^{(n)}$ is equal to the linear combination

$$\varphi_h^{(n)} = \sum_{a \in W_h} \lambda_a (\mu_1)^p e_1 e_3 \cdots e_{2p-1} (a)_1(e_{2p+1}, \dots, e_{n-1}) \quad (5.44)$$

which corresponds only to walk diagrams of $2n$ steps, included in $\mathcal{W}_h^{(n)}$.

The other basis 2 elements with middle height h are obtained by repeated box additions on $\mathcal{W}_h^{(n)}$ (see Fig.8), with the corresponding multiplication rule (4.8). It is then easy to prove recursively that any basis 2 element with middle height h , of the form $(b)_2$, is a linear combination of basis 1 elements whose walk diagrams are included in b , namely

$$[\mathcal{P}_n(q)]_{a,b} \neq 0 \Rightarrow a \subset b \quad (5.45)$$

Arranging the walk diagrams by growing middle height, we see that $\varphi_h^{(n)}$ is expressed only in terms of lower basis 1 elements: this gives only upper triangular entries in the matrix $\mathcal{P}_n(q)$. More generally, the walk diagrams can be ordered for each fixed middle height h in such a way that all the diagrams included in a come before a : it is sufficient, for instance, to order the diagrams by growing number of boxes added to $\mathcal{W}_h^{(n)}$. With such an ordering of the bases 1 and 2, the matrix $\mathcal{P}_n(q)$ is upper triangular (with nonzero terms on the diagonal). For instance, with the ordering of (3.9) and (4.9), we get the upper triangular matrix

$$\mathcal{P}_3(q) = \begin{pmatrix} \mu_1 & -\mu_1\sqrt{\mu_1\mu_2} & -\mu_1\sqrt{\mu_1\mu_2} & \mu_1^2\mu_2 & -\mu_2 \\ 0 & \sqrt{\mu_1\mu_2} & 0 & -\mu_1\mu_2 & \mu_1\mu_2 \\ 0 & 0 & \sqrt{\mu_1\mu_2} & -\mu_1\mu_2 & \mu_1\mu_2 \\ 0 & 0 & 0 & \mu_2 & -\mu_2 \\ 0 & 0 & 0 & 0 & 1 \end{pmatrix} \quad (5.46)$$

Let us decompose the upper triangular matrix $\mathcal{P}_n(q)$ into the product

$$\mathcal{P}_n(q) = \mathcal{Q}_n(q)\mathcal{N}_n(q) \quad (5.47)$$

where $\mathcal{N}_n(q)$ is a diagonal normalization matrix and $\mathcal{Q}_n(q)$ an upper triangular matrix, with diagonal entries equal to 1. This separates the redefinition of basis elements (which does not affect the Gram determinant), through the matrix $\mathcal{Q}_n(q)$, from the change of overall normalization of the basis vectors (which affects the Gram determinant), through $\mathcal{N}_n(q)$. For $n = 3$, these matrices read

$$\begin{aligned} \mathcal{N}_3(q) &= \begin{pmatrix} \mu_1 & 0 & 0 & 0 & 0 \\ 0 & \sqrt{\mu_1\mu_2} & 0 & 0 & 0 \\ 0 & 0 & \sqrt{\mu_1\mu_2} & 0 & 0 \\ 0 & 0 & 0 & \mu_2 & 0 \\ 0 & 0 & 0 & 0 & 1 \end{pmatrix} \\ \mathcal{Q}_3(q) &= \begin{pmatrix} 1 & -\mu_1 & -\mu_1 & \mu_1^2 & -\mu_2 \\ 0 & 1 & 0 & -\mu_1 & \mu_1\mu_2 \\ 0 & 0 & 1 & -\mu_1 & \mu_1\mu_2 \\ 0 & 0 & 0 & 1 & -\mu_2 \\ 0 & 0 & 0 & 0 & 1 \end{pmatrix} \end{aligned} \quad (5.48)$$

The change of basis 1 \rightarrow 2 translates into the matrix identity

$$\begin{aligned} \Gamma_n(q) &= \mathcal{P}_n(q)^t \mathcal{G}_n(q) \mathcal{P}_n(q) \\ &= \mathcal{N}_n(q) \mathcal{Q}_n(q)^t \mathcal{G}_n(q) \mathcal{Q}_n(q) \mathcal{N}_n(q) \end{aligned} \quad (5.49)$$

hence, as $\det \mathcal{Q}_n(q) = 1$, we have the relation between determinants

$$\det[\Gamma_n(q)] = \det[\mathcal{N}_n(q)]^2 D_n(q) \quad (5.50)$$

with, according to (5.5),

$$\begin{aligned} \det[\Gamma_n(q)] &= \prod_{a \in W_n} U_n^a(q) \\ &= \prod_{p=0}^{\lfloor n/2 \rfloor} [U_{n-2p}(q)]^{(b_{n,n-2p})^2} \end{aligned} \quad (5.51)$$

where $b_{n,n-2p}$ is the number of half-walks of n steps with final height $h = n - 2p$, and constrained by $\ell_i \geq 0$, for $i = 0, 1, \dots, n$. The walk diagrams of middle height $h = n - 2p$ are simply obtained by taking arbitrary left and right halves of final height h , hence their number is $(b_{n,n-2p})^2$.

The number $b_{n,n-2p}$ is obtained by subtracting from $\binom{n}{p}$, the total number of unconstrained walks with $\ell_0 = 0$ and $\ell_n = h$, the number of those which touch the line $\ell = -1$, namely $\binom{n}{p-1}$. Indeed, by a simple reflection (mirror image) with respect to the line $\ell = -1$ of the portion of walk between its origin and the first encounter with $\ell = -1$, we get a one-to-one mapping with unconstrained walks such that $\ell'_0 = -2$ and $\ell'_n = h$; the number of such walks is $\binom{n}{p-1}$. Hence we have

$$b_{n,n-2p} = \binom{n}{p} - \binom{n}{p-1} \quad (5.52)$$

The normalization $\mathcal{N}_n(q)$. To get $D_n(q)$ from (5.50), we are left with the calculation of $\det[\mathcal{N}_n(q)]$. The diagonal entries of $\mathcal{N}_n(q)$ are computed as follows. For the diagram $\mathcal{W}_h^{(n)}$, the entry reduces to the global normalization of the vector $\varphi_h^{(n)}$, namely

$$[\mathcal{N}_n(q)]_{\mathcal{W}_h^{(n)}, \mathcal{W}_h^{(n)}} = (\mu_1)^p \quad (5.53)$$

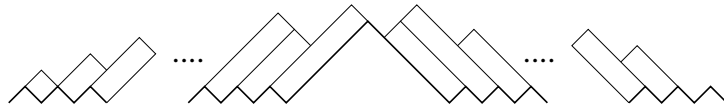


Fig. 12: The left and right strip decomposition of a diagram of middle height h . the strip lengths are given by the numbers ℓ_i^a corresponding to the maxima i of a , $i \neq n$.

The entries corresponding to other walk diagrams of middle height h are simply the product of this factor by the product over all the box additions to $\mathcal{W}_h^{(n)}$ of the normalization factors $\sqrt{\mu_{\ell_i+2}/\mu_{\ell_i+1}}$ which enter the multiplication rule (4.8). In other words

$$[\mathcal{N}_n(q)]_{a,a} = (\mu_1)^p \prod_{\text{box additions } i} \sqrt{\frac{\mu_{\ell_i+2}}{\mu_{\ell_i+1}}} \quad (5.54)$$

To make this formula more explicit, let us arrange the box additions needed to generate a from $\mathcal{W}_h^{(n)}$ into p left and p right *strips* of consecutive boxes, oriented respectively to the right and left as indicated on Fig.12. This is called the *strip decomposition* of a . Each strip ends at a local maximum of a , namely at the vertical of a point i with $\ell_{i+1} = \ell_{i-1} = \ell_i - 1$. The *length* of the corresponding strip is defined to be ℓ_i (there are actually $\ell_i - 1$ boxes in a strip of length ℓ_i ; a strip with no box has indeed $\ell_i = 1$). The expression (5.54) becomes

$$[\mathcal{N}_n(q)]_{a,a} = (\mu_1)^p \prod_{\text{strips}} \sqrt{\frac{\mu_\ell}{\mu_1}} \quad (5.55)$$

where ℓ denotes the length of each strip. As there are p left and p right strips, the factors μ_1 cancel out, and we are left with

$$\boxed{[\mathcal{N}_n(q)]_{a,a} = \prod_{\text{strips}} \sqrt{\mu_\ell}} \quad (5.56)$$

Hence the prefactor in (5.50) reads

$$\det[\mathcal{N}_n(q)]^2 = \prod_{a \in W_n} \prod_{\text{strips of } a} \mu_\ell = \prod_{i=1}^n (\mu_i)^{s_{n,i}} \quad (5.57)$$

where $s_{n,i}$ denotes the *total* number of strips of length i in the strip decompositions of *all* the walk diagrams of W_n , or equivalently the number of distinct diagrams of W_n , with a marked top of strip of length i .

Using the relation $U_i = 1/(\mu_1 \mu_2 \cdots \mu_i)$, we can rewrite $\det[\Gamma_n(q)]$ (5.51) as

$$\det[\Gamma_n(q)] = \prod_{i=1}^n (\mu_i)^{-h_{n,i}} \quad (5.58)$$

where

$$h_{n,i} = \sum_{\substack{i \leq k \leq n \\ k = n \pmod{2}}} (b_{n,k})^2 \quad (5.59)$$

is the total number of walk diagrams of $2n$ steps with middle height larger or equal to i . We finally get

$$D_n(q) = \prod_{i=1}^n (\mu_i)^{-s_{n,i} - h_{n,i}} \quad (5.60)$$

Let us now prove that

$$s_{n,i} + h_{n,i} = b_{2n,2i} \quad (5.61)$$

namely that the total number of walk diagrams of $2n$ steps with final height $2i$ is equal to the *total* number of strips of length i plus the total number of walk diagrams in W_n with middle height larger or equal to i . To prove this, we establish a map between the walk diagrams of length $2n$ and final height $2i$ and (i) the walk diagrams of W_n with a *marked* top of strip of height i or (ii) the diagrams of W_n with middle height $\ell_n \geq i$.

The mapping of walk diagrams. Starting from a given walk diagram w of $2n$ steps from $\ell_0 = 0$ to $\ell_{2n} = 2i$, with $\ell_k \geq 0$, for all k , the construction proceeds in three steps.

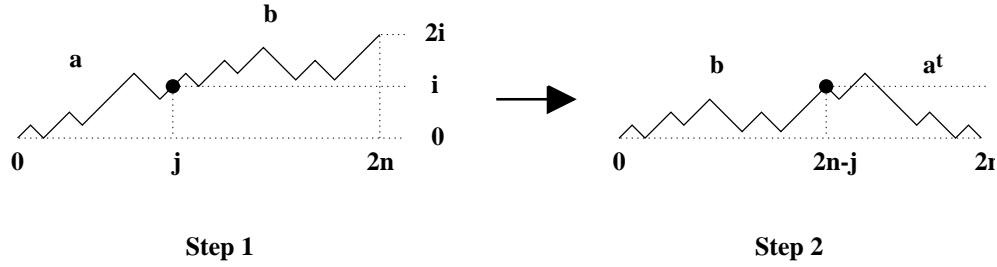


Fig. 13: Reflection-translation of the diagram w . The rightmost crossing point between w and the line of constant height $\ell = i$, at an ascending slope, is marked by a black dot. The dot separates w into a left piece a and a right piece b . The reflection-translation consists in a reflection of $a \rightarrow a^t$, followed by a translation of a^t in order to glue the two walks b and a^t . The gluing point is indicated by a black dot on the second diagram.

Step 1. Let j be the largest point $0 \leq j \leq 2n$ of height $\ell_j = i$ on w , and such that $\ell_{j-1} = \ell_j - 1 = \ell_{j+1} - 2$. As shown on Fig.13, this separates the walk diagram w into a left piece a , with j steps and final height i (namely $\ell_0^a = 0$, $\ell_j^a = i$ and $\ell_k^a \geq 0$ for all k), and a right piece b , with $(2n - j)$ steps, initial height i and final height $2i$. Note that the heights of b remain above the $\ell = i$ line, by definition of j , hence b can be considered as a walk diagram of $(2n - j)$ steps, with extremal heights $\ell_0^b = 0$, $\ell_{2n-j}^b = i$, and subject to the constraint $\ell_k^b \geq 0$, for all k .

Step 2. Let us perform the following reflection-translation on w , shown in Fig.13: reflect the a diagram ($a \rightarrow a^t$) and translate it so that its height i (left) end is glued to the height

i (right) end of b . Note that the resulting diagram w' is an element of W_n , as all its heights lie above the $\ell = 0$ line. Let us mark this gluing point on the resulting diagram $w' \in W_n$. This procedure maps the diagram w onto a marked diagram $w' \in W_n$.

Step 3. Only two possibilities may occur for the marked point, denoted by j in the following: it is either (1) a maximum of w' ($\ell_{j+1}^{w'} = \ell_{j-1}^{w'} = \ell_j^{w'} - 1$) or (2) a descending slope ($\ell_{j-1}^{w'} = \ell_j^{w'} + 1 = \ell_{j+1}^{w'} + 2$) of w' . Indeed, the point $(j+1)$ on w' has the height $\ell_{j+1}^{w'} = \ell_{j-1}^{w'} = \ell_j^{w'} - 1$.

Case 1. When j is a maximum of w' , the marked point $(j, \ell_j^{w'})$ corresponds to the top end of a strip in the strip decomposition of w' *unless* $j = n$. Therefore we have the two subcases

- (1)(a): If the marked point is a maximum of w' , *not in the middle* of w' (i.e. $j \neq n$), w' is a walk diagram of W_n , with a marked (right or left) top of strip at height i .
- (1)(b): If $j = n$, the diagram w' has a middle height i (hence enters the category of walk diagrams of W_n with middle height $\geq i$).

Case 2. When the walk has a descending slope at j , the marked point $(j, \ell_j^{w'})$ corresponds to the top end of a (left) strip in the strip decomposition of w' *only if* $j < n$. Therefore we have the three subcases

- (2)(a): If the marked point has $j < n$, w' is a diagram with marked top of (left) strip.

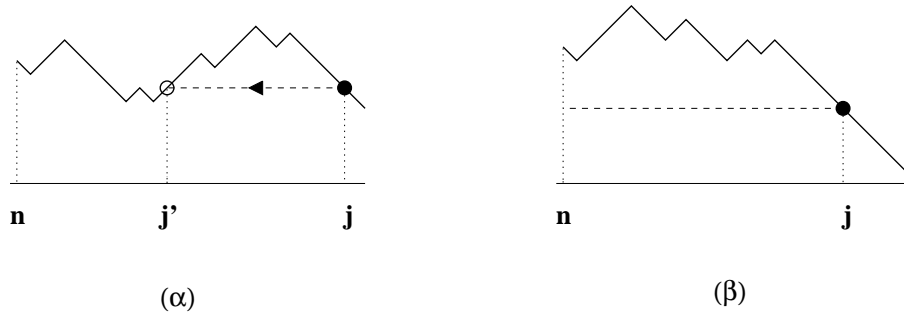


Fig. 14: The cases (2)(b)(α) and (β). We indicate the migration of the marked dot in the (α) case. In the (β) case, the diagram w has a middle height $\geq i$.

(2)(b): If $j > n$, we move the marked point to the left along a line of fixed height $\ell = \ell_j^{w'}$, until we reach a top of (right) strip (see Fig.14 (α)). Of course, one may reach the middle of the diagram before crossing any top of strip (see Fig.14(β)). This leads to two more possibilities

(2)(b)(α): The line of constant height $\ell = \ell_j^{w'}$ crosses an ascending slope of w' at j' ($\ell_{j'-1} = \ell_{j'} - 1 = \ell_{j'+1} - 2$), such that $n < j' < j$. Taking for j' the largest such

integer, we move the mark from j to j' , and end up with a diagram $w' \in W_n$ with a marked top of (right) strip.

(2)(b)(β): The line of constant height $\ell = \ell_j^{w'}$ does not cross any ascending slope of w' between n and j . The diagram $w' \in W_n$ has therefore a middle height $\geq i$. More precisely, we have either possibility

(2)(b)(β)(i): The middle height is $> i$.

(2)(b)(β)(ii): The middle height is $= i$.

(2)(c): The marked point is at $j = n$. The diagram $w' \in W_n$ has middle height i (hence enters the category of walk diagrams of W_n with middle height $\geq i$).

This exhausts all the diagrams with marked top of strips, according to whether

- the top is a maximum (1)(a)
- the top is on a left descending slope (2)(a)
- the top is on a right ascending slope (2)(b)(α)

and all the diagrams with middle height $\geq i$, according to whether

- the middle height is $> i$ (2)(b)(β)
- the middle height is $= i$ and is a maximum (1)(b)
- the middle height is $= i$ and is either an ascending slope or a minimum (2)(b)(β)(ii)
- the middle height is $= i$ and is a descending slope (2)(c)

The inverse map. Conversely, any walk diagram $w' \in W_n$ with a marked top of strip at height i can be mapped onto a walk w of $2n$ steps with $\ell_0^w = 0$, $\ell_{2n}^w = 2i$ and $\ell_k^w \geq 0$ for all k as follows. The marked top of strip $(j, \ell_j^{w'} = i)$ can be either (i) a maximum, (ii) a descending slope in the left half of w' ($j < n$) or (iii) an ascending slope in the right part of w' ($j > n$).

In the cases (i) and (ii), the marked point separates the walk w' into a left piece a (with j steps and $\ell_0^a = 0$, $\ell_j^a = i$, $\ell_k^a \geq 0$ for all k), and a right piece b (with $(2n - j)$ steps and $\ell_0^b = i$, $\ell_{2n-j}^b = 0$, $\ell_k^b \geq 0$ for all k). The diagram w is built by the inverse of the reflection-translation of Fig.13, namely by first reflecting $b \rightarrow b^t$, and then by translating it and gluing its right end to the left end of a . After this transformation, the gluing point, now at position $(2n - j)$ has an ascending slope on w at height i , and is the largest such point.

In the case (iii), the marked point is first moved to the right until the first crossing of the line of constant height $\ell = i$ with a descending slope is reached: such a point always exists, because the height $\ell_{2n}^{w'} = 0$ must be eventually reached. One then applies the above inverse reflection-translation to this new marked diagram. This produces again a diagram

$w \in W_n$ where the gluing point is the *largest* point on w with ascending slope and height i .

Finally, any walk diagram $w' \in W_n$ with middle height $\geq i$ may first be marked as follows. Mark the first crossing $j > n$ between the line of constant height $\ell = i$ and the walk w' at a descending slope. Then apply the above inverse reflection-translation.

In all cases, we have associated a walk diagram w to each diagram w' with either a marked end of strip of height i or a middle height $\geq i$. This concludes the proof of (5.61).

Conclusion. Eq. (5.60) implies that

$$D_n(q) = \prod_{i=1}^n (\mu_i)^{-b_{2n,2i}} \quad (5.62)$$

or, reexpressed in terms of U_i through $\mu_i = U_{i-1}/U_i$

$$D_n(q) = \prod_{i=1}^n [U_i(q)]^{(b_{2n,2i} - b_{2n,2i+2})} \quad (5.63)$$

which takes the desired form (5.6) with

$$\begin{aligned} a_{n,i} &= b_{2n,2i} - b_{2n,2i+2} \\ &= \binom{n-i}{2n} - 2 \binom{n-i-1}{2n} + \binom{n-i-2}{2n} \end{aligned} \quad (5.64)$$

6. Effective meander theory

In this section, we study various properties of the matrix $\mathcal{P}_n(q)$ and its inverse, in relation with the meander and semi-meander polynomials through (3.18). Indeed, rewriting (5.49) as

$$\mathcal{G}_n(q) = (\mathcal{P}_n(q)^t)^{-1} \Gamma_n(q) (\mathcal{P}_n(q))^{-1} \quad (6.1)$$

the relations (3.18) become

$$\begin{aligned} \bar{m}_n(q) &= \vec{v} \cdot \mathcal{G}_n(q) \vec{u} = (\mathcal{P}_n(q)^{-1} \vec{v}) \cdot \Gamma_n(q) \mathcal{P}_n(q)^{-1} \vec{u} \\ m_n(q) &= \vec{u} \cdot \mathcal{G}_n(q) \vec{u} = (\mathcal{P}_n(q)^{-1} \vec{u}) \cdot \Gamma_n(q) \mathcal{P}_n(q)^{-1} \vec{u} \end{aligned} \quad (6.2)$$

where the vectors \vec{u} and \vec{v} are defined in (3.17).

6.1. The matrix $\mathcal{P}_n(q)^{-1}$

By definition, the matrix $\mathcal{P}_n(q)^{-1}$ describes the change of basis $2 \rightarrow 1$, through

$$(a)_1 = \sum_{b \in W_n} [\mathcal{P}_n(q)^{-1}]_{b,a} (b)_2 \quad (6.3)$$

Multiplying both sides to the right by $(c)_2^t$, for some $c \in W_n$, and taking the trace, we get

$$\begin{aligned} \text{Tr}((a)_1(c)_2^t) &= \sum_{b \in W_n} [\mathcal{P}_n(q)^{-1}]_{b,a} \text{Tr}((b)_2(c)_2^t) \\ &= [\mathcal{P}_n(q)^{-1}]_{c,a} \text{Tr}((c)_2(c)_2^t) \end{aligned} \quad (6.4)$$

where we have used the orthogonality of the basis 2 elements. According to (5.3)(5.4), we have $\text{Tr}((c)_2(c)_2^t) = U_{\ell_n^c}(q)$, where ℓ_n^c is the middle height of the diagram c , and we finally get

$$\boxed{[\mathcal{P}_n(q)^{-1}]_{c,a} = \frac{\text{Tr}((a)_1(c)_2^t)}{\text{Tr}((c)_2(c)_2^t)} = \frac{1}{U_{\ell_n^c}(q)} \text{Tr}((a)_1(c)_2^t)} \quad (6.5)$$

6.2. Properties of $\mathcal{P}_n(q)^{-1}$

The formula (6.5) can be used to derive many properties of the matrix $\mathcal{P}_n(q)^{-1}$. Let us take $a = \mathcal{W}_n^{(n)}$ (i.e., $(a)_1 = f_n^{(n)} = 1$) in (6.5). This yields

$$[\mathcal{P}_n(q)^{-1}]_{c, \mathcal{W}_n^{(n)}} = \frac{\text{Tr}((c)_2^t)}{U_{\ell_n^c}(q)} \quad (6.6)$$

writing $c^t = lr$ as a juxtaposition of a left and right half-walk, and using (4.14), we compute

$$\text{Tr}(lr)_2 = \text{Tr}((lr)_2(rr)_2) = \text{Tr}((rr)_2(lr)_2) = \delta_{l,r} \text{Tr}(rr)_2 \quad (6.7)$$

Hence the trace of $(c^t)_2$ vanishes, unless c^t is a symmetric diagram, i.e. with $l = r$, in which case the trace takes the value (5.3)(5.4)

$$\text{Tr}(c^t)_2 = \text{Tr}(rr)_2 = \text{Tr}(\rho_{\ell_n^c} \rho_{\ell_n^c})_2 = U_{\ell_n^c}(q) \quad (6.8)$$

Putting (6.6) and (6.8) together, we simply find that

$$\boxed{[\mathcal{P}_n(q)^{-1}]_{c, \mathcal{W}_n^{(n)}} = \begin{cases} 1 & \text{if } c \text{ is symmetric} \\ 0 & \text{otherwise} \end{cases} \equiv \delta_{c, \text{symmetric}} \quad (6.9)}$$

With the definition (3.17) of the vector \vec{v} , this translates into

$$\mathcal{P}_n(q)^{-1} \vec{v} = \vec{s} \quad (6.10)$$

where the vector \vec{s} has the entries

$$\vec{s}_a = \delta_{a, \text{symmetric}} \quad (6.11)$$

Comparing with (6.2), this permits to rewrite the semi-meander polynomial as

$$\begin{aligned} \bar{m}_n(q) &= \vec{s} \cdot \Gamma_n(q) [\mathcal{P}_n(q)]^{-1} \vec{u} \\ &= \sum_{\substack{a, b \in W_n \\ a \text{ symmetric}}} [\mathcal{P}_n(q)^{-1}]_{a, b} U_{\ell_n^a}(q) \end{aligned} \quad (6.12)$$

whereas the meander polynomial reads

$$\begin{aligned} m_n(q) &= \mathcal{P}_n(q)^{-1} \vec{u} \cdot \Gamma_n(q) \mathcal{P}_n(q)^{-1} \vec{u} \\ &= \sum_{a \in W_n} \left(\sum_{b \in W_n} [\mathcal{P}_n(q)^{-1}]_{a, b} \right)^2 U_{\ell_n^a}(q) \end{aligned} \quad (6.13)$$

Another interesting particular case of formula (6.5) is obtained by taking $c = \mathcal{W}_{\epsilon_n}^{(n)}$, where ϵ_n is the smallest possible middle height in W_n , namely $\epsilon_n = (1 - (-1)^n)/2 = \delta_{n, \text{odd}}$. The heights of a read $\ell_{2i} = 0$ and $\ell_{2i-1} = 1$, for all i . This diagram is the smallest of all the diagrams in W_n , in the sense that it is included in all of them. It corresponds to the first entry of the bases 1 and 2, hence to the vector

$$\vec{w} = (1, 0, 0, \dots, 0) \quad (6.14)$$

The corresponding basis 1 and 2 elements read respectively $f_{\epsilon_n}^{(n)}$ and $\varphi_{\epsilon_n}^{(n)}$. By the definitions (4.5) and (3.6) taken at $h = \epsilon_n$ (in which case $E_{\epsilon_n} = E_0$ or E_1 , hence $E_{\epsilon_n} = 1$), we find the following relation between them

$$\varphi_{\epsilon_n}^{(n)} = (\mu_1)^{[n/2]} f_{\epsilon_n}^{(n)} \quad (6.15)$$

or equivalently

$$(\mathcal{W}_{\epsilon_n}^{(n)})_2 = (\mu_1)^{[n/2]} (\mathcal{W}_{\epsilon_n}^{(n)})_1 \quad (6.16)$$

where we have identified $\epsilon_n = n - 2p$, hence $p = [n/2]$. For the choice $c = \mathcal{W}_{\epsilon_n}^{(n)}$, (6.5) reads

$$\begin{aligned}
[\mathcal{P}_n(q)^{-1}]_{\mathcal{W}_{\epsilon_n}^{(n)}, a} &= \frac{\text{Tr}((a)_1(\mathcal{W}_{\epsilon_n}^{(n)})_2)}{U_{\ell_n^c}(q)} \\
&= (\mu_1)^{[n/2]} \frac{\text{Tr}((a)_1(\mathcal{W}_{\epsilon_n}^{(n)})_1)}{U_{\epsilon_n}(q)} \\
&= (\mu_1)^{[(n+1)/2]} [\mathcal{G}_n(q)]_{a, \mathcal{W}_{\epsilon_n}^{(n)}} \\
&= (\mu_1)^{[(n+1)/2] - c(a, \mathcal{W}_{\epsilon_n}^{(n)})}
\end{aligned} \tag{6.17}$$

In the second line, we have used the relation (6.16), whereas in the third line, we have used the fact that $U_{\epsilon_n}(q) = q^{\epsilon_n} = (\mu_1)^{-\epsilon_n}$ and that $\epsilon_n + [n/2] = [(n+1)/2]$. The last expression uses the definition of the Gram matrix (3.15): the quantity $c(a, \mathcal{W}_{\epsilon_n}^{(n)})$ is, in the arch configuration picture, the number of connected components of the meander obtained by superimposing the upper configuration a and the lower configuration $b \equiv \mathcal{W}_{\epsilon_n}^{(n)}$, made of a sequence of n consecutive single arches, linking the bridges $(2i-1)$ and $(2i)$, for $i = 1, 2, \dots, n$. The (meander) polynomial corresponding to the closings of $\mathcal{W}_{\epsilon_n}^{(n)}$ was computed in [6] and reads⁴

$$i_n(q) = \vec{w} \cdot \mathcal{G}_n(q) \vec{u} = \sum_{a \in W_n} q^{c(a, \mathcal{W}_{\epsilon_n}^{(n)})} = \sum_{k=1}^n \frac{1}{n} \binom{k}{n} \binom{k-1}{n} q^k \tag{6.18}$$

with the vectors \vec{u} and \vec{w} defined respectively in (3.17) and (6.14). Note that the polynomial $i_n(q)$ is reciprocal, i.e. $q^n i_n(1/q) = i_n(q)$. Hence, from (6.17), we get a sum rule for the first line of the matrix $\mathcal{P}_n(q)^{-1}$

$$\begin{aligned}
\sum_{a \in W_n} [\mathcal{P}_n(q)^{-1}]_{\mathcal{W}_{\epsilon_n}^{(n)}, a} &= (\mu_1)^{[(n+1)/2]} i_n\left(\frac{1}{\mu_1}\right) \\
&= i_n(\mu_1) / (\mu_1)^{[n/2]}
\end{aligned} \tag{6.19}$$

by using the reciprocity of $i_n(q)$.

⁴ In ref.[6], it has been shown that the number of closings of $\mathcal{W}_{\epsilon_n}^{(n)}$ with k connected components is identical to that of arch configurations of order n with k interior arches (i.e., arches linking two neighboring bridges i and $(i+1)$). In turn, this is nothing but the number of walk diagrams in W_n with exactly k maxima (the notion of interior arch in an arch configuration is equivalent to that of a maximum in the corresponding walk diagram). This number is $\binom{k}{n} \binom{k-1}{n} / n$.

6.3. Recursion relation for the matrix $\mathcal{Q}_n(q)^{-1}$

The matrix $\mathcal{Q}_n(q)$ is constructed in a similar way as $\mathcal{P}_n(q)$, as the matrix of a redefinition of basis 1, except that all the normalization factors are dropped, namely the prefactor $(\mu_1)^p$ in the definition (4.5) of $\varphi_h^{(n)}$ is dropped, as well as the prefactor $\sqrt{\mu_{\ell_i+2}/\mu_{\ell_i+1}}$ in the multiplication rule (4.8). This results in a diagonal of 1's for $\mathcal{Q}_n(q)$. $\mathcal{Q}_n(q)$ is the matrix of change of basis 1 to the unnormalized basis 2 (denoted by basis 2'), with elements $(a)_{2'} = (a)_2/\mathcal{N}_{a,a}$.

Let us now derive recursion relations for constructing the inverse matrix $\mathcal{Q}_n(q)^{-1}$. This matrix applies the unnormalized basis 2' into the basis 1, according to the identity

$$(b)_1 = \sum_{a \in W_n} [\mathcal{Q}_n(q)^{-1}]_{a,b} (a)_{2'} \quad (6.20)$$

Recall that the basis 1 elements are constructed by box additions (Fig.8) on the basic elements $f_h^{(n)}$, each box addition corresponding to the multiplication by some e_i .

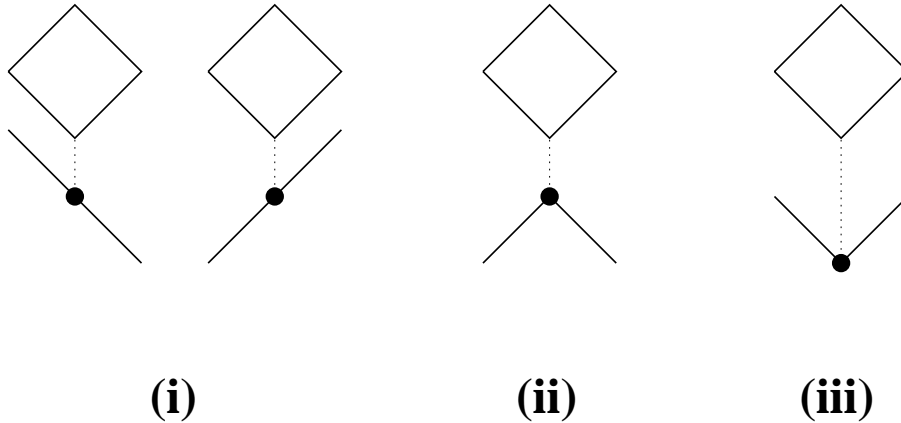


Fig. 15: The three possibilities for the multiplication $e_i(a)_{2'}$, represented as a box addition at the vertical of the point i on a diagram $a \in W_n$. The latter may be above (i) a slope of a , (ii) a maximum of a or (iii) a minimum of a .

Let us study the consequences of a left box addition on b , at a minimum $i < n$ of b . Let us denote by $b + \diamond$ the resulting diagram. Multiplying accordingly (6.20) to the left by e_i , we find a recursion relation for the matrix elements of $\mathcal{Q}_n(q)^{-1}$. Indeed

$$\begin{aligned}
 (b + \diamond)_1 &= \sum_{a \in W_n} [\mathcal{Q}_n(q)^{-1}]_{a, b + \diamond} (a)_{2'} \\
 &= e_i(b)_1 = \sum_{a \in W_n} [\mathcal{Q}_n(q)^{-1}]_{a,b} e_i(a)_{2'}
 \end{aligned} \quad (6.21)$$

gives a relation between $[\mathcal{Q}_n(q)^{-1}]_{a,b+\diamond}$ and elements of the form $[\mathcal{Q}_n(q)^{-1}]_{a',b}$ by identifying the coefficients of the basis 2' elements. Three situations may occur for $e_i(a)_{2'}$, as depicted in Fig.15.

- (i) The box addition is performed on a slope of a ($\ell_{i+1}^a + \ell_{i-1}^a = 2\ell_i^a$). Due to the vanishing property (4.11), we find that the resulting element vanishes, namely

$$\boxed{e_i(a)_{2'} = 0} \quad (6.22)$$

- (ii) The box addition is performed on a maximum of a ($\ell_{i+1}^a = \ell_{i-1}^a = \ell_i^a - 1$). For $(a)_{2'}$, this maximum is itself the result of an (unnormalized) box addition with the rules of basis 2, hence a factor $(e_i - \mu_k)$, where $k = \ell_i^a - 1$, according to (4.8). The multiplication by e_i results in

$$e_i(e_i - \mu_k) = \left(\frac{1}{\mu_1} - \mu_k\right)e_i = \frac{1}{\mu_{k+1}} \times (e_i - \mu_k) + \frac{\mu_k}{\mu_{k+1}} \times 1 \quad (6.23)$$

where we have used the recursion relation (4.4) for the μ 's. The first term in (6.23) restores the box of $(a)_{2'}$, while in the second term the box is removed, yielding $(a-\diamond)_{2'}$, where $a-\diamond$ denotes the walk diagram a with the box below the maximum removed. Hence

$$\boxed{e_i(a)_{2'} = \frac{1}{\mu_{k+1}} \left((a)_{2'} + \mu_k (a-\diamond)_{2'} \right)} \quad (6.24)$$

with $k = \ell_i^a - 1$.

- (iii) The box addition is performed on a minimum of a ($\ell_{i+1}^a = \ell_{i-1}^a = \ell_i^a + 1$). We are left with the multiplication of $(a)_{2'}$ by

$$e_i = (e_i - \mu_k) + \mu_k \times 1 \quad (6.25)$$

where $k = \ell_i^a + 1$. Hence

$$\boxed{e_i(a)_{2'} = (a+\diamond)_{2'} + \mu_k (a)_{2'}}$$
(6.26)

Substituting (6.22)(6.24)(6.26) in (6.21), we get

$$\begin{aligned} \sum_{a \in W_n} [\mathcal{Q}_n(q)^{-1}]_{a, b+\diamond} (a)_{2'} &= \sum_{a \in W_n} [\mathcal{Q}_n(q)^{-1}]_{a, b} \\ &\times \left\{ \frac{1}{\mu^{\ell_i^a}} \delta_{a, \max(i)} \left((a)_{2'} + \mu^{\ell_i^a - 1} (a - \diamond)_{2'} \right) \right. \\ &\left. + \delta_{a, \min(i)} \left((a + \diamond)_{2'} + \mu^{\ell_i^a + 1} (a)_{2'} \right) \right\} \end{aligned} \quad (6.27)$$

where we use the notation

$$\begin{aligned} \delta_{a, \max(i)} &= \begin{cases} 1 & \text{if } \ell_{i+1}^a = \ell_{i-1}^a = \ell_i^a - 1 \\ 0 & \text{otherwise} \end{cases} \\ \delta_{a, \min(i)} &= \begin{cases} 1 & \text{if } \ell_{i+1}^a = \ell_{i-1}^a = \ell_i^a + 1 \\ 0 & \text{otherwise} \end{cases} \end{aligned} \quad (6.28)$$

The identification of coefficients of $(a)_{2'}$ yields the relation

$$\begin{aligned} [\mathcal{Q}_n(q)^{-1}]_{a, b+\diamond} &= \delta_{a, \max(i)} \left(\frac{1}{\mu^{\ell_i^a}} [\mathcal{Q}_n(q)^{-1}]_{a, b} + [\mathcal{Q}_n(q)^{-1}]_{a-\diamond, b} \right) \\ &+ \delta_{a, \min(i)} \left(\mu^{\ell_i^a + 1} [\mathcal{Q}_n(q)^{-1}]_{a, b} + \frac{\mu^{\ell_i^a + 1}}{\mu^{\ell_i^a + 2}} [\mathcal{Q}_n(q)^{-1}]_{a+\diamond, b} \right) \end{aligned}$$

(6.29)

where we have used

$$\begin{aligned} \delta_{a, \max(i)} &= \delta_{a-\diamond, \min(i)} \\ \delta_{a, \min(i)} &= \delta_{a+\diamond, \max(i)} \\ \ell_i^{a \pm \diamond} &= \ell_i^a \pm 2 \end{aligned} \quad (6.30)$$

Together with the initial condition

$$[\mathcal{Q}_n(q)^{-1}]_{a, \mathcal{W}_{\epsilon_n}^{(n)}} = \delta_{a, \mathcal{W}_{\epsilon_n}^{(n)}} \quad (6.31)$$

eq.(6.29) is an actual recursion relation, yielding all the entries of \mathcal{Q}^{-1} , column by column starting from the left.

A first remark is in order: the entries of $\mathcal{Q}_n(q)^{-1}$ satisfy the property

$$[\mathcal{Q}_n(q)^{-1}]_{a, b} \neq 0 \Rightarrow a \subset b \quad (6.32)$$

easily proved by recursion using (6.29). This last condition has been previously derived for the entries of $\mathcal{P}_n(q)$ (cf. (5.45)), but holds as well for the inverse matrix. Note that (6.29) also implies that

$$[\mathcal{Q}_n(q)^{-1}]_{a, a} = 1 \quad (6.33)$$

in agreement with the normalization of \mathcal{Q} .

6.4. The matrix $\mathcal{Q}_n(q)^{-1}$

The recursion relation (6.29) will be solved in two steps. The idea is to treat separately the question of finding when $[\mathcal{Q}_n(q)^{-1}]_{a,b}$ vanishes or not, and that of determining its precise value when it does not vanish. This suggests to separate the matrix element $[\mathcal{Q}_n(q)^{-1}]_{a,b}$ into a product

$$[\mathcal{Q}_n(q)^{-1}]_{a,b} = w_{a,b} f_{a,b} \quad (6.34)$$

where $f_{a,b}$ is subject to the recursion relation

$$\begin{aligned} f_{a,b+\diamond} &= \delta_{a,\max(i)}(f_{a,b} + f_{a-\diamond,b}) \\ &\quad + \delta_{a,\min(i)}(f_{a,b} + f_{a+\diamond,b}) \end{aligned} \quad (6.35)$$

and

$$f_{a,\mathcal{W}_{\epsilon_n}^{(n)}} = \delta_{a,\mathcal{W}_{\epsilon_n}^{(n)}} \quad (6.36)$$

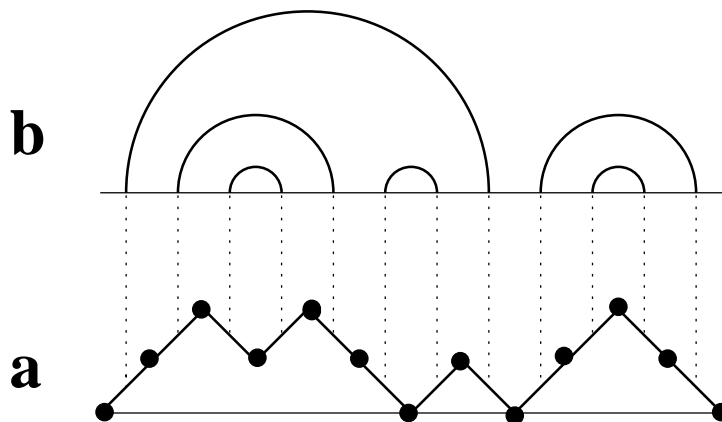


Fig. 16: An example of walks $a \subset b$, where a is b -symmetric. b is represented in the arch configuration picture, and a in the walk diagram picture. The dotted lines continuing the arches of b indicate the links of a which have to be symmetrical: the two links connected to the same arch must be mirror image of each other.

Solving for f . From (6.35)(6.36), it is clear that the f 's are nonnegative integers. In fact, the f 's may only take the values 0 or 1, and act as selection rules on the couples of diagrams $a \subset b$. To describe the solution of (6.35)(6.36), we need one more definition. We will need a mixed representation of a couple $a \subset b$ of walk diagrams in W_n , namely $a \in W_n$

is represented as a walk diagram, but $b \in A_n \equiv W_n$ is represented as an arch configuration of order n . The diagram b is therefore represented by the permutation σ_b of the bridges, with $\sigma_b^2 = 1$, describing the arches (namely $\sigma_b(i) = j$ iff the bridges i and j are linked by an arch). The diagram $a \subset b$ is said to be *b-symmetric* iff it satisfies

$$\boxed{\ell_{\sigma_b(i)}^a - \ell_{\sigma_b(i)-1}^a = -(\ell_i^a - \ell_{i-1}^a)} \quad (6.37)$$

In other words, we may represent on the same figure the arch configuration b and the walk diagram a , as illustrated in Fig.16. Each bridge i of b sits at the vertical of the link $(i-1, i)$ of a . Then a is *b-symmetric* iff the links of a are pairwise symmetrical under the pairs of bridges linked by an arch on b . In particular, if a is *b-symmetric*, then, below an interior arch of b (i.e., an arch linking two consecutive bridges $i, (i+1)$), a must have a maximum or a minimum (the only two left-right symmetrical link configurations around i). Note also that a diagram a is symmetric iff it is $\mathcal{W}_n^{(n)}$ -symmetric, and that the diagram $\mathcal{W}_{\epsilon_n}^{(n)}$ is *b-symmetric* for all $b \in W_n$.

With this definition, the solution of the recursion relation (6.35)(6.36) reads

$$\boxed{f_{a,b} = \begin{cases} 1 & \text{if } a \text{ is } b\text{-symmetric} \\ 0 & \text{otherwise} \end{cases}} \quad (6.38)$$

Hence, in (6.34), f selects the couples of diagrams $a \subset b$ such that a is *b-symmetric*⁵.

With $f_{a,b}$ as in (6.38), let us now check (6.35)(6.36). The relation (6.36) amounts to the fact that a is *a-symmetric*. Indeed, an arch of a always starts (say, at the bridge i) above an ascending link of a ($\ell_i^a = \ell_{i-1}^a + 1$) and ends (say, at the bridge $j = \sigma_a(i)$) over a descending link of a ($\ell_j^a - \ell_{j-1}^a = -1$); these two links are therefore symmetrical.

To check (6.35), let us consider a diagram $a \subset b + \diamond$, which is *b + \diamond-symmetric*. Noting that $b + \diamond$ has an interior arch linking the bridges i and $(i+1)$ (this is equivalent to a maximum above i on the corresponding walk diagram), by virtue of the abovementioned

⁵ Note, with the above definition, that $f_{a,b} \neq 0 \Rightarrow a \subset b$. Indeed, if $f_{a,b} \neq 0$, a cannot cross b , otherwise one would have $\ell_i^a = \ell_i^b$ and $\ell_{i+1}^a = \ell_i^a + 1$, $\ell_{i+1}^b = \ell_i^a - 1$, for some i . Take the smallest such i , this means that an arch of b ends at the bridge i . Let $i' < i$ be the bridge where it starts, then by *b-symmetry*, we must have $\ell_{i'+1}^a = \ell_{i'+1}^b$ and $\ell_{i'}^a = \ell_{i'+1}^a + 1$, $\ell_{i'}^b = \ell_{i'+1}^a - 1$, which contradicts the fact that i is the first crossing between a and b .

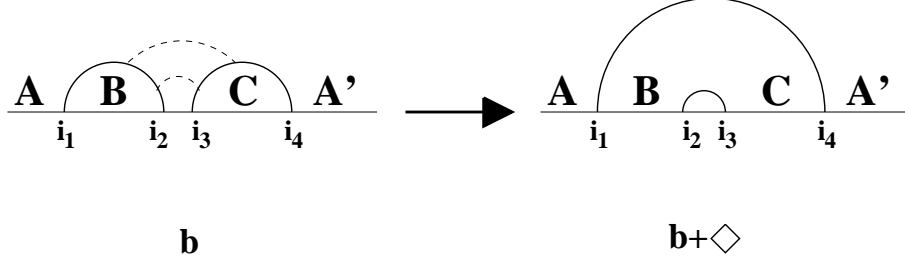


Fig. 17: The bridge move $b \rightarrow b + \diamond$ on the corresponding arch configurations. b has a minimum at $i = i_2$, hence an arch ends at the bridge $i = i_2$, and another starts at the bridge $i_3 = (i + 1)$. In $b + \diamond$, this minimum has been changed into a maximum, hence the bridges (i_1, i_4) and (i_2, i_3) are connected. All the other parts A, B, C and A' of b are unchanged.

property, the $b + \diamond$ -symmetric diagram a must have either a maximum or a minimum above i . These two possibilities correspond to the two lines of (6.35). To complete the check of (6.35), we must prove that in either case one and only one of the two diagrams a and $a \pm \diamond$ is b -symmetric (then (6.35) simply reads $1 = 1$).

More precisely, the box addition on $b \rightarrow b + \diamond$ is interpreted in the arch configuration picture as the *bridge move* illustrated in Fig.17. Before the box addition, b has a minimum at the vertical of i . This means that an arch (starting, say, at the bridge $i_1 < i$) ends at the bridge $i_2 = i$, and that another starts from the bridge $i_3 = (i + 1)$ (and ends, say, at the bridge $i_4 > (i + 1)$). The bridge move of Fig.17 replaces these two arches by an arch connecting the bridges i_1 and i_4 , and an *interior* arch connecting i_2 and i_3 . The creation of an interior arch corresponds to that of a maximum (the top of the box) on b . Let us denote by A, B, C, A' (like in Fig.17), the regions of b lying respectively to the left of i_1 , between i_1 and i_2 , between i_3 and i_4 and to the right of i_4 . Note that the regions A and A' may be connected to each other by arches passing above the (i_1, i_2) and (i_3, i_4) arches, but B and C are only connected to themselves.

Let us consider a walk diagram a which is $b + \diamond$ -symmetric (cf. Fig.18). The portions $\alpha, \beta, \gamma, \alpha'$ of the walk a lying respectively below A, B, C, A' satisfy the following properties: β is B -symmetric, γ is C -symmetric, and $\alpha\alpha'$ is AA' -symmetric⁶. All these portions of a remain untouched in $a \pm \diamond$. Only the two links $(i_2 - 1, i_2)$ and $(i_3 - 1, i_3)$ of a will be affected. The $b + \diamond$ -symmetry of a implies that

$$\begin{aligned} (\ell_{i_1}^a - \ell_{i_1-1}^a) &= (\ell_{i_4-1}^a - \ell_{i_4}^a) \equiv \sigma_1 = \pm 1 \\ (\ell_{i_2}^a - \ell_{i_2-1}^a) &= (\ell_{i_3-1}^a - \ell_{i_3}^a) \equiv \sigma_2 = \pm 1 \end{aligned} \tag{6.39}$$

⁶ Here we extend slightly the notion of respective symmetry to walks $c \subset d$, with initial and final heights not necessarily equal to 0, by still imposing the condition (6.37).

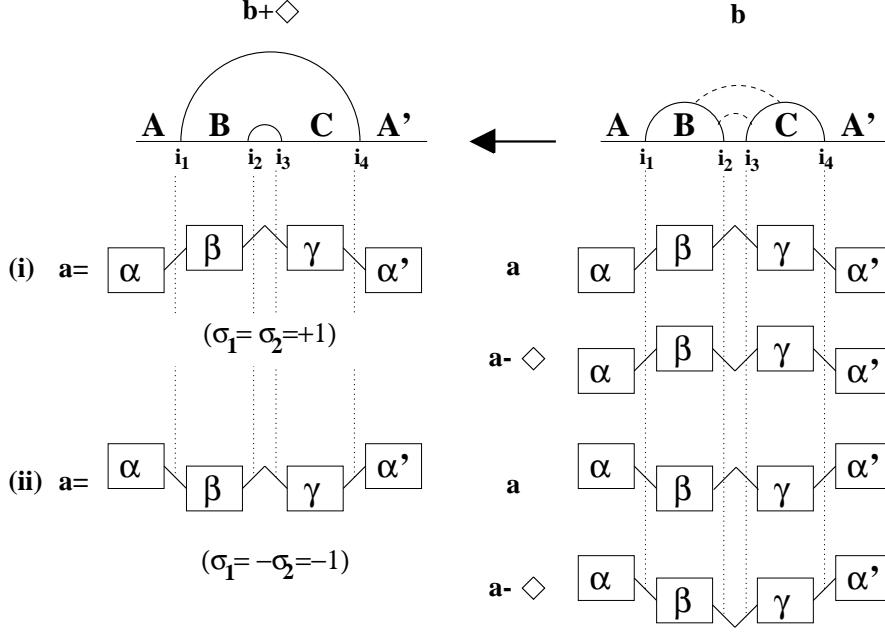


Fig. 18: Example of a walk a , which is $b + \diamond$ -symmetric. The two possibilities (i) $\sigma_1 = \sigma_2 = 1$ and (ii) $\sigma_1 = -\sigma_2 = -1$ are represented. In both cases, one and only one of the two diagrams a and $a - \sigma_2 \diamond$ is b -symmetric.

as the bridges (i_1, i_4) and (i_2, i_3) are connected in $b + \diamond$. Two situations may now occur, according to the relative values of σ_1 and σ_2 .

(i) $\sigma_1 = \sigma_2$: a is not b -symmetric, because the links $(i_1 - 1, i_1)$ and $(i_2 - 1, i_2)$ of a are not symmetrical (the same holds for the links $(i_3 - 1, i_3)$ and $(i_4 - 1, i_4)$). On the contrary, $a - \sigma_2 \diamond$ is b -symmetric, because both links $(i_2 - 1, i_2)$ and $(i_3 - 1, i_3)$ are flipped by the box addition/subtraction. This is illustrated on Fig.18-(i).

(ii) $\sigma_1 = -\sigma_2$: a is b -symmetric, but $a - \sigma_2 \diamond$ is not, as the situation of the previous case is reversed. This is illustrated in Fig.18-(ii).

Hence, we have shown that, when a is $b + \diamond$ -symmetric, one and only one of the two diagrams a and $a - \sigma_2 \diamond$ appearing on the rhs of (6.35) is b -symmetric. This completes the check of the recursion relation (6.35) (which reduces in both cases $\sigma_2 = \pm 1$ to $1 = 1$). Eq. (6.38) is the unique solution to (6.35)(6.36).

In addition to their defining recursion relation, the f 's satisfy a number of interesting properties, which will prove crucial in the study of meander and semi-meander polynomials. Among the many interpretations of the condition $f_{a,b} = 1$, the set of a 's such that $f_{a,b} = 1$ for a given $b \in W_n$, may be obtained as shown in Fig.19. First represent b as a walk diagram of $2n$ steps. Then draw horizontal lines joining the couples of points (of the form $(i, \ell_i^b) - (j, \ell_j^b \equiv \ell_i^b)$, $i, j \geq 1$) corresponding to the beginning and end of all arches of b

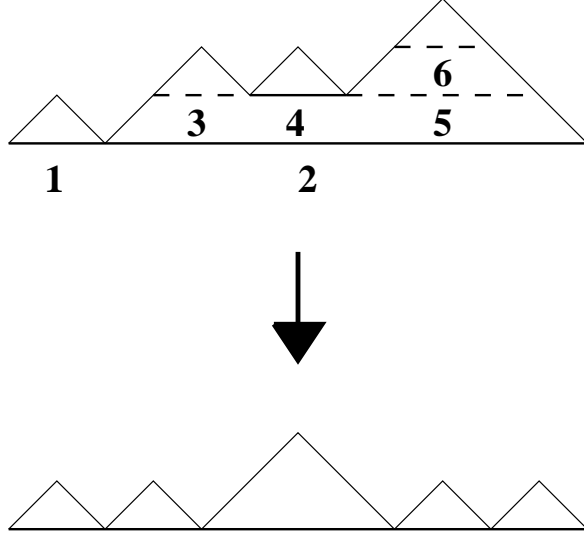


Fig. 19: A particular folding of the walk diagram $b \in W_n$, leading to an $a \in W_n$, such that a is b -symmetric. The solid horizontal lines represent the unfolded folding lines, while the horizontal dashed lines represent the lines along which b is effectively folded (lines number 3,5,6). The total number of folding lines is n , the order of the diagrams ($n = 6$ here).

(the arch starts at the bridge $(i + 1)$ and ends at the bridge j). It is easy to see that there are exactly n such lines. The set of admissible a 's is simply obtained by *folding* the path b arbitrarily along these lines (see Fig.19). Indeed, the folding operation preserves the b -symmetry of a , by simply reversing all the quantities $(\ell_{i+1}^a - \ell_i^a)$ along the folding line. If no additional constraint was imposed on the a 's, we would get 2^n possible foldings for each diagram b . However, a is further constrained to have nonnegative heights, which reduces this number, but we expect it to still behave as 2^n for most b 's, in the large n limit.

Conversely, here is an algorithm to generate, for fixed $a \in W_n$, all the walks $b \in W_n$ such that $f_{a,b} = 1$. The path $b = a$ is always admissible. Let us represent it by the sequence of signs $t_i(a) = \ell_i^a - \ell_{i-1}^a$, $i = 1, 2, \dots, 2n$, and consider the modified sequence

$$\sigma_i(a) = (-1)^{i-1} t_i(a) = (-1)^{i-1} (\ell_i^a - \ell_{i-1}^a) \quad (6.40)$$

Interpreting these indices i as bridge numbers (from 1 to $2n$), the set of b 's such that $f_{a,b} = 1$ is simply the set of arch configurations linking these $2n$ bridges, such that each arch connects two bridges with the *same* value of the sign $\sigma_i(a)$. An example is displayed in Fig.20. The number of admissible b 's for fixed a seems to depend strongly on a .

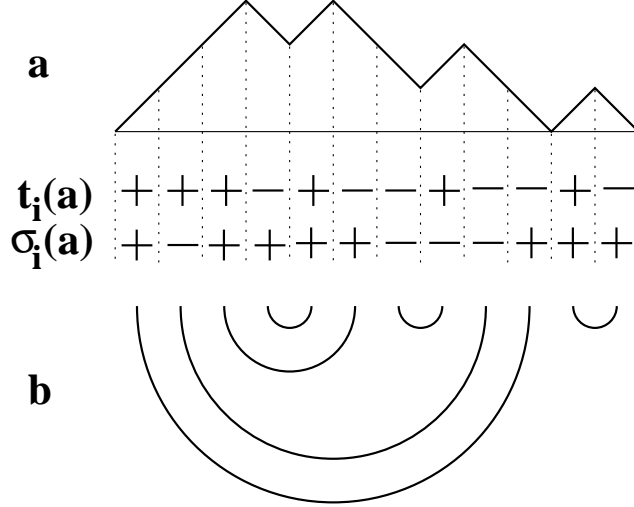


Fig. 20: For fixed a , the b 's such that $f_{a,b} = 1$ are the arch configurations connecting bridges with the same value of $\sigma_i(a) = (-1)^{i-1}t_i(a)$, where $t_i(a) = \ell_i^a - \ell_{i-1}^a$, for $i = 1, 2, \dots, 2n$. Here $n = 6$, and we have represented one of the admissible b 's.

Let us finally mention the following sum rule, proved in detail in Appendix C

$$\boxed{\sum_{a,b \in W_n} f_{a,b} = 3 \frac{2^{n-1}(2n)!}{n!(n+2)!} = 3 \frac{2^{n-1}}{n+2} c_n} \quad (6.41)$$

expressing the total number of couples $(a, b) \in W_n \times W_n$, where a is b -symmetric. By Stirling's formula, we see that

$$\sum_{a,b \in W_n} f_{a,b} \sim \frac{3}{2\sqrt{\pi}} \frac{8^n}{n^{5/2}} \quad (6.42)$$

The leading behavior 8^n agrees with the expectation that the number of admissible a 's for fixed b behave like 2^n for most b 's (whose number is of the order of 4^n).

Solving for w . To complete the solution of (6.29), we have to compute the weight $w_{a,b} = [\mathcal{Q}^{-1}]_{a,b}$ when a is b -symmetric. The form of $w_{a,b}$ is entirely dictated by the coefficients of the recursion relation (6.29). The result reads

$$\boxed{w_{a,b} = \prod_{i=1}^{2n-1} (w(\ell_{i-1}^a, \ell_i^a, \ell_{i+1}^a))^{\frac{1}{4}(\ell_i^b - \ell_i^a)} \\ w(k, \ell, m) = \frac{\mu_{\ell+1}}{\mu_{\ell}} (\mu_{\ell} \mu_{\ell+1})^{\frac{1}{2}(k+m) - \ell}} \quad (6.43)}$$

In order to check that this is compatible with (6.29), we note that, with the form (6.34), and when a is $b + \diamond$ -symmetric, one and only one of the four terms in the r.h.s. of (6.29) is non-zero. Assuming for instance that a has a maximum at i , it is sufficient to check that

$$\begin{aligned} \frac{w_{a,b+\diamond}}{w_{a,b}} &= \frac{1}{\mu \ell_i^a} \\ \frac{w_{a,b+\diamond}}{w_{a-\diamond,b}} &= 1 \end{aligned} \tag{6.44}$$

irrespectively of which term survives. Eqs.(6.44) follow directly from (6.43), and are exactly what is needed to absorb the coefficients in (6.29). Similarly, if a has a minimum at i , one easily checks that the sufficient conditions

$$\begin{aligned} \frac{w_{a,b+\diamond}}{w_{a,b}} &= \mu \ell_i^{a+1} \\ \frac{w_{a,b+\diamond}}{w_{a+\diamond,b}} &= \frac{\mu \ell_i^{a+1}}{\mu \ell_i^{a+2}} \end{aligned} \tag{6.45}$$

are fulfilled. Note also that $w_{a,a} = 1$ as required.

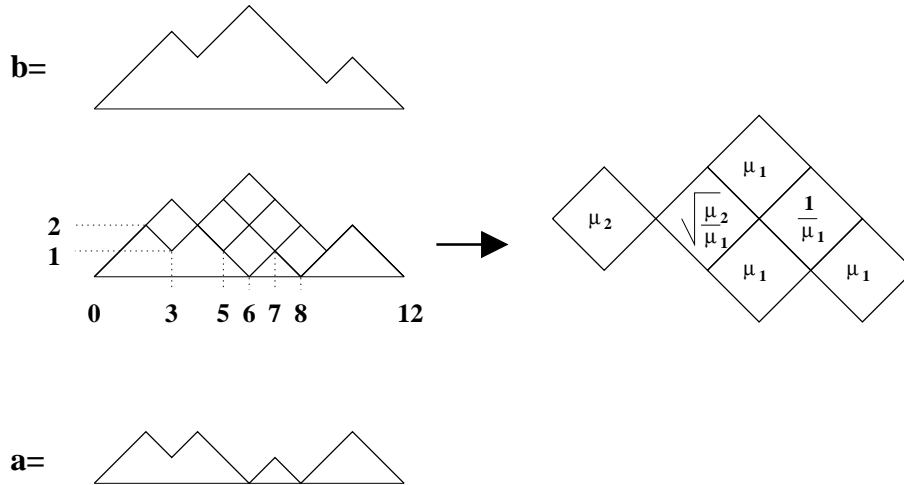


Fig. 21: An example of computation of $w_{a,b}$, for $a \subset b$. b is obtained from a by six box additions. The box weights are computed using the rules (i)-(ii)-(iii). Here we have $w_{a,b} = (\mu_1 \mu_2)^{3/2}$.

Practically, for $a \subset b$ irrespectively of whether a is b -symmetric, the weight (6.43) can be computed as a product of box factors over all the boxes which must be added to a to build b .

- (i) If the box is added at the vertical of a maximum of a , the weight w is multiplied by $1/\mu \ell_i^a$.

(ii) If the box is added at the vertical of a minimum of a , the weight w is multiplied by $\mu_{\ell_i^a+1}$.

(iii) If the box is added at the vertical of a slope of a , the weight w is multiplied by $\sqrt{\mu_{\ell_i^a+1}/\mu_{\ell_i^a}}$.

This is a direct consequence of the expression of $w(k, \ell, m)$ in (6.43), where the power $\frac{1}{2}(k+m) - \ell$ distinguishes between maxima (value -1), minima (value 1) and slopes (value 0). An explicit example is given in Fig.21.

6.5. The normalization matrix $\mathcal{N}_n(q)$

Let us reexpress the (diagonal) matrix elements of $\mathcal{N}_n(q)$ (5.56) in the language of weights $w_{a,b}$ (6.43). The result reads simply

$$\boxed{[\mathcal{N}_n(q)]_{a,a} = w_{a, \mathcal{W}_n^{(n)}}} \quad (6.46)$$

where $\mathcal{W}_n^{(n)}$ is the largest walk diagram of W_n , i.e. containing all the others, with heights

$$\ell_i^{\max} = \min(i, 2n - i) \quad (6.47)$$

This is easily proved as follows. Let us first consider a *symmetric* diagram a . As mentioned before, this diagram is also $\mathcal{W}_n^{(n)}$ -symmetric, hence $f_{a, \mathcal{W}_n^{(n)}} = 1$. By (6.9), we find that

$$\begin{aligned} 1 &= [\mathcal{P}_n(q)^{-1}]_{a, \mathcal{W}_n^{(n)}} \\ &= [\mathcal{N}_n(q)^{-1}]_{a,a} [\mathcal{Q}_n(q)^{-1}]_{a, \mathcal{W}_n^{(n)}} \end{aligned} \quad (6.48)$$

hence

$$[\mathcal{N}_n(q)]_{a,a} = [\mathcal{Q}_n(q)^{-1}]_{a, \mathcal{W}_n^{(n)}} = w_{a, \mathcal{W}_n^{(n)}} \quad (6.49)$$

as $f_{a, \mathcal{W}_n^{(n)}} = 1$. This proves (6.46) for any symmetric diagram a . However, the expression (5.56) for arbitrary a is clearly factorized into products pertaining to the left and right halves of $a = lr$, namely

$$[\mathcal{N}_n(q)]_{a,a} = \prod_{\substack{\text{left strips} \\ \text{on } l}} \sqrt{\mu_\ell} \prod_{\substack{\text{right strips} \\ \text{on } r}} \sqrt{\mu_\ell} = n(l) n(r) \quad (6.50)$$

Analogously, the quantity $w_{a, \mathcal{W}_n^{(n)}}$ factorizes into two products pertaining respectively to the left and right halves of $a = lr$, namely

$$w_{a, \mathcal{W}_n^{(n)}} = w(l) w(r) \quad (6.51)$$

where

$$w(l) = (x(\ell_{n-1}^l, \ell_n^l))^{\frac{n-\ell_n^l}{4}} \prod_{i=1}^{n-1} (w(\ell_{i-1}^l, \ell_i^l, \ell_{i+1}^l))^{\frac{1}{4}(\ell_i^{\max} - \ell_i^l)} \quad (6.52)$$

and

$$\begin{aligned} x(k, \ell) &= (\mu_{\max(k, \ell)})^{k-\ell} \\ &= (\mu_{(k+\ell+1)/2})^{k-\ell} \end{aligned} \quad (6.53)$$

In the above, we have used the formula $\max(k, \ell) = (|k - \ell| + k + \ell)/2 = (k + \ell + 1)/2$, as $k - \ell = \pm 1$. The weights x separate the middle box factors in (6.43) into left and right halves. More precisely, each box factor

$$\boxed{w(k, \ell, m) = x(k, \ell) x(m, \ell)} \quad (6.54)$$

is factorized into a left half (k, ℓ) (described from left to right on a) and a right half (m, ℓ) (described from right to left on a). Eq.(6.54) results from the identity

$$\frac{\mu_{\ell+1}}{\mu_\ell} (\mu_\ell \mu_{\ell+1})^{\frac{1}{2}(k+m)-\ell} = \mu_{\max(k, \ell)}^{k-\ell} \mu_{\max(m, \ell)}^{m-\ell} \quad (6.55)$$

easily proved by inspection. Now the result for symmetric diagrams $a = lr$, $r = l$, reads

$$[\mathcal{N}_n(q)]_{a, a} = n(l)^2 = w(l)^2 \quad (6.56)$$

hence $n(l) = w(l)$. For arbitrary diagrams $a = lr$, we have

$$[\mathcal{N}_n(q)]_{a, a} = n(l)n(r) = w(l)w(r) = w_{a, \mathcal{W}_n^{(n)}} \quad (6.57)$$

which completes the proof of (6.46).

As a by-product of the previous analysis, the local factorization property (6.54) and the obvious relation $x(k, \ell)x(\ell, k) = 1$, enable us to rewrite the general expression (6.43) as

$$\begin{aligned} w_{a, b} &= \prod_{i=1}^{2n-1} [x(\ell_{i-1}^a, \ell_i^a) x(\ell_{i+1}^a, \ell_i^a)]^{\frac{1}{4}(\ell_i^b - \ell_i^a)} \\ &= \prod_{i=0}^{2n-1} [x(\ell_i^a, \ell_{i+1}^a)]^{\frac{1}{4}((\ell_{i+1}^b - \ell_i^b) - (\ell_{i+1}^a - \ell_i^a))} \\ &= \prod_{i=0}^{2n-1} (\mu_{(1+\ell_i^a + \ell_{i+1}^a)/2})^{\frac{1}{4}(1 - (\ell_{i+1}^a - \ell_i^a)(\ell_{i+1}^b - \ell_i^b))} \end{aligned} \quad (6.58)$$

This last expression reduces directly to (5.56) in the case $b = \mathcal{W}_n^{(n)}$, providing us with an alternative proof of (6.46). Indeed, $\ell_{i+1}^b - \ell_i^b = 1$ if $i < n$, and -1 if $i \geq n$, and the factor $\frac{1}{2}(1 - (\ell_{i+1}^a - \ell_i^a)(\ell_{i+1}^b - \ell_i^b))$ takes the value 1 on a 's (left and right) tops of strips, and 0 everywhere else, while $(1 + \ell_i^a + \ell_{i+1}^a)/2$ is the corresponding length of strip.

6.6. The path formulation of (semi)-meanders

We now have all the elements to write alternative expressions for the meander and semi-meander polynomials, as weighted sums over paths. The entries of the matrix $\mathcal{P}_n(q)^{-1}$ read, using (6.43)

$$\begin{aligned}
[\mathcal{P}_n(q)^{-1}]_{a,b} &= [\mathcal{N}_n(q)^{-1}]_{a,a} [\mathcal{Q}_n(q)^{-1}]_{a,b} \\
&= f_{a,b} \frac{w_{a,b}}{w_{a, \mathcal{W}_n^{(n)}}} \\
&= f_{a,b} \prod_{i=1}^{2n-1} [w(\ell_{i-1}^a, \ell_i^a, \ell_{i+1}^a)]^{\frac{1}{4}(\ell_i^b - \ell_i^{\max})} \\
&= f_{a,b} e^{\frac{1}{4} \sum_{i=1}^{2n-1} (\ell_i^b - \ell_i^{\max}) \alpha(\ell_{i-1}^a, \ell_i^a, \ell_{i+1}^a; q)}
\end{aligned} \tag{6.59}$$

where ℓ_i^{\max} is defined in (6.47), and

$$\alpha(k, \ell, m; q) = \log \left(\frac{\mu_{\ell+1}}{\mu_\ell} \right) + \frac{k + m - 2\ell}{2} \log(\mu_\ell \mu_{\ell+1}) \tag{6.60}$$

Using the alternative expression of $w_{a,b}$ (6.58), we may also write

$$[\mathcal{P}_n(q)^{-1}]_{a,b} = f_{a,b} e^{\frac{1}{4} \sum_{i=0}^{2n-1} [(\ell_{i+1}^{\max} - \ell_i^{\max}) - (\ell_{i+1}^b - \ell_i^b)] (\ell_{i+1}^a - \ell_i^a) \log \mu_{(\ell_i^a + \ell_{i+1}^a + 1)/2}} \tag{6.61}$$

The passage from (6.59) to (6.61) may be viewed as a discrete integration by parts in the sum over i .

Substituting the expression (6.61) in (6.12) and (6.13), we get the following expressions for the semi-meander and meander polynomials

$$\begin{aligned}
\bar{m}_n(q) &= \sum_{a,b \in W_n} f_{a,b} f_{a, \mathcal{W}_n^{(n)}} U_{\ell_n^a}(q) \\
&\times e^{\frac{1}{4} \sum_{i=0}^{2n-1} [(\ell_{i+1}^{\max} - \ell_i^{\max}) - (\ell_{i+1}^b - \ell_i^b)] (\ell_{i+1}^a - \ell_i^a) \log \mu_{(\ell_i^a + \ell_{i+1}^a + 1)/2}}
\end{aligned} \tag{6.62}$$

$$\begin{aligned}
m_n(q) &= \sum_{a,b,b' \in W_n} f_{a,b} f_{a,b'} U_{\ell_n^a}(q) \\
&\times e^{\frac{1}{4} \sum_{i=0}^{2n-1} [2(\ell_{i+1}^{\max} - \ell_i^{\max}) - (\ell_{i+1}^b - \ell_i^b) - (\ell_{i+1}^{b'} - \ell_i^{b'})] (\ell_{i+1}^a - \ell_i^a) \log \mu_{(\ell_i^a + \ell_{i+1}^a + 1)/2}}
\end{aligned} \tag{6.63}$$

Note that the semi-meander expression (6.62) may be viewed as (6.63) in which b' is fixed to be $\mathcal{W}_n^{(n)} \equiv r_n$, the walk diagram corresponding to the rainbow arch configuration of order n , which restricts the sum to symmetric walk diagrams a .

The expressions (6.62)(6.63) should permit a detailed asymptotic study of the semi-meander and meander polynomials for large n .

6.7. Connected components in meanders

For any $b \in A_n \equiv W_n$, let \vec{v}_b be the vector with entries $(\vec{v}_b)_a = \delta_{a,b}$. The matrix elements of $\mathcal{G}_n(q)$ can be expressed as

$$[\mathcal{G}_n(q)]_{b,b'} = \vec{v}_{b'} \cdot \mathcal{G}_n(q) \vec{v}_b = (\mathcal{P}_n(q)^{-1} \vec{v}_{b'}) \cdot \Gamma_n(q) \mathcal{P}_n(q)^{-1} \vec{v}_b = q^{c(b,b')} \quad (6.64)$$

where $c(b,b')$ (3.13) is the number of connected components of the meander obtained by superimposing the arch configurations b and b' . Hence we can write a refined version of (6.63) for fixed b and $b' \in A_n$

$$q^{c(b,b')} = \sum_{a \in W_n} f_{a,b} f_{a,b'} U_{\ell_n^a}(q) \times e^{\frac{1}{4} \sum_{i=0}^{2n-1} [2(\ell_{i+1}^{\max} - \ell_i^{\max}) - (\ell_{i+1}^b - \ell_i^b) - (\ell_{i+1}^{b'} - \ell_i^{b'})] (\ell_{i+1}^a - \ell_i^a) \log \mu_{(\ell_i^a + \ell_{i+1}^a + 1)/2}}$$

(6.65)

Note that the highly non-local quantity $c(b,b')$ is expressed as a sum of *local* weights. However, the non-locality reemerges in a weaker form through the selection factors f , which induce mutually non-local constraints on the walks summed over.

This formula gives an interesting expression for $c(b,b')$ in the limit of large q . Indeed, we have, for $q \rightarrow \infty$

$$U_\ell(q) \sim q^\ell \quad \mu_\ell \sim \frac{1}{q} \quad (6.66)$$

hence (6.65) becomes

$$q^{c(b,b')} \sim \sum_{a \in W_n} f_{a,b} f_{a,b'} q^{\frac{1}{4} \sum_{i=0}^{2n-1} ((\ell_{i+1}^b - \ell_i^b) + (\ell_{i+1}^{b'} - \ell_i^{b'})) (\ell_{i+1}^a - \ell_i^a)} \quad (6.67)$$

where we the contributions of the ℓ_i^{\max} 's and that of the Chebishev polynomial have cancelled each other, thanks to the identity

$$\ell_n^a - \frac{1}{2} \sum_{i=0}^{2n-1} (\ell_{i+1}^{\max} - \ell_i^{\max}) (\ell_{i+1}^a - \ell_i^a) = 0 \quad (6.68)$$

For large q 's, the sum in the rhs of (6.67) is dominated by some $a \in W_n$ for which the exponent of q is maximal. Such a maximum is unique, as the coefficient of $q^{c(b,b')}$ is 1. This yields the following formula for the number of connected components $c(b, b')$

$$c(b, b') = \frac{1}{4} \max_{\substack{a \in W_n, \\ b \text{ and } b' \text{-symmetric}}} \left\{ \sum_{i=0}^{2n-1} [(\ell_{i+1}^b - \ell_i^b) + (\ell_{i+1}^{b'} - \ell_i^{b'})] (\ell_{i+1}^a - \ell_i^a) \right\} \quad (6.69)$$

A particular case corresponding to semi-meanders consists in taking $b' = \mathcal{W}_n^{(n)} \equiv r_n$ the rainbow configuration of order n . Using (6.68), we find

$$c(b) = c(b, \mathcal{W}_n^{(n)}) = \frac{1}{4} \max_{\substack{a \in W_n, \text{ symmetric} \\ \text{and } b\text{-symmetric}}} \left\{ 2\ell_n^a + \sum_{i=0}^{2n-1} (\ell_{i+1}^b - \ell_i^b) (\ell_{i+1}^a - \ell_i^a) \right\} \quad (6.70)$$

Another interesting consequence of the expression (6.65) is obtained if we take $b = b'$, in which case $c(b, b) = n$. It takes the form of a sum rule for $f_{a,b}$, namely, for any $b \in W_n$

$$q^n = \sum_{a \in W_n} f_{a,b} U_{\ell_n^a}(q) e^{\frac{1}{2} \sum_{i=0}^{2n-1} [(\ell_{i+1}^{\max} - \ell_i^{\max}) - (\ell_{i+1}^b - \ell_i^b)] (\ell_{i+1}^a - \ell_i^a) \log \mu_{(\ell_i^a + \ell_{i+1}^a + 1)/2}} \quad (6.71)$$

In particular, for $b = \mathcal{W}_n^{(n)}$, hence $\ell_i^b = \ell_i^{\max}$ for all i , we find, with $f_{a, \mathcal{W}_n^{(n)}} = \delta_{a, \text{symmetric}}$:

$$\begin{aligned} q^n &= \sum_{\substack{a \in W_n \\ a \text{ symmetric}}} U_{\ell_n^a}(q) \\ &= \sum_{p=0}^{\lfloor n/2 \rfloor} b_{n, n-2p} U_{n-2p}(q) \end{aligned} \quad (6.72)$$

which is easily proved by recursion on n (the coefficient $b_{n, n-2p}$, computed in (5.52), is indeed the number of symmetric diagrams with middle height $h = n - 2p$).

6.8. Asymptotics for $q \geq 2$

In this section, we use the expressions (6.62)(6.63) to derive asymptotic formulas for the semi-meander and meander polynomials for large n . Such formulas can only be inferred when all the terms in the sums (6.62)(6.63) over walk diagrams are positive. This is the case for all $q \geq 2$, for which $U_m(q) > 0$ and $\mu_m > 0$ for all m .

q=2. As a preliminary exercise, let us start by taking the limit $q \rightarrow 2$ of the sum rule (6.71). Due to the definition (4.2), we have

$$U_\ell(2) = (\ell + 1) \quad \mu_\ell(2) = \frac{\ell}{\ell + 1} \quad (6.73)$$

therefore, when $q \rightarrow 2$, (6.71) becomes

$$2^n = \sum_{a \in W_n} f_{a,b} (\ell_n^a + 1) e^{\frac{1}{2} \sum_{i=0}^{2n-1} [(\ell_{i+1}^{\max} - \ell_i^{\max}) - (\ell_{i+1}^b - \ell_i^b)] (\ell_{i+1}^a - \ell_i^a) \log \frac{\ell_i^a + \ell_{i+1}^a + 1}{\ell_i^a + \ell_{i+1}^a + 3}} \quad (6.74)$$

Note that, summing (6.74) over $b \in W_n$ we get the result

$$\sum_{a,b \in W_n} f_{a,b} (\ell_n^a + 1) e^{\frac{1}{2} \sum_{i=0}^{2n-1} [(\ell_{i+1}^{\max} - \ell_i^{\max}) - (\ell_{i+1}^b - \ell_i^b)] (\ell_{i+1}^a - \ell_i^a) \log \frac{\ell_i^a + \ell_{i+1}^a + 1}{\ell_i^a + \ell_{i+1}^a + 3}} = 2^n c_n \quad (6.75)$$

which behaves, for large n , like

$$\frac{8^n}{n^{3/2}} \sim n \sum_{a,b \in W_n} f_{a,b} \quad (6.76)$$

by making use of the asymptotics (6.42). Comparing (6.75) and (6.76), we are led to the following scaling hypothesis for the values of ℓ_i^b and ℓ_i^a dominating the sum (6.75):

$$\ell_i^a \sim n^\nu \ell^a(x) \quad \ell_i^b \sim n^\nu \ell^b(x) \quad (6.77)$$

where $x = i/n$ and $\nu \in [0, 1]$ is an exponent characterizing the average height of the walk diagrams a, b . For this hypothesis to be compatible with (6.76), we must necessarily have $\nu = 1$, in which case the exponential in (6.75) tends to a constant⁷ (the sum over i is of

⁷ To see why, note that for large n and ℓ 's the sum in the exponential may be approximated by

$$\begin{aligned} & \frac{1}{2} \sum_{i=0}^{2n-1} [(\ell_{i+1}^{\max} - \ell_i^{\max}) - (\ell_{i+1}^b - \ell_i^b)] \frac{\ell_{i+1}^a - \ell_i^a}{\ell_i^a + 1} \\ & \sim - \sum_{i=0}^{2n-1} \left[\delta_{i,n} - \left(\frac{\ell_{i+1}^b + \ell_{i-1}^b}{2} - \ell_i^b \right) \right] \log(\ell_i^a + 1) \end{aligned}$$

where we have performed a discrete integration by parts. Hence the exponential of this sum is equivalent to

$$(\ell_n^a + 1) \times \frac{\prod_i \min. \text{ of } b (\ell_i^a + 1)}{\prod_i \max. \text{ of } b (\ell_i^a + 1)} \sim \text{const.}$$

The products extend respectively over the i 's which are minima and maxima of the walk b and as there is always one more maximum than minima, the above ratio is exactly balanced, hence is of order 1 for large ℓ_i^a 's.

order n , but the logarithm is of order $1/n$), and the factor $(\ell_i^a + 1)$ tends to $\text{const.} \times n$, which yields (6.76). This is an example of use of a scaling hypothesis on the ℓ 's dominating the sum (6.75), leading to large n asymptotics.

Analogously, if we make the same scaling hypothesis (6.77), with $\nu = 1$, on the ℓ 's dominating the sums (6.62)(6.63), for $q = 2$, we find the asymptotic relations, valid for large n

$$\boxed{\begin{aligned} \bar{m}_n(2) &\sim n \sum_{\substack{a,b \in W_n \\ a \text{ symmetric}}} f_{a,b} \\ m_n(2) &\sim n \sum_{a,b,b' \in W_n} f_{a,b} f_{a,b'} \end{aligned}} \quad (6.78)$$

This expresses the asymptotics of the meander and semi-meander polynomials at $q = 2$ in terms of $f_{a,b}$ only. In going from (6.76) to (6.78), we have assumed that configurations of the *same* order of magnitude dominate both sums. In fact, we have made a scaling hypothesis on the matrix elements of $\mathcal{P}_n^{-1}(q = 2)$ and $\Gamma_n(q = 2)$, namely that the configurations with

$$[\mathcal{P}_n^{-1}(2)]_{a,b} \sim f_{a,b} \quad [\Gamma_n(2)]_{a,a} = (\ell_n^a + 1) \sim n^\nu \quad (6.79)$$

dominate the three sums

$$\begin{aligned} \text{Tr}(\mathcal{G}_n(2)) &\sim n^\nu \sum_{a,b \in W_n} f_{a,b} \\ \vec{v} \cdot \mathcal{G}_n(2) \vec{u} &\sim n^\nu \sum_{\substack{a,b \in W_n \\ a \text{ symmetric}}} f_{a,b} \\ \vec{u} \cdot \mathcal{G}_n(2) \vec{u} &\sim n^\nu \sum_{a,b,b' \in W_n} f_{a,b} f_{a,b'} \end{aligned} \quad (6.80)$$

with the same value of $\nu = 1$. Let us stress, however, that the scaling hypothesis (6.79) leads to a wrong result for the meander determinant, $D_n(2)$, for large n . Indeed, from (6.79), we would conclude that

$$D_n(2) \sim \prod_{a \in W_n} f_{a,a}^2 n^\nu \sim n^{\nu c_n} \quad (6.81)$$

whereas, from the exact result (5.6) for $D_n(2)$, we extract the large n asymptotics

$$\log D_n(2) = \sum_{j=1}^n a_{n,j} \log(j+1) \sim \sqrt{\pi n} c_n \quad (6.82)$$

by the standard saddle point technique (note that we find exactly twice the previous result (5.19) for the large n asymptotics of $\log \det D'_n(0)$). The correct asymptotics (6.82) contradict (6.81). This simply means that the configurations of $a \in W_n$ dominating the meander determinant are very different from those dominating the trace of the Gram matrix or the (semi-)meander polynomial.

q>2. We start again from the sum rule (6.71), with $q = e^\theta + e^{-\theta}$, $\theta > 0$. We again make the hypothesis that, when summed over $b \in W_n$, the sum (6.71) is dominated by large ℓ 's for large n . Noting that

$$U_m(e^\theta + e^{-\theta}) \sim \frac{e^{m\theta}}{1 - e^{-2\theta}} \quad \mu_m \sim e^{-\theta} \quad (6.83)$$

for large m , this gives the asymptotic formula

$$\begin{aligned} c_n (e^\theta + e^{-\theta})^n &\sim \sum_{a,b \in W_n} f_{a,b} \frac{e^{\theta \ell_n^a}}{1 - e^{-2\theta}} e^{-\frac{\theta}{2} \sum_{i=0}^{2n-1} [(\ell_{i+1}^{\max} - \ell_i^{\max}) - (\ell_{i+1}^b - \ell_i^b)] (\ell_{i+1}^a - \ell_i^a)} \\ &= \frac{1}{1 - e^{-2\theta}} \sum_{a,b \in W_n} f_{a,b} e^{\frac{\theta}{2} \sum_{i=0}^{2n-1} (\ell_{i+1}^b - \ell_i^b) (\ell_{i+1}^a - \ell_i^a)} \\ &\sim \frac{4^n}{n^{3/2}} (e^\theta + e^{-\theta})^n \end{aligned} \quad (6.84)$$

where we have used (6.68). This gives an asymptotic sum rule involving the $f_{a,b}$'s and q .

Assuming that the same scaling hypothesis holds for the sums (6.62)(6.63), we find the following asymptotic formulas

$$\begin{aligned} \bar{m}_n(e^\theta + e^{-\theta}) &\sim \sum_{\substack{a,b \in W_n \\ a \text{ symmetric}}} f_{a,b} e^{\frac{\theta}{2} [\ell_n^a + \frac{1}{2} \sum_{i=0}^{2n-1} (\ell_{i+1}^b - \ell_i^b) (\ell_{i+1}^a - \ell_i^a)]} \\ m_n(e^\theta + e^{-\theta}) &\sim \sum_{a,b,b' \in W_n} f_{a,b} f_{a,b'} e^{\frac{\theta}{4} \sum_{i=0}^{2n-1} [(\ell_{i+1}^b - \ell_i^b) + (\ell_{i+1}^{b'} - \ell_i^{b'})] (\ell_{i+1}^a - \ell_i^a)} \end{aligned}$$

(6.85)

where we have dropped the prefactor $1/(1 - e^{-2\theta})$, subleading for $\theta > 0$. Indeed, the limits $\theta \rightarrow 0$ and $n \rightarrow \infty$ do not commute, hence (6.85) is only valid for $\theta > 0$. On the other hand, in the limit $\theta \rightarrow \infty$, we recover the large q asymptotics

$$\begin{aligned} \bar{m}_n(q) &\sim q^n \sim e^{n\theta} \\ m_n(q) &\sim c_n q^n \sim \frac{(4e^\theta)^n}{n^{3/2}} \end{aligned} \quad (6.86)$$

by using the two formulas (6.70)(6.69).

As before, we can test the scaling hypothesis used above against the large n asymptotics of the meander determinant for $q > 2$. This hypothesis amounts to writing

$$\begin{aligned} [\mathcal{P}_n^{-1}(e^\theta + e^{-\theta})]_{a,b} &\sim f_{a,b} e^{\frac{\theta}{4} [-2\ell_n^a + \sum_{i=0}^{2n-1} (\ell_{i+1}^b - \ell_i^b)(\ell_{i+1}^a - \ell_i^a)]} \\ [\Gamma_n(e^\theta + e^{-\theta})]_{a,a} &\sim e^{\theta \ell_n^a} \end{aligned} \quad (6.87)$$

The corresponding large n estimate of the meander determinant reads

$$D_n(e^\theta + e^{-\theta}) \sim \prod_{a \in W_n} f_{a,a}^2 e^{n\theta} \sim e^{nc_n \theta} \quad (6.88)$$

whereas the exact formula (5.6) leads to the asymptotics

$$\log D_n(e^\theta + e^{-\theta}) = \theta \sum_{j=1}^n a_{n,j} \log \frac{\sinh(j+1)\theta}{\sinh \theta} \sim nc_n \theta \quad (6.89)$$

by the standard saddle point method. The agreement between the two estimates (6.88)-(6.89) is a confirmation *a posteriori* that the scaling hypothesis (6.87) holds for a very large class of properties of the gram matrix $\mathcal{G}_n(q)$, for $q > 2$ and large n .

Finally, in view of the assumed $q = 2$ value $\nu(2) = 1$, and the exact $q \rightarrow \infty$ value $\nu(\infty) = 1$ (the semi-meander polynomial (6.86) is indeed dominated by the single diagram $b = \mathcal{W}_n^{(n)}$, with winding $\ell_n^b = n \sim n^{\nu(\infty)}$), it is reasonable to infer that $\nu(q)$ is identically equal to 1 for all $q \geq 2$.

6.9. Meander and semi-meander polynomials as SOS partition functions

The asymptotic formulas (6.85) are to be compared with the following exact formulas

$$\begin{aligned} \bar{m}_n(e^\theta + e^{-\theta}) &= \sum_{\substack{a \in P_n, b \in W_n \\ a \text{ symmetric}}} f_{a,b} e^{\frac{\theta}{2} [\ell_n^a + \frac{1}{2} \sum_{i=0}^{2n-1} (\ell_{i+1}^b - \ell_i^b)(\ell_{i+1}^a - \ell_i^a)]} \\ m_n(e^\theta + e^{-\theta}) &= \sum_{\substack{a \in P_n \\ b, b' \in W_n}} f_{a,b} f_{a,b'} e^{\frac{\theta}{4} \sum_{i=0}^{2n-1} [(\ell_{i+1}^b - \ell_i^b) + (\ell_{i+1}^{b'} - \ell_i^{b'})](\ell_{i+1}^a - \ell_i^a)} \end{aligned} \quad (6.90)$$

where a runs now over the set P_n of *all* closed paths of $(2n)$ steps (with $\ell_0^a = \ell_{2n}^a = 0$) *not subject to the constraint* $\ell_i^a \geq 0$. The relations (6.90) may indeed be obtained as

consequences of the following alternative formula for $q^{c(b,b')}$, $b, b' \in W_n$ (to be compared with (6.65))

$$(e^\theta + e^{-\theta})^{c(b,b')} = \sum_{a \in P_n} f_{a,b} f_{a,b'} e^{\frac{\theta}{4} \sum_{i=0}^{2n-1} [(\ell_{i+1}^b - \ell_i^b) + (\ell_{i+1}^{b'} - \ell_i^{b'})]} (\ell_{i+1}^a - \ell_i^a) \quad (6.91)$$

Let us now prove (6.91). On the one hand, as a is both b and b' -symmetric, the values of $t_i(a) = (\ell_{i+1}^a - \ell_i^a)$ are fixed, up to an overall sign, along each connected component of the meander (b, b') , and alternate on successive bridges along the connected component.

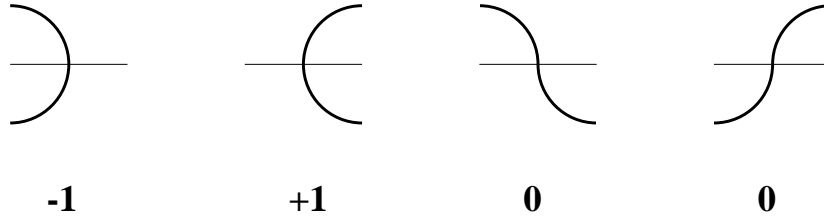


Fig. 22: The four possible local environments of the $(i+1)$ -th bridge together with the corresponding value $s_i(b, b') = \pm 1, 0$.

On the other hand, the quantity $s_i(b, b') = [(\ell_{i+1}^b - \ell_i^b) + (\ell_{i+1}^{b'} - \ell_i^{b'})]/2$ may only take the three values $-1, 0$ and $+1$, corresponding to the four possibilities of local environment of the $(i+1)$ -th bridge of the meander (b, b') , depicted in Fig.22. Along any connected component of (b, b') , the variable $s_i(b, b')$ alternates as long as it remains nonzero, and discarding all the zeros leaves us with an alternating sign.

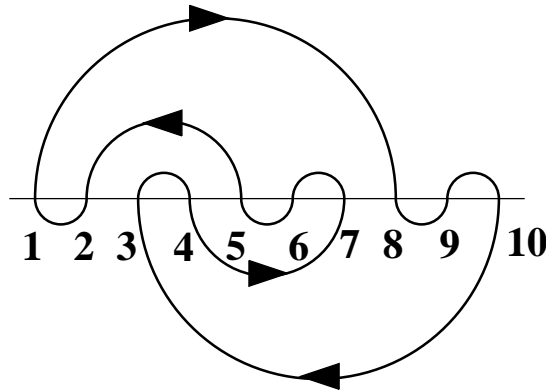


Fig. 23: An oriented connected component K with 10 bridges. Starting from bridge 1, the sequence of visited bridges is 1, 8, 9, 10, 3, 4, 7, 6, 5, 2.

For illustration, with the connected component depicted in Fig.23, this gives the sequence, starting from the bridge 1

bridge i	1	8	9	10	3	4	7	6	5	2
$t_i(a)$	+	-	+	-	+	-	+	-	+	-
$s_i(b, b')$	+	0	0	-	+	0	-	0	0	0
$t_i(a)s_i(b, b')$	+	0	0	+	+	0	-	0	0	0
turn	R	-	-	R	R	-	L	-	-	-

where we also indicated the type of turn (right= R , left= L) taken on the corresponding bridge. The global sign $t_i(a)s_i(b, b')$ is thus constant between two zeros and is reversed through each zero. Since a zero indicates a transition from turning left to right and vice versa along the meander, the quantity

$$\frac{1}{2} \sum_{i \text{ along } K} (\ell_{i+1}^a - \ell_i^a) [(\ell_{i+1}^b - \ell_i^b) + (\ell_{i+1}^{b'} - \ell_i^{b'})] \quad (6.92)$$

summed along any connected component K of the meander (b, b') , is simply equal, up to a sign, to the total number of right turns minus that of left turns ($n_R - n_L$), taken on the bridges along K . As on any closed loop we have $(n_R - n_L) = \pm 2$, we compute

$$\begin{aligned} f(K) &= \sum_{\substack{t_i(a)=\pm 1 \\ i \text{ along } K}} f_{a,b} f_{a,b'} e^{\frac{\theta}{2} \sum_{i \text{ along } K} t_i(a) s_i(a)} \\ &= \sum_{\epsilon=\pm 1} e^{\theta \epsilon (n_R - n_L) / 2} \\ &= e^\theta + e^{-\theta} \end{aligned} \quad (6.93)$$

where the sum over $\epsilon = \pm 1$ corresponds to the only overall sign ambiguity left on the $t_i(a)$ after taking into account the b and b' -symmetry of a on K . The final result (6.91) is simply the product over all the connected components K of (b, b') of the weight $f(K)$ above, which completes the proof of the result.

More generally, the above analysis can be carried over to $q = z + 1/z$, for any complex number z , resulting in

$$(z + 1/z)^{c(b, b')} = \sum_{a \in P_n} f_{a,b} f_{a,b'} z^{\frac{1}{4} \sum_{i=0}^{2n-1} [(\ell_{i+1}^b - \ell_i^b) + (\ell_{i+1}^{b'} - \ell_i^{b'})]} (\ell_{i+1}^a - \ell_i^a) \quad (6.94)$$

This yields the following general expressions for semi-meander and meander polynomials at $q = z + 1/z$ for arbitrary complex z

$$\begin{aligned}
 \bar{m}_n(z + 1/z) &= \sum_{\substack{a \in P_n, b \in W_n \\ a \text{ symmetric}}} f_{a,b} z^{\frac{1}{2}} \left[\ell_n^a + \frac{1}{2} \sum_{i=0}^{2n-1} (\ell_{i+1}^b - \ell_i^b)(\ell_{i+1}^a - \ell_i^a) \right] \\
 m_n(z + 1/z) &= \sum_{\substack{a \in P_n \\ b, b' \in W_n}} f_{a,b} f_{a,b'} z^{\frac{1}{4}} \sum_{i=0}^{2n-1} [(\ell_{i+1}^b - \ell_i^b) + (\ell_{i+1}^{b'} - \ell_i^{b'})] (\ell_{i+1}^a - \ell_i^a)
 \end{aligned}
 \tag{6.95}$$

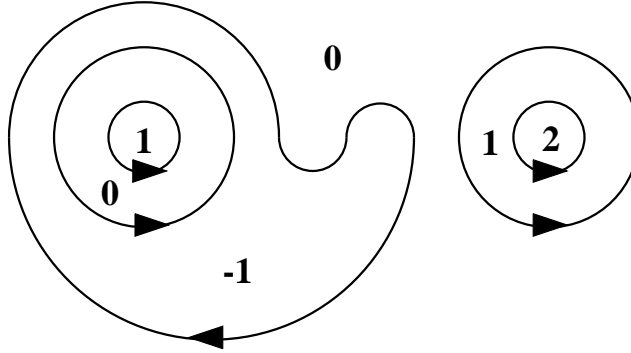


Fig. 24: An example of SOS configuration attached to a meander. We display the value of the height ℓ . Note that it is entirely dictated by the choices of orientation of the connected components of the meander, and the fact that $\ell = 0$ at infinity.

This analysis suggests to interpret the quantity $q^{c(b,b')}$ as the Boltzmann weight of a particular configuration, formed by the meander (b, b') , of a suitably defined *SOS model*. Indeed, the b and b' -symmetry of $a \in P_n$ implies that the variable ℓ_i^a takes identical values on all segments of river which can be connected to each other without crossing any arch of b or b' . Therefore, the variable ℓ_i^a may be considered as a height variable in the plane, constant on each connected component delimited by one or several roads, and undergoing a jump discontinuity of ± 1 across each road (see Fig.24 for an example), and continuous across the river. In particular, $\ell = 0$ at infinity, due to the boundary condition $\ell_0 = \ell_{2n} = 0$. Such an height configuration induces a unique orientation of the various connected components of (b, b') , by taking the convention that $\ell \rightarrow \ell + 1$ (resp. $\ell \rightarrow \ell - 1$) across a road pointing to the right (resp. left). Conversely, a choice of orientation of the connected components of (b, b') specifies uniquely the height configuration, by further demanding that $\ell = 0$ at infinity. The Boltzmann weight

$$z^{\frac{1}{4}} \sum_{i=0}^{2n-1} [(\ell_{i+1}^b - \ell_i^b) + (\ell_{i+1}^{b'} - \ell_i^{b'})] (\ell_{i+1}^a - \ell_i^a)
 \tag{6.96}$$

corresponds to attaching to each bridge of (b, b') one of the following Boltzmann weights

$$\begin{array}{cccc}
 \begin{array}{c} \text{---} \\ \curvearrowright \\ z^{\frac{1}{2}} \end{array} & \begin{array}{c} \text{---} \\ \curvearrowleft \\ z^{\frac{1}{2}} \end{array} & \begin{array}{c} \text{---} \\ \curvearrowright \\ z^{-\frac{1}{2}} \end{array} & \begin{array}{c} \text{---} \\ \curvearrowleft \\ z^{-\frac{1}{2}} \end{array} \\
 \begin{array}{c} \text{---} \\ \curvearrowright \\ 1 \end{array} & \begin{array}{c} \text{---} \\ \curvearrowleft \\ 1 \end{array} & \begin{array}{c} \text{---} \\ \curvearrowright \\ 1 \end{array} & \begin{array}{c} \text{---} \\ \curvearrowleft \\ 1 \end{array}
 \end{array} \tag{6.97}$$

according to the local environment of the bridge, and taking the product over all the bridge weights. Again, summing over the two orientations of each connected component K of (b, b') results in a total weight per connected component

$$\sum_{\epsilon=\pm 1} z^{\epsilon(n_R - n_L)/2} = z + 1/z = q \tag{6.98}$$

where n_R (resp. n_L) is the number of right (resp. left) turns of the road on the bridges of K , and $\epsilon = \pm 1$ accounts for the global orientation of K . In the language of SOS models, the expression (6.65) corresponds to a *Restricted SOS* version, in which the height variable is further restricted to be non-negative (in particular the configuration of Fig.24 is ruled out).

As a first element of comparison with the results of the previous section, if we write (6.95) at $z = 1$, hence $q = 2$, we see that

$$\boxed{
 \begin{array}{l}
 \bar{m}_n(2) = \sum_{\substack{a \in P_n, b \in W_n \\ a \text{ symmetric}}} f_{a,b} \\
 m_n(2) = \sum_{\substack{a \in P_n \\ b, b' \in W_n}} f_{a,b} f_{a,b'}
 \end{array}
 } \tag{6.99}$$

to be compared with the asymptotic estimates (6.78): this gives a relation between sums over P_n and over W_n , involving the same combinations of f . Note that the same type of relation links the cardinals of the two sets over which a is summed, namely

$$\text{card}(P_n) = \binom{n}{2n} = (n+1)c_n = (n+1) \text{card}(W_n) \tag{6.100}$$

and also, using (6.41)

$$\sum_{a \in P_n, b \in W_n} f_{a,b} = 2^n c_n = \frac{2}{3}(n+2) \sum_{a,b \in W_n} f_{a,b} \quad (6.101)$$

The reader could wonder in what the restricted expressions (6.62)(6.63) of the previous section are really different from the simple SOS expressions (6.90) obtained above. Actually, the considerations of the previous section on the heights ℓ dominating the expressions (6.62)(6.63) for the meander and semi-meander polynomials, eventually leading to an exponent $\nu = 1$ for $q = 2$, could not be carried over here, because of the lack of an explicit prefactor proportional to $(\ell + 1)$. Hence, in some sense, the formulas (6.62)(6.63) (at least for $q = 2$) give us access to more precise details on the path formulation.

More generally, it is interesting to compare the $q > 2$ formulas (6.90) and (6.85). We see that these are identical, except for the range of summation over a (W_n in (6.85) and P_n in (6.90)). We conclude that the restriction condition that $\ell_i^a \geq 0$ in (6.85) is not important in the large n limit, for $q > 2$.

7. Generalization: the semi-meander determinant

In this section, we consider a possible generalization of the meander determinant to semi-meanders in the following way.

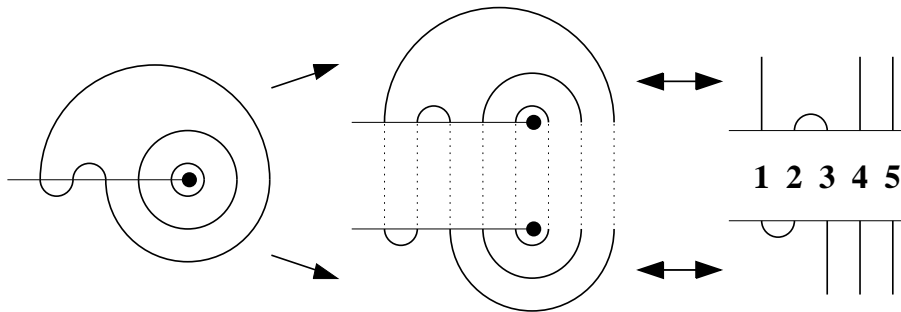


Fig. 25: Any semi-meander may be viewed as the superimposition of an upper and a lower open arch configurations. Here the initial semi-meander has winding 3. The two open arch configurations on the right have $h = 3$ open arches. To recover the initial semi-meander, these open arches must be connected two by two, from the right to the left (the arches number 5,4,1 of the upper configuration are respectively connected to the arches number 5,4,3 of the lower configuration).

Going back to the original river/road formulation of semi-meanders, we see on Fig.25 that any given semi-meander, with winding number h , is obtained as the superimposition of two (upper and lower) *open arch configurations* of order n , with h open arches. By this, we mean that h semi-infinite vertical roads originate from h of the n bridges, otherwise connected by pairs through $(n-h)/2$ nonintersecting arches (the winding h has always the same parity as the order n in the semi-meanders). The semi-meander is re-built in a unique way by connecting the upper and lower open arches from the right to the left. In particular, only open arch configurations with the same number of open arches may be superimposed to yield a semi-meander. Let $A_n^{(h)}$ denote the set of open arch configurations of order n with h open arches. It is a simple exercise to show that

$$\text{card}(A_n^{(h)}) = b_{n,h} = \binom{n}{\frac{n-h}{2}} - \binom{n}{\frac{n-h}{2} - 1} \quad (7.1)$$

Indeed, the open arch configurations of order n with h open arches are in one-to-one correspondence with the half-walk diagrams of n steps, with final height h , namely with $\ell_0 = 0$, $\ell_i \geq 0$ and $\ell_n = h$. Let $W_n^{(h)} \equiv A_n^{(h)}$ denote the set of half-walks of order n with final height h . The number of such half-walks has been derived in eq.(5.52) above. We now define the semi-meander determinant of order n and winding h , as the determinant $D_n^{(h)}(q)$ of the matrix $\mathcal{G}_n^{(h)}(q)$ with entries

$$[\mathcal{G}_n^{(h)}(q)]_{l,l'} = q^{c(l,l')} \quad l, l' \in W_n^{(h)} \equiv A_n^{(h)} \quad (7.2)$$

where $c(l, l')$ denotes the number of connected components of the semi-meander obtained by superimposing the open arch configurations l and l' and connecting their h open arches. For illustration, we list below the matrices corresponding to $n = 4$, $h = 0, 2, 4$

$$\mathcal{G}_4^{(0)}(q) = \begin{pmatrix} q^2 & q \\ q & q^2 \end{pmatrix} \quad \mathcal{G}_4^{(2)}(q) = \begin{pmatrix} q^3 & q^2 & q \\ q^2 & q^3 & q^2 \\ q & q^2 & q^3 \end{pmatrix} \quad \mathcal{G}_4^{(4)}(q) = q^4 \quad (7.3)$$

with the following ordering of open arch configurations

$$h = 0 : \circ \circ, \textcircled{\circ} \quad h = 2 : \circ ||, | \circ |, || \circ \quad h = 4 : ||| | \quad (7.4)$$

Note also that $\mathcal{G}_{2n}^{(0)}(q) = \mathcal{G}_{2n-1}^{(1)}(q) = \mathcal{G}_n(q)$, hence the formula (5.6) applies to the winding zero and one cases. More generally, we conjecture that

$$\boxed{D_n^{(h)}(q) = \det \mathcal{G}_n^{(h)}(q) = \prod_{j=1}^{\frac{n-h}{2}+1} U_j(q)^{\alpha_{n,j}^{(h)}}} \quad (7.5)$$

where the numbers $\alpha_{n,j}^{(h)}$ read, in terms of the $a_{n,j}$ of (5.6)

$$\begin{aligned} \alpha_{2n,j}^{(2h)} &= a_{n,j+h} + 2h a_{n,j+h-1} \\ \alpha_{2n-1,j}^{(2h+1)} &= a_{n,j+h} + 2h (a_{n-1,j+h} + a_{n-1,j+h-1}) \end{aligned} \quad (7.6)$$

We checked the validity of this conjecture up to $n = 9$. For instance, for $n = 8, 9$, we have

$$\begin{aligned} n = 8 \quad \begin{aligned} D_8^{(0)} &= U_1^8 & U_2^{13} & U_3^6 & U_4 \\ D_8^{(2)} &= U_1^{29} & U_2^{32} & U_3^{13} & U_4^2 \\ D_8^{(4)} &= U_1^{58} & U_2^{25} & U_3^4 & \\ D_8^{(6)} &= U_1^{37} & U_2^6 & & \\ D_8^{(8)} &= U_1^8 & & & \end{aligned} \end{aligned} \quad (7.7)$$

$$\begin{aligned} n = 9 \quad \begin{aligned} D_9^{(1)} &= U_1^{15} & U_2^{40} & U_3^{26} & U_4^8 & U_5 \\ D_9^{(3)} &= U_1^{82} & U_2^{64} & U_3^{22} & U_4^3 & \\ D_9^{(5)} &= U_1^{102} & U_2^{36} & U_3^5 & & \\ D_9^{(7)} &= U_1^{50} & U_2^7 & & & \\ D_9^{(9)} &= U_1^9 & & & & \end{aligned} \end{aligned}$$

in agreement with (7.5)(7.6). We have performed various checks on the numbers $\alpha_{n,j}^{(h)}$ (7.6). In particular, the term of highest degree of $D_n^{(h)}(q)$, as a polynomial of q , is given by the product of the diagonal terms in $\mathcal{G}_n^{(h)}(q)$, namely

$$q^{\deg(D_n^{(h)})} = \prod_{l \in W_n^{(h)}} q^{\frac{n+h}{2}} \quad (7.8)$$

hence

$$\deg(D_n^{(h)}) = \frac{n+h}{2} b_{n,h} \quad (7.9)$$

This can actually be derived from (7.6).

We expect that (7.5)(7.6) can be proved by diagonalizing the matrix $\mathcal{G}_n^{(h)}(q)$. This matrix has again a simple interpretation as the Gram matrix of a certain subspace of $TL_n(q)$, generated by some particular basis 1 elements. Inspired by the one-to-one correspondence between walk diagrams of order n and the elements of the basis 1, we attach

to any half-walk l of n steps and final height h in $W_n^{(h)}$ the basis 1 element $(a)_1$ corresponding to the walk diagram $a = lr \in W_n$, where we have completed the half-walk l with a particular choice of right half-walk r of final height h , namely with $\ell_i^r = [1 + (-1)^i]/2$, $i = 0, 1, \dots, n-h$, and $\ell_i^r = i+h-n$ for $i = n-h+1, n-h+2, \dots, n$. This corresponds to only retaining basis 1 elements which are obtained by acting on $f_h^{(n)}$ (defined in (3.6)) through *left* multiplications by e_i . In this new basis, the scalar product between two elements reads

$$(lr, l'r) = \text{Tr}((lr)_1(l'r)_1^t) = q^{c(lr, l'r)} = q^{\frac{n-h}{2}} q^{c(l, l')} \quad (7.10)$$

which coincides with (7.2) up to an overall prefactor of $q^{(n-h)/2}$ due to the addition of $(n-h)/2$ trivial loops to the semi-meander ll' . A proof of (7.5)(7.6) should follow the lines of that of (5.6), by writing a change of basis which diagonalizes the Gram matrix (7.2). Note also that like in the meander case, the formula (7.5)(7.6) gives the multiplicities of the zeros of $D_n^{(h)}(q)$.

Finally, the product over all the possible windings of the semi-meander determinants takes the simple form

$$\boxed{\bar{D}_n(q) = \prod_{\substack{h=0 \\ n-h=0 \pmod{2}}}^n D_n^{(h)}(q) = \prod_{j=1}^n U_j(q)^{\beta_{n,j}}} \quad (7.11)$$

where

$$\boxed{\begin{aligned} \beta_{2n,j} &= 3 \binom{2n}{n-j} - \binom{2n}{n-j-1} \\ \beta_{2n-1,j} &= 3 \binom{2n}{n-j} - 2 \binom{2n-1}{n-j} - \binom{2n}{n-j-1} \end{aligned}} \quad (7.12)$$

as a direct consequence of (7.6), with $\beta_{n,j} = \sum_h \alpha_{n,j}^{(h)}$. Eq.(7.11) may be viewed as the semi-meander counterpart of (5.6).

The semi-meander gram matrix (7.2) also gives access to refined properties of the semi-meanders. Indeed, we may compute

$$\begin{aligned} \bar{m}_n^{(h)}(q^2) &= \text{Tr}(\mathcal{G}_n^{(h)}(q)^2) \\ &= \sum_{k=1}^n \bar{M}_n^{(k)}(h) q^{2k} \end{aligned} \quad (7.13)$$

where $\bar{M}_n^{(k)}(h)$ denotes the total number of semi-meanders of order n with winding h and k connected components. An asymptotic study of these numbers should be made possible by the explicit diagonalization of $\mathcal{G}_n^{(h)}(q)$.

8. Conclusion

In this paper, we have extensively studied the representation of the meander and semi-meander enumeration problems within the framework of the Temperley-Lieb algebra $TL_n(q)$. This representation is induced by the existence of a map between the reduced elements of $TL_n(q)$ and the arch configurations of order n used to build meanders and semi-meanders. Moreover, we have seen that the standard trace over $TL_n(q)$ provides a tool for counting the number of connected components of meandric objects. The first result of this paper is a direct computation of the meander determinant (5.6), interpreted as the Gram determinant of the basis of reduced elements of $TL_n(q)$, and the exact study of its zeros (5.11) and associated multiplicities (5.23)(5.34).

Beyond the meander determinant, we have been able to rewrite the change of basis diagonalizing the Gram matrix in terms of local height variables defining a restricted SOS model (see (6.65)). We also derived an unrestricted SOS model interpretation (see (6.94)) of the Gram matrix elements. These lead to various expressions for the meander and semi-meander polynomials, as weighted sums over discrete paths (walk diagrams). It is tempting to try to approximate these sums by continuous path integrals, in the limit of large number of bridges. In the case $q \geq 2$, where all the SOS Boltzmann weights are positive, this path integral might even be dominated by a simple subset of configurations, obtained for instance through a saddle point approximation.

A generalization of this approach to the semi-meanders with fixed winding (number of times the roads wind around the source of the river) should be possible, in view of the conjectured form (7.5) for the corresponding (fixed winding) semi-meander determinants. A proof of (7.5) should be at hand, by a simple adaptation of the proof of (5.6) presented here. This will be addressed elsewhere.

Acknowledgements

We thank A. Zvonkin for bringing Ref.[4] to our knowledge, R. Balian for helpful discussions, S. Legendre for interesting historical remarks and J.-B. Zuber for a careful reading of the manuscript.

Appendix A. Proof of the formula (5.23) for the multiplicities of the zeros of the meander determinant

In order to prove (5.23), we note that

$$\delta_{j+1,0 \bmod (k+1)} = \frac{1}{k+1} \sum_{m=0}^k (\omega_{k+1})^{m(j+1)} \quad (\text{A.1})$$

where $\omega_{k+1} = e^{2i\pi/(k+1)}$, and rewrite

$$\begin{aligned}
d_n(z_{k,l}) &= \frac{1}{k+1} \sum_{m=0}^k \sum_{j=1}^n (\omega_{k+1})^{m(j+1)} a_{n,j} \\
&= \frac{1}{k+1} \sum_{m=0}^k \sum_{j=1}^n \binom{2n}{n-j} \left[(\omega_{k+1})^{m(j+1)} - 2(\omega_{k+1})^{mj} + (\omega_{k+1})^{m(j-1)} \right] \\
&\quad - \binom{2n}{n-1} \\
&= -\frac{1}{k+1} \sum_{m=0}^k (2 \sin \frac{\pi m}{k+1})^2 \sum_{j=1}^n \binom{2n}{n-j} (\omega_{k+1})^{mj} - \binom{2n}{n-1} \\
&= -\frac{1}{2(k+1)} \sum_{m=0}^k (2 \sin \frac{\pi m}{k+1})^2 \left[(\sqrt{\omega_{k+1}} + \frac{1}{\sqrt{\omega_{k+1}}})^{2n} - \binom{2n}{n} \right] \\
&\quad - \binom{2n}{n-1} \\
&= c_n - \frac{1}{2(k+1)} \sum_{m=1}^k (2 \sin \frac{\pi m}{k+1})^2 (2 \cos \frac{\pi m}{k+1})^{2n}
\end{aligned} \tag{A.2}$$

which is equivalent to (5.23). In the second line of (A.2), we have performed two discrete integrations by parts, which have produced the boundary term $\binom{2n}{n-1}$. In the fourth line of (A.2), we have used the reality of $d_n(z_{k,l})$ to express the sum over j as

$$\sum_{j=1}^n \binom{2n}{n-j} \frac{\omega^j + \omega^{-j}}{2} = \frac{1}{2} \left[(\sqrt{\omega} + \frac{1}{\sqrt{\omega}})^{2n} - \binom{2n}{n} \right] \tag{A.3}$$

In the last line of (A.2), we have used the sum rule

$$\frac{1}{2(k+1)} \sum_{m=0}^k \left(2 \sin \frac{\pi m}{k+1} \right)^2 = 1 \tag{A.4}$$

and recombined $\binom{2n}{n} - \binom{2n}{n-1} = c_n$.

Appendix B. The Gram matrix at $q = \sqrt{2}$

Let us illustrate the conjecture (5.39) in the case $k = 3$, $l = 1$, namely $q = z_{3,1} = \sqrt{2}$. For $n = 3, 4$ we have the following identities relating the last line of $\mathcal{G}_n(\sqrt{2})$ to those corresponding to diagrams of maximal height 2

$$\begin{aligned}
\begin{array}{c} \bullet \\ \diagup \quad \diagdown \\ \bullet \quad \bullet \\ \diagup \quad \diagdown \quad \diagup \quad \diagdown \\ \bullet \quad \bullet \quad \bullet \quad \bullet \\ \diagup \quad \diagdown \quad \diagup \quad \diagdown \quad \diagup \quad \diagdown \\ \bullet \quad \bullet \quad \bullet \quad \bullet \quad \bullet \quad \bullet \end{array} &= \sqrt{2} \left(\begin{array}{c} \bullet \quad \bullet \\ \diagup \quad \diagdown \\ \bullet \quad \bullet \end{array} + \begin{array}{c} \bullet \quad \bullet \\ \diagdown \quad \diagup \\ \bullet \quad \bullet \end{array} \right) - \left(\begin{array}{c} \bullet \quad \bullet \\ \diagup \quad \diagdown \\ \bullet \quad \bullet \end{array} + \begin{array}{c} \bullet \quad \bullet \\ \diagdown \quad \diagup \\ \bullet \quad \bullet \end{array} \right) \\
\begin{array}{c} \bullet \\ \diagup \quad \diagdown \\ \bullet \quad \bullet \\ \diagup \quad \diagdown \quad \diagup \quad \diagdown \\ \bullet \quad \bullet \quad \bullet \quad \bullet \\ \diagup \quad \diagdown \quad \diagup \quad \diagdown \quad \diagup \quad \diagdown \\ \bullet \quad \bullet \quad \bullet \quad \bullet \quad \bullet \quad \bullet \end{array} &= \sqrt{2} \left(\begin{array}{c} \bullet \quad \bullet \quad \bullet \\ \diagup \quad \diagdown \\ \bullet \quad \bullet \quad \bullet \end{array} + \begin{array}{c} \bullet \quad \bullet \quad \bullet \\ \diagdown \quad \diagup \\ \bullet \quad \bullet \quad \bullet \end{array} \right) - \left(\begin{array}{c} \bullet \quad \bullet \quad \bullet \\ \diagup \quad \diagdown \\ \bullet \quad \bullet \quad \bullet \end{array} + \begin{array}{c} \bullet \quad \bullet \quad \bullet \\ \diagdown \quad \diagup \\ \bullet \quad \bullet \quad \bullet \end{array} \right)
\end{aligned} \tag{B.1}$$

where each line vector is represented by its labeling diagram. In turn, the labeling diagram represents a basis 1 element for $TL_n(q = \sqrt{2})$. The equations (B.1) translate into the fact that the element

$$E_3(e_1, e_2) = 1 - \sqrt{2}(e_1 + e_2) + (e_2e_1 + e_1e_2) \quad (\text{B.2})$$

is *orthogonal* (with respect to the scalar product (3.12)) to all the elements of respectively $TL_3(\sqrt{2})$ and $TL_4(\sqrt{2})$. This is a direct consequence of the following identities

$$\begin{aligned} e_1 E_3(e_1, e_2) &= e_2 E_3(e_1, e_2) = 0 \\ \text{Tr}(1 E_3(e_1, e_2)) &= \eta U_3(\sqrt{2}) = 0 \\ \text{Tr}(e_3 E_3(e_1, e_2)) &= \sqrt{2} U_3(\sqrt{2}) = 0 \end{aligned} \quad (\text{B.3})$$

where the first and second lines are valid in both $TL_3(\sqrt{2})$ ($\eta = 1$) and $TL_4(\sqrt{2})$ ($\eta = \sqrt{2}$), and the third line holds only in $TL_4(\sqrt{2})$.

More generally, the element (B.2) is orthogonal to all the elements of $TL_n(\sqrt{2})$ for any $n \geq 5$ as the e_i commute with $E_3(e_1, e_2)$ for $i \geq 4$. For $n \geq 5$ however, all the linear combinations we get involve diagrams with some heights ≥ 3 . For instance, for $n = 5$, the first combination reads

$$\triangle = \sqrt{2} \left(\begin{array}{c} \diagup \diagdown \\ \diagup \diagdown \\ \diagup \diagdown \end{array} + \begin{array}{c} \diagup \diagdown \\ \diagup \diagdown \\ \diagup \diagdown \end{array} \right) - \left(\begin{array}{c} \diagup \diagdown \\ \diagup \diagdown \\ \diagup \diagdown \end{array} + \begin{array}{c} \diagup \diagdown \\ \diagup \diagdown \\ \diagup \diagdown \end{array} \right) \quad (\text{B.4})$$

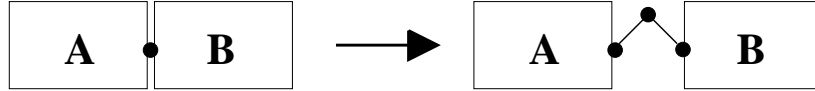


Fig. 26: The enhancement transformation of a walk diagram. The walk diagram $a = AB \in W_n$ is enhanced at the point marked by a dot, by simply inserting a maximum at this point. Here $A = l$ and $B = r^t$, as the marked point lies in the middle of the diagram. The enhanced diagram belongs to W_{n+1} .

Note that going from TL_4 to TL_5 (as well as going from TL_3 to TL_4) amounts simply to enhancing the middle part of the diagrams, as depicted in Fig.26, which results in a middle height $\ell_4 = 2 \rightarrow \ell'_5 = 3$ for the four diagrams on the r.h.s. of (B.4). To reexpress the combination (B.4) in terms of diagrams of $W_{5,2}$, we note that the four diagrams appearing in the r.h.s. of (B.4) contain a middle sequence of heights of the form $(\ell_3 = 1, \ell_4 = 2, \ell_5 = 3, \ell_6 = 2, \ell_7 = 1)$, as the result of two successive enhancements. Using

the first line of (B.1), we may rewrite this central part as a linear combination of four diagrams with central height ≤ 2 , which results in the four combinations

$$\begin{aligned}
\text{Diagram 1} &= \sqrt{2} (\text{Diagram 1.1} + \text{Diagram 1.2}) - (\text{Diagram 1.3} + \text{Diagram 1.4}) \\
\text{Diagram 2} &= \sqrt{2} (\text{Diagram 2.1} + \text{Diagram 2.2}) - (\text{Diagram 2.3} + \text{Diagram 2.4}) \\
\text{Diagram 3} &= \sqrt{2} (\text{Diagram 3.1} + \text{Diagram 3.2}) - (\text{Diagram 3.3} + \text{Diagram 3.4}) \\
\text{Diagram 4} &= \sqrt{2} (\text{Diagram 4.1} + \text{Diagram 4.2}) - (\text{Diagram 4.3} + \text{Diagram 4.4})
\end{aligned} \tag{B.5}$$

which, upon substitution into (B.4), yield the desired expression of the last line of $\mathcal{G}_5(\sqrt{2})$ as a linear combination of the $2^{5-1} = 16$ lines corresponding to the elements of $W_{5,2}$. Note that all these diagrams have middle height 1. For general n , we have the following recursive algorithm to generate the desired linear combination expressing the last line of $\mathcal{G}_n(\sqrt{2})$ in terms of the lines $a \in W_{n,2}$, denoted by $K_n = \sum_{a \in W_{n,2}} \lambda_a^n(a)$. The combinations K_3 , K_4 and K_5 have been constructed above. Suppose we have constructed K_n . Two situations may occur for K_{n+1} .

- (i) If $n = 2p - 1$, the combination K_{2p} is simply obtained by enhancing (see Fig.26) the middle of all the diagrams of $W_{2p-1,2}$ appearing in K_{2p-1} , and keeping the coefficients of the combination fixed. But as the middle heights always satisfy $\ell_n = n \bmod 2$, for all n , the diagrams of $W_{2p-1,2}$ have all middle height $\ell_{2p-1} = 1$. Therefore, the combination K_{2p} only contains elements of $W_{2p,2}$, with middle height $\ell_{2p} = 2$.
- (ii) If $n = 2p$, the combination K_{2p+1} is obtained in two steps. First enhance the middle of all the diagrams in K_{2p} to get another linear combination L_{2p+1} . According to the previous discussion, the enhanced diagrams in L_{2p+1} have all middle height equal to 3. But they actually arise from the diagrams appearing in K_{2p-1} , after *two successive* enhancements. This means that they all contain a middle sequence of heights of the form $(\ell_{n-1} = 1, \ell_n = 2, \ell_{n+1} = 3, \ell_{n+2} = 2, \ell_{n+3} = 1)$. The second step consists in using the first line of (B.1) to reexpress this middle piece as a linear combination of diagrams with middle height $1 \leq 2$. This yields K_{2p+1} after substitution in L_{2p+1} .

By carefully following the above algorithm, we find the following compact expression for the linear combination K_{2p+1} .

$$\boxed{(\mathcal{W}_{2p+1}^{(2p+1)}) = K_{2p+1} = \sum_{j=0}^p (-1)^j (\sqrt{2})^{p-j} \sum_{a \in I_j} (a)} \tag{B.6}$$

where the sets $I_j \subset W_{2p+1,2}$ are constructed recursively as follows. I_0 is the set of symmetric diagrams of $W_{2p+1,2}$. I_k is the set of diagrams of $W_{2p+1,2}$ which may be obtained from diagrams in I_{k-1} by *one* box addition, and which are not already elements of some I_{k-l} , $l \geq 1$. One can easily show that $\text{card}(I_j) = 2^p \binom{p}{j}$. The reader will easily check (B.6) for $n = 3, 4, 5$, with the previous expressions (B.1)(B.4)(B.5). The expression for K_{2p+2} is easily obtained by enhancing K_{2p+1} (case (i) above).

This leads to the relation (5.39) linking the semi-meander polynomial of degree $(2p+1)$ at $q = \sqrt{2}$ to the polynomials (5.40) corresponding to the closures of all $a \in W_{2p+1,2}$, at the same value of q

$$\boxed{\bar{m}_{2p+1}(\sqrt{2}) = \sum_{j=0}^p (-1)^j (\sqrt{2})^{p-j} \sum_{a \in I_j} \bar{m}(a, \sqrt{2})} \quad (\text{B.7})$$

This proves the conjectured relation (5.39) in the case $k = 3, l = 1$. Note also that changing $\sqrt{2} \rightarrow -\sqrt{2}$ in (B.7) gives an analogous relation in the case $k = 3, l = 2$.

More generally, the element $\varphi_n^{(n)} = E_n(e_1, \dots, e_{n-1})$ (4.5) is orthogonal to all the elements of $TL_n(q = 2 \cos \pi/(n+1))$, as a consequence of the identities

$$\begin{aligned} e_i \varphi_n^{(n)} &= 0 \quad \text{for } i = 1, 2, \dots, n-1 \\ \text{Tr} \varphi_n^{(n)} &= U_n(q = 2 \cos \frac{\pi}{n+1}) = 0 \end{aligned} \quad (\text{B.8})$$

This permits to express the last line of $\mathcal{G}_n(q = 2 \cos \pi/(n+1))$ (corresponding to the diagram $\mathcal{W}_n^{(n)}$ or equivalently to the element $(\mathcal{W}_n^{(n)})_1 = 1$) as a linear combination of the $(c_n - 1)$ other lines, corresponding to diagrams with heights $\leq (n-1)$, and middle height $(n-2)$. This implies in particular that $r_n(2 \cos \pi/(n+1)) \leq c_n - 1$, and agrees with the conjectured relation (5.36), which reads here

$$d_n(2 \cos \frac{\pi}{n+1}) = 1 \quad r_n(2 \cos \frac{\pi}{n+1}) = c_n - 1 \quad (\text{B.9})$$

For $m > n$, $E_n(e_1, \dots, e_{n-1})$ remains orthogonal to all the elements of $TL_m(2 \cos \pi/(n+1))$. This results in an expression of the last line of $\mathcal{G}_m(2 \cos \pi/(n+1))$ as a linear combination of the $(c_n - 1)$ repeated $(m - n)$ times) enhancements of the elements of $W_{n,n-1}$, which belong to $W_{m,m-1}$. For $m = n+1$, the elements of the enhanced linear combination still lie in $W_{n,n-1}$ as only the middle heights have been affected, and changed from $(n-2)$ to $(n-1)$. Hence all the linear combinations corresponding to $m = kn+1$ are the trivial enhancements of the linear combination at $m = kn$. In all the other cases, many reductions must be applied to the diagrams to eventually get a linear combination of elements of $W_{m,n-1}$ only. We will not discuss the details of this mechanism here.

Appendix C. Proof of the sum rule (6.41)

We wish to establish the following result

$$\boxed{\sum_{a,b \in W_n} f_{a,b} = 2^n c_n - \frac{1}{8} 2^{n+1} c_{n+1}} \quad (\text{C.1})$$

valid for $n \geq 1$ (we set the number on the lhs of (C.1) to be 1 when $n = 0$). By a simple rearrangement of factorials, this is readily seen to be equivalent to (6.41). Our strategy will be the following. First we write a system of recursion relations linking the numbers (C.1) to other numbers, to be defined below. We proceed and show that this set completely determines all the numbers, provided we take some suitable boundary conditions. Finally, we solve the system explicitly, and extract back the exact value (C.1).

Like in Sect. 6.9, we denote by P_n the set of unrestricted walks a , such that $\ell_0^a = \ell_{2n}^a = 0$, without the positivity constraint on the ℓ_i^a 's. Let $P_n^{(-k)}$ denote the set of walks $a \in P_n$, whose (possibly negative) heights are bounded from below by $-k$, k a given nonnegative integer.

$$P_n^{(-k)} = \{a \in P_n, \text{s.t. } \ell_0^a = \ell_{2n}^a = 0 \text{ and } \ell_i^a \geq -k, \forall i\} \quad (\text{C.2})$$

In particular, $P_n^{(0)} = W_n$. Note also that if $k \geq n$, the above restriction amounts to no restriction at all, hence $P_n^{(-k)} = P_n$. We define $\eta_n^{(k)}$ to be the total number of couples (a, b) , $a \in P_n^{(-k)}$ and $b \in W_n$, such that a is b -symmetric

$$\eta_n^{(k)} = \sum_{a \in P_n^{(-k)}, b \in W_n} f_{a,b} \quad (\text{C.3})$$

and E_k the generating function

$$E_k(x) = \sum_{n=0}^{\infty} \eta_n^{(k)} x^n \quad (\text{C.4})$$

Again, whenever $k \geq n$, we simply have

$$\eta_n^{(k)} = \sum_{a \in P_n, b \in W_n} f_{a,b} = 2^n c_n \quad (\text{C.5})$$

as shown in (6.101).

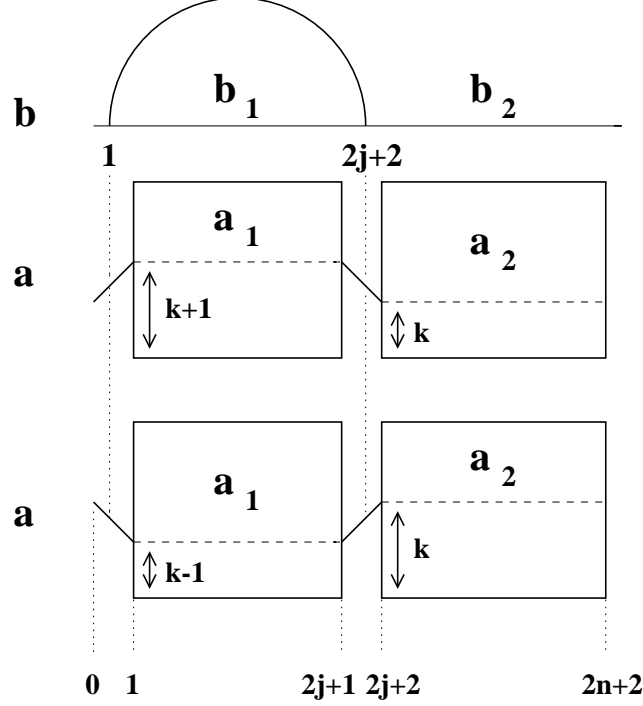


Fig. 27: The recursion for $\eta_{n+1}^{(k)}$. The diagram $b \in W_{n+1}$ is represented as an arch configuration, and we have represented its leftmost arch, separating its interior piece $b_1 \in W_j$ from its exterior piece $b_2 \in W_{n-j}$. The a 's $\in P_{n+1}^{(-k)}$ which are b -symmetric are of either form depicted. In the first case, $\ell_1^a = \ell_{2j+1}^a = 1$. The piece a_1 of a between these two points is b_1 -symmetric, and has its restriction condition lowered by 1: $a_1 \in P_j^{(-k-1)}$ (the dashed line represents the $\ell = 0$ line in the a_i 's). There are $\eta_j^{(k+1)}$ such couples (a_1, b_1) . In the second case, $\ell_1^a = \ell_{2j+1}^a = -1$. a_1 is b_1 -symmetric, but now its restriction condition is raised by 1: $a_1 \in P_j^{(-k+1)}$. There are $\eta_j^{(k-1)}$ such couples (a_1, b_1) . The piece a_2 is b_2 -symmetric and has its restriction condition unchanged in both cases: $a_2 \in P_{n-j}^{(-k)}$. There are $\eta_{n-j}^{(k)}$ couples (a_2, b_2) .

The desired result (C.1) amounts to writing that

$$E_0(x) = C(2x) - \frac{1}{8x}(C(2x) - 1 - 2x) \quad (\text{C.6})$$

where $C(x)$ denotes the generating function (5.35) of the Catalan numbers (the subtractions in the second term are *ad hoc* to yield the initial value $\eta_0^{(0)} = 1$).

Let us now derive a system of recursion relations for the numbers $\eta_n^{(k)}$. Let us count the pairs of walk diagrams $(a \in W_{n+1}, b \in W_{n+1})$ such that a is b -symmetric. Representing b in the arch configuration picture as in Fig.27, let us concentrate on its leftmost arch, connecting the first bridge (1) to, say, the bridge $(2j+2)$ (the bridge number must clearly

be even). This arch isolates its interior, corresponding to the bridges $2, 3, \dots, (2j+1)$ from its exterior, corresponding to the bridges $(2j+3), \dots, (2n+2)$: these two sets of bridges cannot be connected to each other. Let us now count the a 's which are b -symmetric, and consider an $a \in W_{n+1}$, such that $f_{a,b} = 1$. The part a_1 of a corresponding to the interior b_1 of the leftmost arch of b is symmetric w.r.t. this piece of b . The same holds for the part a_2 of a corresponding to the exterior b_2 of this arch, which may be simply seen as a walk with $2(n-j)$ steps, i.e. an element of W_{n-j} . In addition, we also have $\ell_1^a - \ell_0^a = 1 = \ell_{2j+1}^a - \ell_{2j+2}^a$ by symmetry w.r.t. the leftmost arch of b , which implies that $\ell_1^a = \ell_{2j+1}^a = 1$, while $\ell_i^a \geq 0$ for $i = 1, 2, \dots, 2j+1$. Therefore, by a trivial translation of the heights and bridge numbers $\ell'_i = \ell_{i+1} - 1$, the part of a corresponding to the interior of the arch may be seen as a walk of $(2j)$ steps with $\ell_0^{a'} = \ell_{2j}^{a'} = 0$, but with the constraint that $\ell_i^{a'} \geq -1$ for $i = 0, 1, \dots, 2j$, hence as an element of $P_j^{(-1)}$. Conversely, we may build any a which is b -symmetric by the juxtaposition of a walk in $P_j^{(-1)}$ and one in W_{n-j} , with the respective conditions that they are b -symmetric w.r.t. the corresponding portions of b , and elevating the interior portion by shifting the ℓ^a 's of $P_j^{(-1)}$ by $+1$, and adding $\ell_0^a = \ell_{2j+2}^a = 0$. This is summarized in the following recursion relation

$$\eta_{n+1}^{(0)} = \sum_{j=0}^n \eta_j^{(1)} \eta_{n-j}^{(0)} \quad (\text{C.7})$$

More generally, the same reasoning applies to $\eta_{n+1}^{(k)}$, with the result (see Fig.27)

$$\eta_{n+1}^{(k)} = \sum_{j=0}^n (\eta_j^{(k+1)} + \eta_j^{(k-1)}) \eta_{n-j}^{(k)} \quad (\text{C.8})$$

where two situations may now occur for the part of a corresponding to the interior of the arch: either $\ell_1^a = \ell_{2j+1}^a = 1$, in which case the restriction condition on a is lowered by 1 (term $\eta_j^{(k+1)}$), or $\ell_1^a = \ell_{2j+1}^a = -1$, which may occur as soon as $k \geq 1$, in which case the restriction condition is raised by 1 (term $\eta_j^{(k-1)}$). The exterior part of a is unaffected and keeps the restriction condition at level $-k$ (term $\eta_{n-j}^{(k)}$). We may take (C.8) as generic recursion relation, also valid for $k = 0$, provided we define $\eta_n^{(-1)} \equiv 0$ for all $n \geq 0$. In addition to this boundary condition, we set $\eta_0^{(k)} = 1$ for all k (there is exactly one walk diagram of 0 steps, with $\ell_0 = 0$, whatever the restriction k).

The recursion relations (C.8) together with the boundary conditions

$$\eta_n^{(-1)} = 0 \quad \eta_0^{(k)} = 1 \quad (\text{C.9})$$

determine all the numbers $\eta_n^{(k)}$ completely. Indeed, (C.8) expresses η_{n+1} in terms of η_j , $j \leq n$, hence by repeated applications, we may express all the numbers $\eta_n^{(k)}$ in terms of the collection of numbers $\eta_0^{(k)}$. This establishes the uniqueness of the solution to (C.8)(C.9), provided it exists. To show the existence, we next exhibit the solution explicitly. It is best expressed in terms of the generating functions $E_k(x)$ (C.4), in terms of the variable

$$y = \frac{C(2x) - 1}{2} = \sum_{n=1}^{\infty} 2^{n-1} c_n x^n \quad (\text{C.10})$$

easily invertible as

$$x = \frac{y}{(2y + 1)^2} \quad (\text{C.11})$$

by use of (5.35). The general solution reads

$$E_{2k}(x) = 2y + 1 - \frac{y + 1}{U_k(1/y)U_{k+1}(1/y)}$$

$$E_{2k+1}(x) = 2y + 1 - \frac{(2y + 1)(y + 1)}{y(U_k(1/y) + U_{k+1}(1/y))(U_{k+1}(1/y) + U_{k+2}(1/y))}$$

(C.12)

where $U_k(z)$ denote the Chebishev polynomials (4.2). Note in particular that for $k = 0$, we recover $E_0(x) = 1 + 2y - y(y + 1) = 1 + y - y^2$, which yields the desired result (C.6), and therefore proves (C.1). The first few generating functions read

$$\begin{aligned} E_0(x) &= 1 + y - y^2 \\ E_1(x) &= \frac{(1 - y)(2y + 1)^2}{1 + y - y^2} \\ E_2(x) &= \frac{1 + y - 2y^2 - y^3}{1 - y} \\ E_3(x) &= \frac{(1 - 2y^2)(2y + 1)^2}{(1 + y - y^2)(1 + y - 2y^2 - y^3)} \end{aligned} \quad (\text{C.13})$$

Note also that the expressions (C.12) make it clear that the $E_k(x)$ converge uniformly towards $(2y + 1) = C(2x)$ when $k \rightarrow \infty$, for small enough x (indeed, when expanded at small y , (C.12) reads $E_k(x) = 2y + 1 + O(y^{k+1}) \rightarrow 2y + 1$ when $k \rightarrow \infty$). This is not surprising, as letting k tend to infinity amounts to progressively removing the constraints on the counted paths, whose numbers tend to $2^n c_n$ (they are actually exactly equal to this for all $n \leq k$), and $2y + 1 = C(2x)$ is precisely the generating function for unconstrained paths.

To prove (C.12), let us rephrase the recursion relations (C.8) in terms of generating functions. We have

$$E_k(x) - 1 = xE_k(x)(E_{k+1}(x) + E_{k-1}(x)) \quad (\text{C.14})$$

where we have used the boundary condition $\eta_0^{(k)} = 1 \Rightarrow E_k(0) = 1$. The remainder of (C.9) implies that

$$E_{-1}(x) = 0 \quad (\text{C.15})$$

It is now a straightforward but tedious exercise to check that (C.14) is satisfied by (C.12).

For odd $k = 2p + 1$, we have

$$\begin{aligned} 1 - x(E_{2p+2}(x) + E_{2p}(x)) &= 1 - \frac{2y}{2y+1} + \frac{y(y+1)}{(2y+1)^2} \frac{U_{p+2}(1/y) + U_p(1/y)}{U_p(1/y)U_{p+1}(1/y)U_{p+2}(1/y)} \\ &= \frac{1}{2y+1} + \frac{y+1}{(2y+1)^2 U_p(1/y)U_{p+2}(1/y)} \\ &= \frac{(2y+1)U_p(1/y)U_{p+2}(1/y) + y+1}{(2y+1)^2 U_p(1/y)U_{p+2}(1/y)} \end{aligned} \quad (\text{C.16})$$

where, in the second line, we have used the recursion relation (4.1). On the other hand, we compute

$$\frac{1}{E_{2p+1}(x)} = \frac{y(U_p + U_{p+1})(U_{p+1} + U_{p+2})}{(2y+1)\left(y(U_p + U_{p+1})(U_{p+1} + U_{p+2}) - y - 1\right)} \quad (\text{C.17})$$

Using the multiplication rule

$$U_k(t)U_m(t) = \sum_{\substack{j=|m-k| \\ j=m+k \bmod 2}}^{m+k} U_j(t) \quad (\text{C.18})$$

easily proved by recursion, and implying in particular that $U_{p+1}^2 = U_p U_{p+2} + 1$, we reexpress

$$\begin{aligned} (U_p(t) + U_{p+1}(t))(U_{p+1}(t) + U_{p+2}(t)) &= U_{p+1}(U_p + U_{p+2}) + U_{p+1}^2 + U_p U_{p+2} \\ &= (t+1)U_{p+1}^2 + U_p U_{p+2} \\ &= (t+1)(U_p U_{p+2} + 1) + U_p U_{p+2} \\ &= (t+2)U_p(t)U_{p+2}(t) + t + 1 \end{aligned} \quad (\text{C.19})$$

by various applications of (C.18). Substituting this into (C.17), with $t = 1/y$, this gives exactly (C.16), thus proving (C.14) for $k = 2p + 1$.

For even $k = 2p$, we have

$$\begin{aligned}
1 - x(E_{2p+1}(x) + E_{2p-1}(x)) &= \frac{1}{2y+1} + \frac{y+1}{2y+1} \frac{U_{p-1} + U_p + U_{p+1} + U_{p+2}}{(U_{p-1} + U_p)(U_p + U_{p+1})(U_{p+1} + U_{p+2})} \\
&= \frac{1}{2y+1} + \frac{y+1}{y(2y+1)(U_{p-1} + U_p)(U_{p+1} + U_{p+2})} \\
&= \frac{(U_{p-1} + U_p)(U_{p+1} + U_{p+2}) + (y+1)/y}{(2y+1)(U_{p-1} + U_p)(U_{p+1} + U_{p+2})}
\end{aligned} \tag{C.20}$$

We then compute

$$\begin{aligned}
&(U_{p-1}(t) + U_p(t))(U_{p+1}(t) + U_{p+2}(t)) + t + 1 \\
&= (U_{p-1}U_{p+1} + U_pU_{p+2}) + U_{p-1}U_{p+2} + U_pU_{p+1} + t + 1 \\
&= (tU_pU_{p+1} - 1) + (U_pU_{p+1} - U_1) + U_pU_{p+1} + t + 1 \\
&= (t+2)U_p(t)U_{p+1}(t)
\end{aligned} \tag{C.21}$$

Finally, we write

$$\frac{1}{E_{2p}(x)} = \frac{U_p(1/y)U_{p+1}(1/y)}{(2y+1)U_p(1/y)U_{p+1}(1/y) - y - 1} \tag{C.22}$$

which, upon the substitution of (C.21), with $t = 1/y$, is equal to (C.20). This completes the proof of (C.14) for $k = 2p$.

References

- [1] K. Hoffman, K. Mehlhorn, P. Rosenstiehl and R. Tarjan, *Sorting Jordan sequences in linear time using level-linked search trees*, Information and Control **68** (1986) 170-184.
- [2] A. Phillips, *La topologia dei labirinti*, in M. Emmer, ed. *L'occhio di Horus: itinerario nell'immaginario matematico*, Istituto della Enciclopedia Italia, Roma (1989) 57-67.
- [3] V. Arnold, *The branched covering of $CP_2 \rightarrow S_4$, hyperbolicity and projective topology*, Siberian Math. Jour. **29** (1988) 717-726.
- [4] K.H. Ko, L. Smolinsky, *A combinatorial matrix in 3-manifold theory*, Pacific. J. Math **149** (1991) 319-336.
- [5] S. Lando and A. Zvonkin, *Plane and Projective Meanders*, Theor. Comp. Science **117** (1993) 227-241, and *Meanders*, Selecta Math. Sov. **11** (1992) 117-144.
- [6] P. Di Francesco, O. Golinelli and E. Guitter, *Meander, folding and arch statistics*, to appear in Journal of Mathematical and Computer Modelling (1996).
- [7] Y. Makeenko, *Strings, Matrix Models and Meanders*, proceedings of the 29th Inter. Ahrenshoop Symp., Germany (1995).
- [8] J. Touchard, *Contributions à l'étude du problème des timbres poste*, Canad. J. Math. **2** (1950) 385-398.
- [9] W. Lunnon, *A map-folding problem*, Math. of Computation **22** (1968) 193-199.
- [10] H. Temperley and E. Lieb, *Relations between the percolation and coloring problem and other graph-theoretical problems associated with regular planar lattices: some exact results for the percolation problem*, Proc. Roy. Soc. **A322** (1971) 251-280.
- [11] P. Martin, *Potts models and related problems in statistical mechanics*, World Scientific (1991).